

**Molecular pharmacological investigation of archazolid  
for the intervention with inflammation and cancer**

**Dissertation**

To Fulfill the  
Requirements for the Degree of  
**„doctor rerum naturalium“ (Dr. rer. nat)**

**Submitted to the Council of the Faculty  
of Biology and Pharmacy  
of the Friedrich Schiller University Jena**

**by Dipl.-Pharm. Lea Maria Thomas  
born on June 2<sup>nd</sup>, 1987 in Aschaffenburg**

Date of disputation: March 10<sup>th</sup>, 2017

1<sup>st</sup> Reviewer: Prof. Dr. Oliver Werz – University of Jena

2<sup>nd</sup> Reviewer: Prof. Dr. Gerhard K. E. Scriba – University of Jena

3<sup>rd</sup> Reviewer: Prof. Dr. Eugen Proschak – University of Frankfurt

# TABLE OF CONTENTS

|   |           |
|---|-----------|
| ABBREVIATIONS.....  | IV        |
| SUMMARY.....  | VII       |
| ZUSAMMENFASSUNG.....  | IX        |
| <b>1 INTRODUCTION.....</b>  | <b>1</b>  |
| 1.1 Inflammation.....   | 1         |
| 1.1.1 Acute inflammation.....   | 1         |
| 1.1.2 Chronic inflammation.....   | 2         |
| 1.1.3 Inflammation-related diseases.....                                | 3         |
| 1.1.3.1 Cancer.....   | 3         |
| 1.1.4 Molecular signaling in bacteria-induced inflammation.....         | 4         |
| 1.1.4.1 Protein Kinases involved in LPS signaling and inflammation..... | 4         |
| 1.1.4.2 Transcription factors involved in inflammation.....             | 5         |
| 1.1.5 Cytokines.....  | 7         |
| 1.1.5.1 TNF $\alpha$ .....  | 8         |
| 1.1.6 Eicosanoids in inflammation and resolution.....                   | 9         |
| 1.1.6.1 Key enzymes in eicosanoid formation.....                        | 9         |
| 1.1.6.2 PGE <sub>2</sub> and other prostanoids.....                     | 11        |
| 1.1.6.3 Lipoxygenase products.....                                      | 12        |
| 1.2 Macrophages.....  | 15        |
| 1.2.1 M1 and M2 polarization.....                                       | 16        |
| 1.2.2 Role of M1 and M2 in cancer occurrence.....                       | 17        |
| 1.3 Vacuolar-type H <sup>+</sup> -ATPase.....                           | 19        |
| 1.3.1 Structure and function.....                                       | 19        |
| 1.3.2 Inhibition of the v-ATPase by myxobacterial compounds.....        | 21        |
| 1.3.3 Role of the v-ATPase in disease.....                              | 22        |
| <b>2 AIM OF THE THESIS.....</b>   | <b>24</b> |
| <b>3 MATERIALS AND METHODS.....</b>                                     | <b>25</b> |
| 3.1 Materials.....  | 25        |
| 3.2 Methods.....  | 30        |
| 3.2.1 Cell isolation and cell culture.....                              | 30        |
| 3.2.1.1 Monocyte isolation from leukocyte concentrates.....             | 30        |
| 3.2.1.2 Macrophage differentiation and polarization.....                | 30        |

---

|          |   |           |
|----------|---|-----------|
| 3.2.1.3  | MDA-MB-231 .....  | 30        |
| 3.2.2    | Determination of cell viability.....  | 31        |
| 3.2.3    | Analysis of vesicular pH.....   | 31        |
| 3.2.4    | Investigation of phagocytic activity.....   | 32        |
| 3.2.5    | Immunofluorescence microscopy.....  | 33        |
| 3.2.6    | Live cell imaging .....   | 34        |
| 3.2.7    | Determination of extracellular cytokine levels.....   | 34        |
| 3.2.8    | Determination of extracellular PGE <sub>2</sub> levels.....                                   | 34        |
| 3.2.9    | Determination of eicosanoid release.....  | 35        |
| 3.2.10   | Solid phase extraction.....   | 35        |
| 3.2.11   | UPLC-MS/MS analysis .....   | 36        |
| 3.2.12   | Determination of kinase activation, STAT1/3- and IκB phosphorylation, and NF-κB activity..... | 37        |
| 3.2.13   | Determination of v-ATPase, COX-2, and 5-LO expression.....                                    | 37        |
| 3.2.14   | Subcellular fractionation.....  | 37        |
| 3.2.15   | Generation of whole cell lysates for Western blot.....  | 38        |
| 3.2.16   | SDS-PAGE and Western blot.....  | 39        |
| 3.2.17   | Generation of cell homogenates .....  | 40        |
| 3.2.18   | Analysis of mRNA expression and degradation.....  | 40        |
| 3.2.19   | Determination of [ <sup>3</sup> H]-AA release.....  | 42        |
| 3.2.20   | Determination of reactive oxygen species (ROS) .....  | 42        |
| 3.2.21   | Statistics.....   | 43        |
| <b>4</b> | <b>RESULTS.....</b>   | <b>44</b> |
| 4.1      | Influence of archazolid on macrophage function .....  | 44        |
| 4.1.1    | v-ATPase expression and functionality .....   | 44        |
| 4.1.2    | Viability of M, M1, and M2 .....  | 46        |
| 4.1.3    | Morphology of M, M1, and M2 .....   | 47        |
| 4.1.4    | Phagocytosis .....  | 47        |
| 4.2      | Effects of archazolid on macrophages.....   | 48        |
| 4.2.1    | Cytokine release.....   | 48        |
| 4.2.2    | pH elevation and TNFα release .....   | 50        |
| 4.2.3    | TNFα mRNA expression and degradation .....  | 51        |
| 4.2.4    | Transcription factors.....  | 52        |
| 4.2.5    | Kinases involved in LPS signal transduction .....   | 54        |
| 4.2.6    | ROS levels .....  | 55        |

|          |  |            |
|----------|--|------------|
| 4.2.7    | Viability of MDA-MB-231.....   | 55         |
| 4.3      | Influence of archazolid on eicosanoid metabolism .....   | 56         |
| 4.3.1    | COX-2 products.....  | 56         |
| 4.3.2    | pH-elevating drugs.....  | 58         |
| 4.3.3    | Arachidonic acid release.....  | 59         |
| 4.3.4    | COX-2 activity, protein-, and mRNA expression .....  | 59         |
| 4.3.5    | Lipoxygenase product formation.....  | 61         |
| 4.3.5.1  | 5-LO translocation.....  | 63         |
| 4.3.6    | 5- and 15-LO product formation in cell homogenates.....  | 64         |
| 4.3.7    | 5-LO protein expression .....  | 65         |
| <b>5</b> | <b>DISCUSSION.....</b>   | <b>66</b>  |
| 5.1      | Archazolid B inhibits the v-ATPase functionality by simultaneous unimpaired macrophage integrity ..... | 67         |
| 5.2      | Archazolid elevates TNF $\alpha$ levels in M and M1 due to increased transcription .....               | 68         |
| 5.3      | Enzymes of the eicosanoid metabolism are differently affected by archazolid .....                      | 73         |
| <b>6</b> | <b>REFERENCES.....</b>   | <b>78</b>  |
|          | <b>APPENDIX 1: Acknowledgements.....</b>   | <b>I</b>   |
|          | <b>APPENDIX 2: List of publications.....</b>   | <b>III</b> |
|          | <b>APPENDIX 3: Eigenständigkeitserklärung.....</b>   | <b>IV</b>  |

## ABBREVIATIONS

|                      |  |
|----------------------|--|
| [ <sup>3</sup> H]-AA | Tritium labeled arachidonic acid       |
| AA                   | Arachidonic acid                       |
| ATF                  | Activating transcription factor        |
| ATP                  | Adenosine triphosphate                 |
| BSA                  | Bovine serum albumin                   |
| CAIA                 | Collagen-antibody induced arthritis    |
| CCL                  | Chemokine (C-C motif) ligand           |
| CD                   | Cluster of differentiation             |
| CLP                  | Coactosin-like protein                 |
| COX                  | Cyclooxygenase                         |
| cPGES                | Cytosolic prostaglandin E synthase     |
| cPLA <sub>2</sub>    | Cytosolic phospholipase A <sub>2</sub> |
| CQ                   | Chloroquine                            |
| CRE                  | cAMP-responsive element                |
| CXCL                 | Chemokine (C-X-C motif) ligand         |
| cysLT                | Cysteinyl leukotrienes                 |
| D'PBS                | Dulbecco's phosphate buffered saline   |
| DAPI                 | 4',6-diamidino-2-phenylindole          |
| DC                   | Dendritic cells                        |
| DCFH-DA              | 2'-7'-dichlorofluorescein diacetate    |
| DGLA                 | Dihomo-gamma-linolenic acid            |
| DMEM                 | Dulbecco's modified eagle medium       |
| E-box                | Enhancer box                           |
| EDTA                 | Ethylenediaminetetraacetic acid        |
| EGF                  | Epithelial growth factor               |
| EPA                  | Eicosapentaenoic acid                  |
| ER                   | Endoplasmic reticulum                  |
| ERK                  | Extracellular-signal regulated kinase  |
| FCS                  | Fetal calf serum                       |
| FITC                 | Fluorescein isothiocyanate             |
| FLAP                 | Five-lipoxygenase activating protein   |
| GPCR                 | G-protein coupled receptor             |
| H(p)ETE              | Hydro(pero)xyeicosatetraenoic acid     |
| HBSS                 | Hank's balanced salt solution          |
| HIF                  | Hypoxia-inducible factor               |
| HODE                 | Hydroxyoctadecadienoic acid            |
| HSC                  | Haematopoietic stem cell               |
| IFN                  | Interferon                             |
| IKK                  | IκB kinase                             |
| IL                   | Interleukin                            |
| iNOS                 | Inducible nitric oxide synthase        |
| ITC                  | Inflammation triggered cancer          |
| IκB                  | Inhibitor of kappa B                   |
| Jak                  | Janus activated kinase                 |

|                |   |
|----------------|---|
| JNK            | c-Jun N-terminal kinase   |
| LBP            | LPS-binding protein   |
| LO             | Lipoxygenase  |
| LPS            | Lipopolysaccharide  |
| LT             | Leukotriene   |
| Lx             | Lipoxin   |
| m/cPGES        | Microsomal/cytosolic prostaglandin E synthase                         |
| MAPEG          | Membrane-associated proteins in eicosanoid and glutathione metabolism |
| MAPK           | Mitogen activated protein kinase                                      |
| MCP-1          | Monocyte chemotactic protein-1  |
| MD             | Myeloid differentiation protein                                       |
| MEK            | MAPK kinase   |
| MEKK           | MAPK kinase kinase  |
| MHC            | Major histocompatibility complex                                      |
| MMP            | Matrix metalloproteinase  |
| MPS            | Mononuclear phagocyte system  |
| MRP-4          | Multidrug resistance protein  |
| MTT            | 3-(4,5-dimethylthiazol-2-yl)-2,5-diphenyltetrazolium bromide          |
| MyD88          | Myeloid differentiation primary response gene 88                      |
| NAK            | NF- $\kappa$ B activating kinase                                      |
| NF- $\kappa$ B | Nuclear factor- $\kappa$ B  |
| NK             | Neutral killer cells  |
| NO             | Nitric oxide  |
| NSAID          | Non-steroidal anti-inflammatory drug                                  |
| PAF            | Platelet activating factor  |
| PBMC           | Peripheral blood mononuclear cells                                    |
| PC             | Phosphatidylcholine   |
| PDK            | Phosphoinositide-dependent kinase                                     |
| PFA            | Paraformaldehyde  |
| PG             | Prostaglandin   |
| PI             | Phosphatidylinositol  |
| PI3-K          | Phosphoinositide 3-kinase   |
| PIP3           | Phosphoinositol (3,4,5) triphosphate                                  |
| PK             | Protein kinase  |
| PMSF           | Phenylmethylsulfonyl fluoride   |
| PPAR           | Peroxisome proliferator activated receptor                            |
| PRR            | Pattern recognition receptor  |
| PUFA           | Polyunsaturated fatty acid  |
| RHD            | Rel homology domain   |
| rhM-CSF        | recombinant human Macrophage colony stimulating factor                |
| RNS            | Reactive nitrogen species   |
| ROS            | Reactive oxygen species   |
| RSK            | Ribosomal subunit kinase  |
| SDS            | Sodium dodecyl sulfate  |
| SDS-PAGE       | SDS-polyacrylamide gel electrophoresis                                |
| SHIP           | Src homology 2-containing inositol phosphatase                        |
| SPE            | Solid phase extraction  |

|                     |  |
|---------------------|--|
| SRS-A               | Slow-reacting substance of anaphylaxis                           |
| STAT                | Signal transducer and activator of transcription                 |
| STI                 | Trypsin inhibitor from soybean                                   |
| TAD                 | Transactivation domain   |
| TAM                 | Tumor associated macrophage                                      |
| TBS                 | Tris-buffered saline   |
| TGF                 | Transforming growth factor                                       |
| TGN                 | Trans-Golgi network  |
| T <sub>H</sub> cell | T helper cell  |
| TLR                 | Toll-like receptor   |
| TNF(R)              | Tumor necrosis factor (receptor)                                 |
| Tris                | Trimethanolamine   |
| Tx                  | Thromboxane  |
| UPLC-MS/MS          | Ultra performance liquid chromatography tandem mass spectrometry |
| v-ATPase            | Vacuolar-type H <sup>+</sup> -ATPase                             |
| VEGF                | Vascular endothelial growth factor                               |

## SUMMARY

The vacuolar H<sup>+</sup>-ATPase (v-ATPase) constitutes a crucial enzyme in regulating cellular pH and maintaining pH homeostasis to ensure essential cellular processes in view of processing, trafficking and degradation. Being involved in such indispensable mechanisms, deregulation of the proton translocating enzyme has been linked to diseases of the renal system, osteoclast dysfunction and cancer [1-3], when the tight control of the pH cannot be maintained. The v-ATPase has thus been emphasized as potential drug target. The myxobacterial compound archazolid inhibits the v-ATPase in the low nanomolar range [4] and has further been evidenced to potently induce apoptotic mechanisms in tumor cells [5]. As promising agent for future anti-cancer therapies it was of particular relevance to investigate whether archazolid also affects primary immune cells that are components of the tumor microenvironment. In this context, macrophages as representative cells of the innate and adaptive immune system were addressed in this work. Thus, several assays with macrophages differentiated from freshly isolated monocytes were performed. The ability of macrophages to polarize upon activating stimuli into the pro-inflammatory but anti-tumoral M1 phenotype and the M2 phenotype with opposing properties [6] was further addressed in the investigation of archazolid. Especially concerning cancer occurrence the predominating macrophage subtype (i.e. M2) is significant for tumor development and disease progress. This is mainly attributable to a variety of mediators formed by macrophages dependent on their polarization [7]. This thesis comprises two parts, which focus on distinct groups of mediators and whether they are affected by archazolid.

The first part concerns a selection of tumor-relevant pro- and anti-inflammatory cytokines, produced upon inflammatory stimuli by cells of the immune system, such as macrophages. Once released, they aim at the communication between these cells whereby they exhibit pro- or anti-inflammatory potential. Signaling pathways, also studied in this work, regulate their formation and determine their time-dependent release [8]. Tumor necrosis factor (TNF) $\alpha$  belongs to the most prominent cytokines that was discovered about 50 years ago as inducer of malignant cell necrosis [9]. M1-like macrophages are an abundant source of TNF $\alpha$  which is further closely related to pro-inflammatory events which limited the cytokine's use in systemic administration to cancer patients although it can still be used when administered by a specific technique [10]. Archazolid elevated TNF $\alpha$  levels selectively in M1, attributable to a transcriptional induction, whereas M2 were not

affected. As underlying mechanism it could be established that archazolid affects the transcription factor nuclear factor kappa B (NF- $\kappa$ B). Thus, it was hypothesized that elevated TNF $\alpha$  levels induced by archazolid in M1 might exhibit cancer cell death inducible activity supporting the compound's direct cytotoxic activities on cancer cells while sparing the host macrophages.

The second part of this thesis approaches the modulation of the arachidonic acid (AA) cascade by archazolid, where in turn both pathways, lipoxygenase (LO) and cyclooxygenase (COX) pathway, were considered. The first route uses 5-LO to convert AA to leukotrienes (LT). LTs are potent lipid mediators that have originally been found to mediate the characteristic symptoms of diseases of the respiratory system like asthma, while their contribution to cardiovascular diseases (CVD), auto-immune diseases, and cancer have been established later [11]. 15-HETE, which is in turn metabolized into lipoxins, is another metabolite of AA formed by 15-LO. Contrarily to 5-LO products, 15-LO-derived mediators have been evidenced to be involved in the resolution of inflammation [12]. Archazolid was demonstrated to affect the LOs in a different manner, since 5-LO product formation was inhibited in M1 and M2 while 15-HETE was increased only in M1. Although it was emphasized that archazolid seems to affect the enzymes directly, the distinct role of M1 and M2 in this context could only be elucidated partly. The COX-2 is another key enzyme in the AA metabolism converting the substrate into prostanoids, of which prostaglandin (PG)E<sub>2</sub> is the most prominent representative. It mediates some of the characteristic symptoms of an acute inflammation, such as fever, pain, redness and swelling [13], but recently, it has also been identified to induce the resolution phase of inflammation due to its context dependent effects [14]. PGE<sub>2</sub> is produced especially by M1-like macrophages in which PGE<sub>2</sub> levels were elevated by archazolid due to an induction of COX-2 mRNA in M1 but not in M2. This led to the conclusion that the underlying mechanism is related to the transcriptional induction of TNF $\alpha$ .

Together, it is notable that the v-ATPase inhibitor archazolid elevated the levels of the M1-related mediators TNF $\alpha$  and PGE<sub>2</sub> selectively in M1, whereas they remained unaffected in M2. The LO pathway of M1 is modulated by archazolid in favor of the anti-inflammatory pro-resolving metabolite 15-HETE. The results of this thesis provide novel insights into the impact of v-ATPase inhibition on primary cells, they emphasize the advantage of investigating different macrophage phenotypes and elucidate the possibility of their specific manipulation. In particular, the results suggest that archazolid increases M1 specific properties that might potentiate the anti-tumoral activity of this v-ATPase inhibitor and links important roles of the V-ATPase in this context.

## ZUSAMMENFASSUNG

Die ATPase des Vakuolen-Typ (v-ATPase) stellt ein entscheidendes Enzym für die Regulierung des zellulären pH Wertes und die Aufrechterhaltung der pH Homöostase dar, wodurch grundlegende zelluläre Vorgänge, wie Prozessierung, Transport und Abbau gewährleistet werden [3]. Als Bestandteil dieser essentiellen Mechanismen kann eine Fehlfunktion dieses Enzyms zu Nierenerkrankungen, veränderter Osteoklastentätigkeit oder Krebs führen [1, 2], wenn die notwendige exakte Kontrolle des pH Wertes nicht mehr aufrechterhalten werden kann. Die V-ATPase stellt aus diesem Grund ein mögliches Arzneistofftarget dar. Archazolid, eine ursprünglich aus Myxobakterien isolierte Verbindung, hemmt die V-ATPase im niederen nanomolaren Bereich [4] und wurde bereits als Substanz identifiziert, die die Apoptose in Tumorzellen potent zu induzieren vermag [5]. Da Archazolid eine vielversprechende Substanz für zukünftige Krebsbehandlungen darstellt, war die Untersuchung dieser Verbindung in Hinblick auf deren Einfluss auf primäre Immunzellen, die in der Tumormikroumgebung anzutreffen sind, von besonderem Interesse. Als repräsentative Vertreter der Immunzellen innerhalb der angeborenen und adaptiven Immunantwort wurden Makrophagen verwendet, die aus frisch isolierten Monozyten differenziert und für verschiedene Tests kultiviert wurden. Die Fähigkeit von Makrophagen in Folge entsprechender Stimuli zu entzündungsfördernden, Tumor bekämpfenden M1 Makrophagen oder M2 Makrophagen, die durch entgegengesetzte Eigenschaften charakterisiert sind, zu polarisieren [6] wurde ebenfalls in die Forschungsarbeit über Archazolid einbezogen. Der vorherrschende Makrophagen Subtyp (d.h. M2) ist besonders im Krebsgeschehen von zentraler Bedeutung, da er Tumorentwicklung und Krankheitsverlauf mitbestimmt. Dies ist vorwiegend auf die Vielfalt an Mediatoren zurückzuführen, die entsprechend des jeweiligen Polarisierungstyps von Makrophagen gebildet werden [7]. Die vorliegende Arbeit umfasst zwei Teile, welche jeweils unterschiedliche Gruppen dieser Mediatoren behandeln und deren Beeinflussung durch Archazolid darlegen.

Der erste Teil bezieht sich auf eine Auswahl an Tumor-relevanten entzündungsfördernden und -hemmenden Zytokinen, die in Folge der Stimulation von Zellen des Immunsystems, wie beispielsweise Makrophagen, gebildet und freigesetzt werden. Freigesetzte Zytokine mit unterschiedlichem entzündungsförderndem oder -hemmendem Potential ermöglichen eine Kommunikation zwischen den Zellen. Verschiedene Signalwege, die ebenfalls in dieser Arbeit

untersucht wurden, regulieren dabei die Bildung und Freisetzung dieser Zytokine [8]. Tumor Nekrose Faktor (TNF) $\alpha$  ist eines der bekanntesten Zytokine, das vor ungefähr 50 Jahren durch seine Fähigkeit entdeckt wurde, Nekrose bösartiger Zellen hervorzurufen [9]. Makrophagen des M1 Phänotyps produzieren große Mengen an TNF $\alpha$ , welches allerdings auch eng mit entzündungsfördernden Prozessen verknüpft ist, die seine systemische Verabreichung an Krebspatienten limitierte. Wird jedoch eine spezielle Verabreichungstechnik angewandt, kann TNF $\alpha$  dennoch in Krebstherapien eingesetzt werden [10]. Durch Archazolid wurden die TNF $\alpha$  Level in M1 Makrophagen selektiv erhöht, was auf eine Induktion auf transkriptioneller Ebene zurückzuführen war, während M2 Makrophagen nicht beeinflusst wurden. Als zugrundeliegender Mechanismus hierfür wurde die Beeinflussung des Transkriptionsfaktors Nuclear Factor kappa B (NF- $\kappa$ B) durch Archazolid nachgewiesen. Dies führte zu der Hypothese, dass die durch Archazolid verursachten erhöhten TNF $\alpha$  Level in M1 den Tod von Krebszellen induzieren, dadurch die direkte Zelltoxizität von Archazolid auf Tumorzellen unterstützen, jedoch gleichzeitig die Makrophagenviabilität nicht beeinträchtigen sollten.

Im zweiten Teil dieser Arbeit wird die Modulation der Arachidonsäure (AA)-Kaskade durch Archazolid behandelt, wobei sowohl der Lipoxygenase-(LO), als auch der Cyclooxygenase-(COX) Weg berücksichtigt wurde. Dem ersten Weg folgend wird AA durch die 5-LO zu Leukotrienen (LT) umgesetzt. Bei diesen handelt es sich um potente Lipidmediatoren, die charakteristische Symptome von Atemwegserkrankungen, wie Asthma, hervorrufen. Ihre Beteiligung an kardiovaskulären Erkrankungen (CVD), Autoimmunerkrankungen und Krebs wurde erst später festgestellt [11]. 15-HETE stellt einen weiteren Metaboliten innerhalb der AA-Kaskade dar, welcher durch die 15-LO gebildet und nachfolgend zu den Lipoxinen weiter umgesetzt wird. 15-LO Produkte wurden jedoch im Gegensatz zu den LT mit der Auflösung einer Entzündung in Verbindung gebracht [12]. Archazolid beeinflusste die beiden LOs in unterschiedlicher Weise: Mediatoren des 5-LO Weges wurden von Archazolid unabhängig des Makrophagen Subtyps inhibiert, während 15-HETE Level in M1 gesteigert wurden. Obwohl durch mehrere Experimente herausgestellt werden konnte, dass Archazolid einen direkten Einfluss auf die Enzyme ausübt, konnte die unterschiedliche Rolle von M1 und M2 in diesem Zusammenhang nur teilweise aufgeklärt werden. Die COX-2 stellt ein weiteres Schlüsselenzym der AA-Kaskade dar, welches das Substrat zu Prostanoiden umsetzt, unter denen Prostaglandin (PG) $E_2$  der prominenteste Vertreter ist. PGE $_2$  vermittelt einige der charakteristischen Symptome einer akuten

Entzündungsreaktion, zu denen Fieber, Schmerz, Rötung und Schwellung gehören [13], wobei kürzlich ebenso sein Beitrag zur Induktion der Auflösungsphase der Entzündung diskutiert wurde [14]. PGE<sub>2</sub> wird vorwiegend vom M1 Phänotyp gebildet, in welchem eine Erhöhung der PGE<sub>2</sub> Level durch Archazolid aufgrund einer Induktion der COX-2 mRNA nachgewiesen werden konnte. Dies führte zu der Schlussfolgerung, dass die zugrundeliegenden Mechanismen denen entsprechen, die die transkriptionelle Induktion von TNF $\alpha$  verursachten.

Zusammenfassend zeigte der V-ATPase Inhibitor Archazolid eine bemerkenswerte selektive Steigerung der M1-verwandten Mediatoren TNF $\alpha$  und PGE<sub>2</sub> ausschließlich im M1 Makrophagen Phänotyp, während M2 Makrophagen unbeeinflusst blieben. Der Lipoxigenase-Weg wird durch Archazolid zugunsten des entzündungshemmenden und die Phase der Auflösung unterstützenden Mediators 15-HETE beeinflusst. Die in dieser Arbeit dargestellten Ergebnisse liefern somit neue Erkenntnisse über den Einfluss der V-ATPase Inhibition in Primärzellen, machen dabei einerseits die Notwendigkeit der Untersuchung verschiedener Makrophagen Phänotypen deutlich und offenbaren andererseits, dass deren spezifische Beeinflussung möglich ist. Im Speziellen deuten die Resultate darauf hin, dass Archazolid M1-spezifische Eigenschaften steigert, wodurch dessen anti-tumorale Aktivität potenziert werden könnte und neue Einsichten zur Rolle der v-ATPase offenbart werden.

# 1 INTRODUCTION

## 1.1 Inflammation

Inflammation is a physiological process closely connected to the innate immunity as it is an essential response of an organism to secure survival in case of injury or against invading pathogens that cause infection. Due to the conspicuousness of an inflammatory reaction, the five main symptoms have already been defined long time ago: redness, heat, swelling, pain and loss of function are the consequences of diverse mediators formed from the beginning of an inflammation. Whereas in non-infectious inflammation the triggers causing tissue injury are still incompletely understood, the molecular mechanisms of a bacterial, viral or parasitic elicited inflammatory response are well-characterized [15].

### 1.1.1 Acute inflammation

When the body is attacked by invading pathogens it will respond by an immediate immune reaction, the acute inflammation, to avoid infection and tissue injury and to maintain homeostasis. Due to the rapidity of this first defense system it is unspecific and consists of several events [16]. In case of a bacterial infection macrophages recognize foreign particles by specific receptors (see 1.1.4) which lead to the production and delivery of inflammatory mediators, including lipid mediators, cytokines, and chemokines. Thereby, neutrophils are recruited to the site of inflammatory origin and become activated. Releasing toxic agents like reactive oxygen species (ROS) from their granules, they eliminate pathogens but can also damage host cells [17]. Additionally, monocytes enter the tissue and thereby differentiate into inflammatory macrophages. Furthermore, activation of the complement system supports the destruction of bacterial invaders by facilitating their phagocytosis and further chemoattraction of neutrophils. Delivery of nitric oxide (NO) and prostaglandins (PG) at the site of inflammation leads to vasodilatation, enhancing the release of soluble factors while evoking redness and warmth of the affected tissue. For the same purpose, leukotrienes (LT), histamine and other metabolites increase vascular permeability, thereby contributing to the formation of edema due to an opening of endothelial cell tight junctions [18, 19]. The common aspect of all these mechanisms is the elimination of the pathogen and protection of the host, avoiding infection and initiating repair systems. One of the most important

mechanisms beneath these, however, is to secure the termination of the inflammatory processes and to activate the resolution of inflammation before the host suffers from the inflammatory activities. The termination sequences are already activated shortly after the inflammatory response has begun. They include the shift from pro- to anti-inflammatory mediators, the cessation of neutrophil infiltration and recruitment to the inflamed tissue, the initiation of programmed cell death by apoptosis of neutrophils, and their engulfment by phagocytic macrophages [20]. This way the affected tissue returns to its pre-infected status.

### 1.1.2 Chronic inflammation

Chronic inflammation arises from a persisting and non-resolving acute inflammation. While acute inflammation is self-limiting and thus represents the necessary and beneficial response of the immune system for protection against pathogens, the failure of initiating the resolution phase provokes a chronic inflammatory environment which damages the host [21]. The mechanisms which may lead to a prolonged inflammatory status are multifaceted and an exact identification is sometimes impossible due to functional interactions. Phagocytosis of apoptotic neutrophils by macrophages triggers the release of anti-inflammatory cytokines. Deficiency in this event leads to necrosis of neutrophils which elicits pro-inflammatory signals, similarly to that caused by microbial products [22]. Attenuation of the pro-inflammatory state of monocytes and macrophages constitutes another critical event. Phagocytosis of tissue debris by monocytes induces their phenotypic switch from pro- to anti-inflammatory and, furthermore, the release of anti-inflammatory cytokines which suppress the activity of pro-inflammatory macrophages [23]. Too strong or too weak T-cell responses as well as an impaired function of T regulatory cells promote the prolongation of inflammation [22]. Apart from the cellular involvement, soluble factors, released from immune cells, determine the development of inflammation: Cytokines, ROS and reactive nitrogen species (RNS), and lipid mediators are, among others, involved in preservation or resolution of inflammation [17, 22]. Naturally, also the persistence of exogenous inflammatory stimuli in the form of toxins or antigens are essential events in chronification, even if this is not an indispensable requirement. Often, the inflammatory events themselves are harming the host [22]. Notably, inhibition of inflammation is not the key to return to homeostasis, although it improves the cardinal signs of acute inflammation. In fact, inhibition even prolongs the inflammatory status due to its resolution-impairing effect [24, 25].

Ultimately, an inflammatory environment which persists a longer period of time facilitates the emergence of diverse diseases or, even if it is not their underlying reason, promotes disease progress by the given mechanisms [26, 27].

### 1.1.3 Inflammation-related diseases

If inflammation escapes from its protective function due to deficiencies of inflammation resolving mechanisms, therefore sliding into chronic inflammation, it is strongly associated with diverse diseases. Cardiovascular and renal diseases, type 2 diabetes, autoimmune diseases as rheumatoid arthritis, asthma, and cancer are, for instance, affected in their initiation and progression by a chronic inflammation [28].

#### 1.1.3.1 Cancer

Long lasting inflammatory processes cause pathological changes and concerning cancer, can affect different phases of disease development: Tumorigenesis by survival mechanisms, including cellular transformation and escape from immune surveillance as well as tumor spread by invasion, angiogenesis and metastasis [26]. The link to chronic inflammation concerns many different types of cancer and for some of them the inflammatory stimulus responsible for the manifestation of the neoplasm is even known. Examples are lung carcinoma caused by bronchitis, colorectal carcinoma induced by inflammatory bowel diseases and bladder carcinoma triggered by cystitis [29]. The arising tumor microenvironment still shows strong similarities to the initial inflammatory site, where immigration of immune cells and the production of specific mediators are essential events [30]. However, the tumor enables its survival by changing the infiltrating immune cell status in favor of an anti-inflammatory and immune suppressive phenotype and therefor exploits the plasticity of many immune cells. Macrophages are influenced by the tumor to develop towards the tumor associated macrophages (TAM), promoting proliferation, angiogenesis, invasion, and metastasis by production of corresponding factors and enzymes [31] (see 1.2.1). Furthermore, dendritic cells (DC) are impeded to mature, thus preventing the activation of T-cells that trigger an anti-tumoral immune response [32]. T-cells themselves are induced to develop towards the immune suppressive type 2 phenotype, ineffective in fighting against the tumor. This illustrates that the tumor microenvironment is not lacking immune cells or inflammatory cytokines in general. Instead, it generates an anti-inflammatory, immune suppressive environment with their

help. This is supported by the finding that in some cancer patients a systemic inflammatory response seems to be impossible [31], thus shielding the tumor from an attack of the immune system.

#### 1.1.4 Molecular signaling in bacteria-induced inflammation

There are diverse signaling pathways leading to the formation of pro-inflammatory mediators. Of importance for the detection of bacterial inducers are the so-called Toll-like receptors (TLR), a family of transmembrane proteins pertaining to the signaling pattern recognition receptors (PRR). These are localized on immune cells, especially on antigen-presenting cells such as macrophages and play a major role by recognizing microbial components leading to the production of several effector molecules: transcription factors, cytokines (interleukin (IL)-1, IL-6, tumor necrosis factor (TNF) $\alpha$ ), chemokines (monocyte chemotactic protein (MCP)-1, IL-8) and eicosanoids as part of the early immune reaction, causing themselves the induction of further mediators [15, 33]. In case of the gram-negative bacterial membrane component lipopolysaccharide (LPS), the detection occurs by TLR4 on macrophages leading to the activation of intracellular signaling cascades. The exact mechanism of detection starts with the LPS-binding protein (LBP), which transfers LPS monomers to the cluster of differentiation (CD) 14 receptor on the cell membrane. However, lacking a transmembrane domain, CD14 demands TLR4 and its associated myeloid differentiation protein (MD)-2 for transducing the LPS signal and thus activating one of the intracellular downstream cascades [34, 35].

##### 1.1.4.1 Protein Kinases involved in LPS signaling and inflammation

In response to LPS, mitogen activated protein kinases (MAPK) play a major role in transferring the inflammatory signal. Their signaling results in promotion of transcription factor expression and induced cytokine production. The classical activation of a MAPK is initiated by phosphorylation by a MAPK kinase (MEK), which is in turn activated by a MEK kinase (MEKK). Extracellular signal-regulated kinase (ERK), p38 and c-Jun N-terminal kinase (JNK) belong to the most important MAPK involved in inflammation [36]. In this manner, ERK1/2 becomes activated by MEK1/2, p38 activity is regulated by MEK3/6, and JNK phosphorylation is performed by MEK4/7. The prominent involvement of these three kinases in the inflammatory response is, for instance, represented by their regulation of TNF $\alpha$ , the paragon of inflammatory cytokines [37].

Whereas JNK is involved in TNF $\alpha$  transcription and translation [38] and p38 regulates TNF $\alpha$  mRNA in post-transcriptional processes, such as stability and translation [39-41], ERK affects the transport of the TNF $\alpha$  transcript from the nucleus to the cytoplasm [42]. However, besides TNF $\alpha$ , gene expression of many other inflammatory target proteins is induced [43, 44].

Apart from MAPK, the serine/threonine kinase Akt (also called protein kinase B/PKB), likewise activated upon TLR4 activation, is involved in the inflammatory occurrence [36]. Signaling of Akt proceeds via the phosphoinositide 3-kinase (PI3-K) pathway, which includes the phosphatidylinositol (3,4,5) triphosphate (PIP3) mediated translocation of Akt to the plasma membrane and activating phosphorylation by phosphoinositide-dependent kinase 1 (PDK1) [45]. In this way, the transcription factor nuclear factor kappa B (NF- $\kappa$ B) becomes activated and thus contributes to the pro-inflammatory effects of Akt [46]. However, Akt is also implicated in anti-inflammatory actions since it induces the LPS-stimulated production of IL-10 [47, 48]. Furthermore, elevated activity of Akt, for instance due to the repression of deactivating factors, has been observed in some types of tumors, leading to enhanced cancer cell survival and proliferation [49].

#### 1.1.4.2 Transcription factors involved in inflammation

Transcription factors are proteins with the ability to bind specific DNA sequences, thereby regulating the transcription of the appropriate target gene. Thus, they are essential for physiological processes, but equally important if deregulated mechanisms result in disease.

Probably the most prominent transcription factor involved in inflammatory processes is NF- $\kappa$ B. NF- $\kappa$ B consists of a dimer of two of five possible mammalian subunits: NF- $\kappa$ B1 (p105, proteolytically processed to p50), NF- $\kappa$ B2 (p100, proteolytically processed to p52), RelA (p65), RelB, and c-Rel. The Rel homology domain (RHD) is the common structure of all these subunits and is responsible for DNA binding, dimerization, nuclear localization, and inhibitor of kappa B (I $\kappa$ B) binding [50]. The five Rel family members are expressed in every cell type and are able to affect a huge number of genes which enables NF- $\kappa$ B to possess a large variety of functions. However, it is especially of relevance when stress conditions demand rapid gene transcription since activation of NF- $\kappa$ B via the classical pathway up to DNA binding of the target gene occurs within minutes [50, 51]. The classical or so-called “canonical pathway” is activated upon stimulation with LPS or the cytokines IL-1 and TNF. Thus, the I $\kappa$ B kinase complex (IKK),

consisting of the IKK $\alpha$ , IKK $\beta$ , and IKK $\gamma$  subunits, becomes activated by phosphorylating upstream kinases. IKK $\beta$  then phosphorylates the inhibitory NF- $\kappa$ B-binding protein I $\kappa$ B $\alpha$ , resulting in its ubiquitination and therefore proteasomal degradation. Free NF- $\kappa$ B is hence enabled to translocate into the nucleus, where it binds to the DNA for regulating the expression of the respective target genes [50]. Furthermore, there are several mechanisms to regulate NF- $\kappa$ B activity in strength and duration: phosphorylation at different sites of NF- $\kappa$ B subunits, hyperphosphorylation of IKK, processing of NF- $\kappa$ B precursors (p100 and p105) or induction of I $\kappa$ B synthesis. The specificity of NF- $\kappa$ B binding to special sites in the promoters of target genes is enabled by the distinct composition of NF- $\kappa$ B dimers [50-53]. The amount and diversity of NF- $\kappa$ B-regulated genes is a possible explanation for the different roles of this transcription factor in disease, especially in cancer [54, 55]. Several regulatory functions of NF- $\kappa$ B expose it as tumor promoting factor: NF- $\kappa$ B regulates cell proliferation by stimulating cytokine and growth factor expression and affecting cell cycle proteins [54]. It regulates expression of chemokines and growth factors, promoting angiogenesis, and regulates the expression of adhesion molecules, facilitating invasion and metastasis [56]. Deregulation of NF- $\kappa$ B controlling mechanisms and therefore overexpression of constitutively activated NF- $\kappa$ B are present in many types of cancer [55]. Nevertheless, NF- $\kappa$ B also mediates indispensable functions of the immune system. It regulates the expression of cytokines, occupying a key function in innate immunity by interferon (IFN)- $\gamma$  expression in T-cells, IL-6 expression in B-cells, TNF $\alpha$  expression in macrophages, and IL-12 expression in dendritic cells. In addition, it promotes lymphocyte proliferation and cell survival, hematopoiesis as well as apoptosis [54]. Whether NF- $\kappa$ B expresses tumor promoting or suppressing functions depends on the conditions and cannot be predicted generally.

Another class of transcription factors with diverse contribution to cancer development is the signal transducer and activator of transcription (STAT) family. There are seven STATs which exist as cytoplasmic transcription factors that become activated after recruitment to and phosphorylation by protein tyrosine kinases. The cytokine receptor-associated Janus activated kinases (Jak), growth factor receptors and cytoplasmic tyrosine kinases are able to phosphorylate STAT proteins. Activation of STAT results in translocation of dimerized STATs into the nucleus, where they regulate gene transcription after binding to their response elements in the target gene [57]. A large number of cytokine receptors, for instance IL-2, IL-4, IL-6, IL-12, IFN, and growth factors signal through the Jak/STAT pathway. Consequently, STATs are extensively involved in B-cell

development, T-cell stimulation, neutrophil function and macrophage activation [58] that explains their essential role in inflammation and immunity as well as related diseases in case of deregulation. Indeed, key functions of STAT1, STAT3, and STAT5 have been found in many types of cancer [59-61]. Physiologically activated STAT3 and STAT5 contribute to cell growth and proliferation and an aberrant activity is therefore not surprisingly involved in tumor growth, progression, cancer cell survival and chemoresistance mechanisms [59]. Additionally, elevated levels of phosphorylated STAT3 are characteristic for a tumor infiltrating M2 macrophage phenotype [62] (see 1.2.2). Contrarily, STAT1 is associated with growth inhibition, apoptosis induction and is, due to its activation by IFNs, essential for a functional immune system [59], according to their expression in the anti-tumoral M1 phenotype [62] (see 1.2.2). Whereas inhibition of STAT3 and STAT5 has already been found to be beneficial for an anti-tumor therapy, the overexpression of STAT1 found in some tumors is not yet completely understood but seems to be positive in anti-cancer treatments since it acts as a tumor suppressor [60, 61].

### 1.1.5 Cytokines

Cytokines belong to a group of small proteins, ranging in their molecular weight from 8 to 40,000 Da, and are categorized according to their biological function (pro-/anti-inflammatory), since the most cells are able to synthesize and even respond to them [63]. Cytokines are produced and released upon inflammatory stimuli for the communication between cells and their common orchestration of an immune response [8]. Chemokines are even identifiable by their name (chemotactic cytokines) to be specialized in initiating chemotaxis and thereby enabling the communication between cells. However, not only the communication between host cells but also of malignant cells among themselves or to the host's immune cells, affecting them in favor of malignant cell growth, are enabled by a number of cytokines. To the class of pro-inflammatory cytokines belong TNF $\alpha$ , IFN- $\gamma$ , IL-1 $\beta$ , IL-6, IL-12, IL-18, IL-8, and MCP-1 whereas IL-4, IL-10, IL-13, and transforming growth factor (TGF)- $\beta$  are attributed to the anti-inflammatory cytokines [31, 63-65]. Nevertheless, a strict division into pro- and anti-inflammatory is not always possible, since their effects depend on the context [63]. Stimulation of production and release of cytokines as well as effective stop mechanisms for their formation have to be tightly controlled in a biological system. Hence, it is obvious that intracellular trafficking of cytokines follows diverse pathways, being an option to coordinate and regulate their formation and release [8].

### 1.1.5.1 TNF $\alpha$

TNF was first identified in 1962 [66] and its activity demonstrated in 1975 [9] before 1985 two TNFs with 50% sequence homology were structurally identified and separated into TNF $\alpha$  and TNF $\beta$  [67]. The TNFs are mainly formed by monocytes/macrophages, B-, and T-lymphocytes, as they are physiologically responsible for the immunological host defense against microbial infections [68]. LPS belongs to one of the most potent inducers of TNF $\alpha$  production and regulates it at the transcriptional and translational level. [69]. According to the classic secretory pathway, the initially in the endoplasmic reticulum (ER) formed membrane associated precursor protein (26 kDa) underlies further processing in the Golgi. Subsequently, TNF $\alpha$  is transported from the trans-Golgi network (TGN) via recycling endosomes, after sorting from other cargo, to phagocytic cups at the membrane. There it is cleaved by matrix metalloproteinases (MMP) into the 17 kDa soluble protein prior to release [8, 68]. TNF $\alpha$  reaches maximum levels after its release within very short times compared to other cytokines, but likewise, there are effective mechanisms to eliminate circulating TNF $\alpha$  in short time periods to prevent pathological conditions. The pro-inflammatory and immunomodulatory effects of TNF $\alpha$  are mediated by two cell surface receptors, TNFR1 and TNFR2. In this way TNF $\alpha$  induces the production of further inflammatory cytokines and activates cells of the immune system. The main inflammatory events, however, are attributable to TNF $\alpha$ 's effects on endothelial cells, whereby leukocyte populations are attracted to the site of infection. Consequently, fever and tissue injury, cell proliferation, differentiation and apoptosis are directly and indirectly caused by TNF $\alpha$  [69, 70].

TNF $\alpha$  was discovered as an endogenous agent that induces necrosis of malignant cells [9]. Accordingly, after isolation and purification, TNF $\alpha$  was used in a variety of anti-cancer studies [71-75]. Nevertheless, the effects of TNF $\alpha$  in cancer occurrence are paradoxical, even due to its undisputed role in inflammation [10, 76, 77]. However, there is evidence that several mechanisms both, directly and indirectly, contribute to the destruction of tumor cells by TNF $\alpha$ . Local injections into the tumor with high and continuous doses of TNF $\alpha$  are important for an effective treatment [74, 78]. Thus, growth inhibition of established tumors, necrosis and apoptosis, platelet adherence and therefore destruction of the tumors's vasculature can be achieved. Potentiation of efficacy is possible by combination of TNF $\alpha$  with IFN- $\gamma$ . Another possibility to further increase the cytotoxic effects of TNF $\alpha$  on tumor cells consists of its combination with the chemotherapeutics melphalan or doxorubicin [79]. Representing an effective immunostimulatory cytokine, it is not surprising

that TNF $\alpha$  additionally mediates its anti-tumoral effects by inducing T-cell mediated immunity and stimulated macrophage cytotoxicity against cancer cells [71, 76, 80].

### 1.1.6 Eicosanoids in inflammation and resolution

In addition to cytokines, eicosanoids are a class of mediators extensively involved in processes regulated by the immune system. Eicosanoids are omega-6 polyunsaturated fatty acid (PUFA) derived lipid mediators, including PG, thromboxanes, LTs, hydroperoxyeicosatetraenoic acids (HpETE), hydroxyeicosatetraenoic acids (HETE), and lipoxins. All eicosanoids contribute to the inflammatory occurrence, even though their effects are diverse [81].

#### 1.1.6.1 Key enzymes in eicosanoid formation

Eicosanoids arise from the  $\omega$ -6 PUFA arachidonic acid (AA) which is incorporated into phospholipids of cell membranes and upon stimulation cleaved by phospholipases, predominantly by the cytosolic phospholipase A<sub>2</sub> (cPLA<sub>2</sub>). AA can subsequently be metabolized via two different pathways, the cyclooxygenase (COX) or the lipoxygenase (LO) pathway, both of them using AA as substrate [82].

The integral membrane protein COX, located primarily at the ER and perinuclear regions, exists in two isoforms. COX-1 is constitutively expressed, whereas COX-2 expression is induced by stimulation. Both enzymes are composed of an amino-terminal epidermal growth factor (EGF)-like domain, a membrane-binding domain, and a large catalytic domain, including the heme-binding site at the C-terminal end. The sequence identity of COX-1 and COX-2 is about 60-65%. An important structural difference of both enzymes is the larger active site of COX-2 allowing its specific inhibition by bulky inhibitors [83]. Regulation of enzyme expression and therefore prostanoid formation occurs by transcription elements in the promoter regions of the two COX genes. Here, NF- $\kappa$ B, cAMP-responsive element (CRE) and enhancer box (E-box) are solely present in the COX-2 gene, being involved in the specific regulation of COX-2 mRNA expression [84, 85]. Glucocorticoids, inhibiting prostanoid formation, act partly by suppression of NF- $\kappa$ B dependent transcription [86, 87], whereas non-steroidal anti-inflammatory drugs (NSAIDs) suppress COX-2 NF- $\kappa$ B-independently [83].

5-Lipoxygenase (5-LO) is another key enzyme converting AA into bioactive lipid mediators. It is composed of an amino-terminal "C2-like" domain with binding sites for regulatory factors and a

catalytic domain with the non-heme catalytic iron [88]. 5-LO is, unlike other lipoxygenases, a tightly regulated enzyme and conversion of AA thus controlled by multiple mechanisms.  $\text{Ca}^{2+}$ , phosphatidylcholine (PC), coactosin-like protein (CLP), and adenosine triphosphate (ATP) affect the activity of 5-LO via direct binding [89].  $\text{Ca}^{2+}$  stimulates 5-LO activity, shown *in vitro* by  $\text{Ca}^{2+}$ -mobilizing ionophores as A23187, which results in abundant leukotriene formation [90]. PC is a membrane component and a further stimulating factor for 5-LO activity [91]. It directs the enzyme, especially in presence of  $\text{Ca}^{2+}$ , to the nuclear envelope [92, 93]. The F-actin binding protein CLP stimulates  $\text{Ca}^{2+}$ -induced 5-LO activity and additionally increases stimulatory effects of PC, similarly acting as scaffold for 5-LO [94]. Another 5-LO-stimulating factor with a direct binding site is ATP which is supposed to promote enzyme stability stronger than other nucleotides [95, 96]. An indispensable requirement for substrate conversion by 5-LO is the redox status. Lipidhydroperoxides oxidize the inactive ferrous ( $\text{Fe}^{2+}$ ) form into the active ferric ( $\text{Fe}^{3+}$ ) form. The catalytic iron in the catalytic domain is thus either electron donor or acceptor and holds the enzyme in an active or inactive state. Nevertheless, also external stimuli contribute to the activity of 5-LO. Signaling via the MAPK p38 and ERK1/2 increase leukotriene synthesis by phosphorylation on Ser271 and Ser663, respectively [89]. Phosphorylation on Ser523 by the serine/threonine kinase protein kinase A (PKA) results in an inactivation of 5-LO due to an impaired nuclear import [89, 97]. Even inadequate substrate supply limits leukotriene formation, for instance caused by an impaired functioning of the AA releasing cPLA<sub>2</sub> [98]. Likewise, the 5-LO activating protein (FLAP) is an essential protein of the membrane-associated proteins in eicosanoid and glutathione metabolism (MAPEG) family in intact cells, responsible for the transfer of cleaved AA to the 5-LO. FLAP is crucial for 5-LO product formation as shown by inhibitor studies where leukotriene synthesis is significantly reduced by its inhibition [99].

Apart from 5-LO there are two other lipoxygenases, i.e., 12-LO and 15-LO, both members of the non-heme iron dioxygenase family converting AA into H(p)ETEs. 12-LO is separated into platelet-type and leukocyte-type, both forming 12-HETE [100]. Even 15-LO includes a reticulocyte-type (15-LOX-1) and an epidermis-type (15-LOX-2), converting AA into 15-HETE. The leukocyte-type 12-LO and the reticulocyte-type 15-LO share high sequence conservation, substrate specificity and enzyme kinetics and are therefore often referred to as 12/15-LO [101]. Besides translational and post-translational regulation, 15-LOX-1 can be transcriptionally regulated by the cytokines IL-4 and IL-13, that were found to induce 15-LOX-1 expression in

monocytes [102]. Due to 15-LOX-1 preferring linoleic acid as substrate, its main product is 13-(S)-HODE. 15-LOX-2, different from 15-LOX-1 with respect to its unique tissue distribution and higher substrate specificity for AA leading to 15-HETE [103], is upregulated by inflammation-related IFN- $\gamma$  in human epidermal keratinocytes [104]. Thus, 15-LOX-2 expression predominates in the LPS/INF- $\gamma$  primed M1 macrophage phenotype, whereas the IL-4-related M2 subtype mainly expresses 15-LOX-1 [105]. Both 15-LO subtypes, however, are reported to be tumor suppressing as low expression of 15-LOX-1 is connected to pancreatic carcinogenesis [106] and reduction of 15-LOX-2 expression associated with prostate cancer [107].

#### 1.1.6.2 PGE<sub>2</sub> and other prostanoids

COX-2 is a dual acting enzyme in converting its substrate. In the first step, AA is dioxygenated by the enzyme's COX activity to PGG<sub>2</sub> which is in the second step immediately reduced to PGH<sub>2</sub> by the hydroperoxidase functionality of COX [85]. PGH<sub>2</sub> serves then as starting point for further degradation by specific enzymes to PGE<sub>2</sub>, thromboxane (Tx)A<sub>2</sub>/B<sub>2</sub>, PGD<sub>2</sub>/15d-PGJ<sub>2</sub>, PGF<sub>2 $\alpha$</sub> , and PGI<sub>2</sub>, respectively, which are, except for the conversion to PGF<sub>2 $\alpha$</sub> , nonoxidative reactions [13] (Figure 1.1). PGE<sub>2</sub> can be synthesized by three PGE synthases, namely the inducible microsomal PGE synthase-1, the microsomal PGE synthase-2, and the cytosolic PGE synthase and mediates its effects through the four G-protein coupled receptors (GPCR) EP<sub>1</sub>, EP<sub>2</sub>, EP<sub>3</sub>, and EP<sub>4</sub> [13]. For a long time it has been known to be a key factor in acute inflammation eliciting typical signs of an inflammatory response: vasodilatation and increased vascular permeability are caused by PGE<sub>2</sub> together with other factors like histamine and bradykinin. This results in an increased blood flow into the affected tissue, becoming visible in redness and edemas. By interaction with central sites PGE<sub>2</sub> leads to pain and fever [108]. However, it becomes more and more evident that PGE<sub>2</sub> is further involved in the resolution of inflammation [14, 109, 110]. As shown by Serhan et al. [110] in a collagen-antibody induced arthritis (CAIA) model in mice lacking mPGES-1, reduced PGE<sub>2</sub> levels led to increased disease severity. This is caused by a raise in neutrophil recruitment to the inflamed tissue whereas macrophage recruitment, important for the elimination of apoptotic neutrophils, remains unaffected, therefore supposing a key role for PGE<sub>2</sub> in neutrophil-mediated inflammation. Uptake of dying neutrophils by macrophages further contributes to the inhibition of pro-inflammatory cytokine release by the release of PGE<sub>2</sub> together with platelet activating factor (PAF) and TGF- $\beta$  [111]. Moreover, neutrophil engulfment by macrophages induces the switch of

their eicosanoid profile [112] towards the anti-inflammatory metabolites 15-HETE/lipoxins. Even in neutrophils a phenotypic switch can be induced by PGE<sub>2</sub>, as well as the production of enzymes forming anti-inflammatory and pro-resolving eicosanoids, an event also referred to as “lipid mediator class switching” [113]. In a recent study PGE<sub>2</sub> was shown to mediate anti-inflammatory properties by a pleurisy-resolving effect in rats [114]. Likewise, another report proposed an anti-inflammatory role of COX-2 in pleurisy of rats in the resolution phase, partly due to PGE<sub>2</sub>, but also induced by the COX-2 metabolites PGD<sub>2</sub>/15d-PGJ<sub>2</sub> [25]. Like PGE<sub>2</sub>, PGD<sub>2</sub> mediates pro- and anti-inflammatory effects [115] by its DP<sub>1</sub> and DP<sub>2</sub> GPCRs [108]. PGD<sub>2</sub> promotes the induction of anti-inflammatory enzymes [113], and its dehydration product 15d-PGJ<sub>2</sub> additionally acts regulatory concerning cytokine production and immune cell trafficking, especially via DP<sub>1</sub> [116]. TxA<sub>2</sub> and its stable but less bioactive hydrolysis product TxB<sub>2</sub> bind to the TP receptor, expressed in platelets, endothelial cells, smooth muscles and other cells [117, 118]. There, they mediate vasoconstriction and platelet aggregation [119], explaining their role in cardiovascular diseases (CVD) [120] and atherosclerosis [121]. Whereas platelets with predominant expression of COX-1 are the major source of TxA<sub>2</sub>, also macrophages synthesize abundant amounts of this metabolite, using both, COX-1 and COX-2 for biosynthesis [117]. The role of TxA<sub>2</sub> in tumor development is controversially discussed, as TxA<sub>2</sub> promotes the expression of adhesion molecules on the endothelium [122] and cell migration [123]. But it has both, promoting and inhibiting effects in angiogenesis [123, 124], probably due to the two splice variants of the TP receptor TP $\alpha$  and TP $\beta$  [117]. PGI<sub>2</sub> represents a further metabolite of the COX-pathway, functioning via its IP receptor that acts opposing to TxA<sub>2</sub>: Vasodilation and platelet inhibition are the main effects of PGI<sub>2</sub> [120]. However, PGI<sub>2</sub> is rapidly metabolized non-enzymatically into the inactive 6-keto-PGF<sub>1 $\alpha$</sub> . [118]. PGF<sub>2 $\alpha$</sub>  is formed from PGH<sub>2</sub> by PGF synthases and binds the FP receptor, including two splice variants FP $\alpha$  and FP $\beta$ , thus especially mediating functions in the renal and female reproductive system [118]. Ultimately, mediators formed in the COX-pathway express diverse, sometimes overlapping but partially opposing physiological and pathological effects.

### 1.1.6.3 Lipoxygenase products

5-LO as well as cPLA<sub>2</sub> are soluble enzymes that translocate to the nuclear membrane upon stimulation [125], where they fulfill different functions. The cPLA<sub>2</sub> cleaves AA from phospholipids, which is transferred by FLAP to the 5-LO [126]. The 5-LO converts AA in a two-

step reaction, where it holds two different enzyme functions (Figure 1.1). By its dioxygenase activity oxygen is inserted into AA leading to 5-HpETE. This first reaction is common for all lipoxygenases, except for the position of oxygen insertion which occurs at the carbon for which the lipoxygenase is named: C-5, C-12, or C-15. The second function is unique for 5-LO and consists in an LTA<sub>4</sub> synthase activity. By this, 5-HpETE is transformed into the unstable epoxide LTA<sub>4</sub>, which is either hydrolyzed to LTB<sub>4</sub> or converted by the LTC<sub>4</sub>-synthase to the cysteinyl LTs (cysLT), including LTC<sub>4</sub>, LTD<sub>4</sub>, and LTE<sub>4</sub> [127]. Alternatively, non-enzymatic hydrolysis of LTA<sub>4</sub> into LTB<sub>4</sub>-isomeric DiHETEs [128] or transformation into the two stereoisomers trans-LTB<sub>4</sub> and epi/trans-LTB<sub>4</sub> are possible [129]. Glutathione peroxidases convert 5-HpETE into the corresponding alcohol 5-HETE [127]. LTB<sub>4</sub> is a potent chemotactic agent for neutrophils, enabling their adhesion to the endothelium, extravasation, and degranulation causing the release of toxic mediators. It furthermore activates cells of the immune system such as monocytes/macrophages and lymphocytes. These effects are attributable to LTB<sub>4</sub> binding to its GPCRs BLT<sub>1</sub> and BLT<sub>2</sub> [130]. Even the peroxisome proliferator-activated receptor (PPAR) $\alpha$  was found to be activated by LTB<sub>4</sub>, though mediating anti-inflammatory effects [131]. The cysLTs, also called slow-reacting substances of anaphylaxis (SRS-A), mediate smooth muscle contraction of the airways and vascular permeability by their CysLT<sub>1</sub> and CysLT<sub>2</sub> receptors, playing a huge role in diseases of the respiratory system like asthma [132, 133]. Apart from 5-LO there is 12-LO producing 12-H(p)ETE and 15-LO forming 15-(S)-H(p)ETE. 15-(S)-HETE acts as precursor for the production of the trihydroxytetraenes lipoxin (Lx)A<sub>4</sub> and LxB<sub>4</sub> [134] via the intermediate epoxytetraene, a reaction catalyzed by 5-LO [135]. Two other pathways are known to yield lipoxins in a transcellular manner. The first route uses leukocyte 5-LO to form LTA<sub>4</sub>, which is transformed by platelet-type 12-LO, owning a lipoxin synthase activity, into LxA<sub>4</sub>/B<sub>4</sub>. In a second pathway, aspirin provoked acetylation of COX-2 results in the synthesis of 15-(R)-HETE leading to 15-epi-lipoxins by 5-LO activity [135, 136]. Contrarily to the products of 5-LO that predominantly mediate pro-inflammatory events, 15-LO products possess several counterbalancing effects which contribute to limit the inflammatory response and to initiate the resolution phase [12]. 15-HETE inhibits neutrophil adhesion to endothelial cells and transmigration processes due to its esterification into neutrophil phospholipids, mainly into phosphatidylinositol (PI) involved in signal transduction processes. Thus, 15-HETE can furthermore act as stored precursor for lipoxin formation. Remodeling of neutrophil phospholipids

by 15-HETE causes affinity reduction of  $\text{LTB}_4$  to its receptors and impairs the production of second messengers. Interaction of neutrophils with endothelial membranes is thus disturbed and

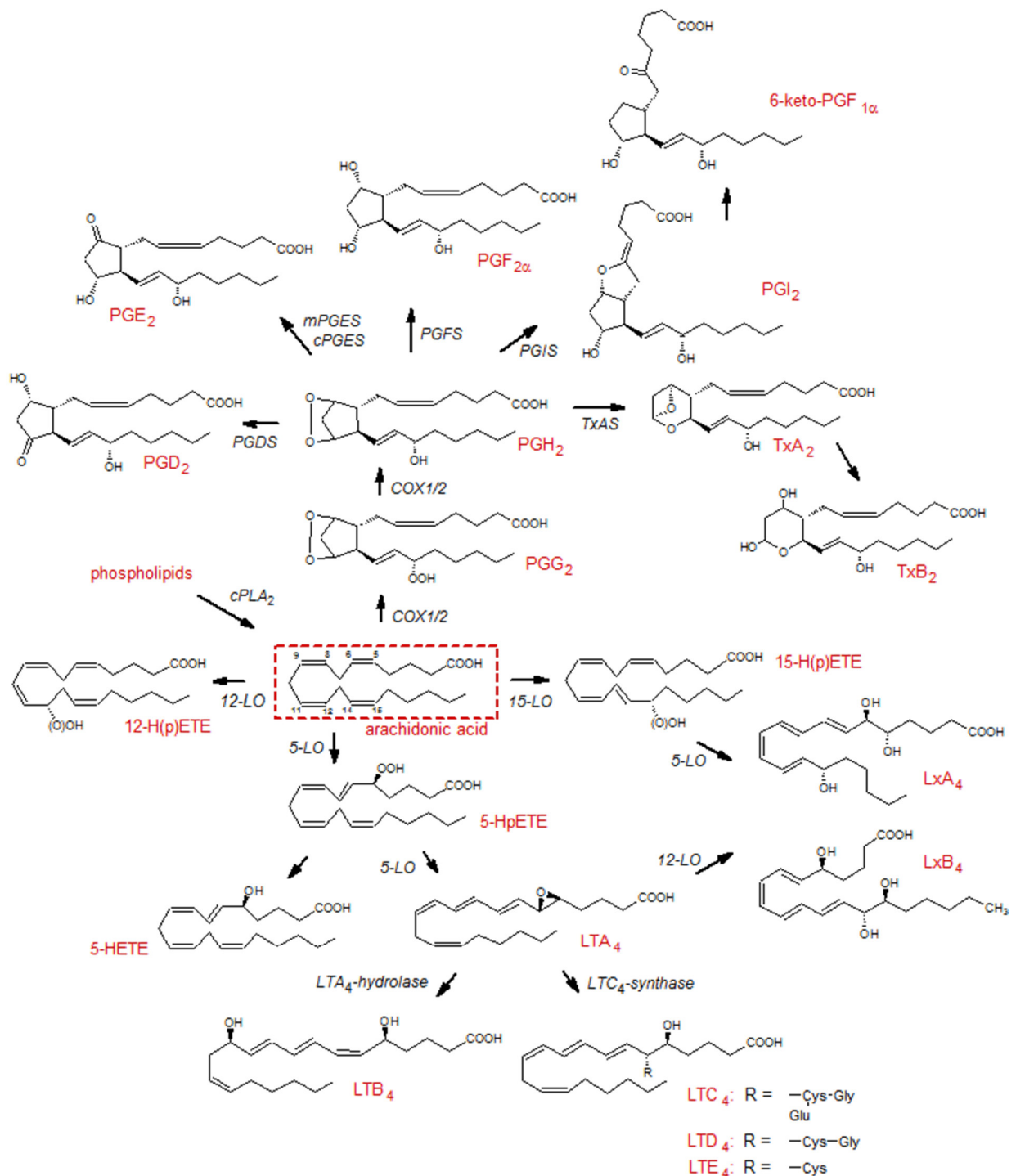


**Figure 1.1: Eicosanoid biosynthesis.** AA is starting point for both, COX-pathway (upper half) and LOX-pathway (lower half). Prostaglandins, prostacyclin, and thromboxanes are formed by two COX-catalyzed steps resulting in  $\text{PGG}_2$  and  $\text{PGH}_2$ , respectively, followed by the activity of several specific synthases. Stereospecificity of the different LOX lead to H(p)ETEs, leukotrienes, and lipoxins.

might limit the neutrophil mediated inflammatory response [137, 138]. Lipoxins, belonging to the anti-inflammatory eicosanoids as well, interact with inflammation promoting properties of neutrophils, for instance by inhibiting leukotriene induced vascular permeability [139]. Additionally, they impair neutrophil recruitment and infiltration [24]. Instead, mononuclear cells are recruited by lipoxins to enable tissue repair [140] and phagocytosis of apoptotic neutrophils by macrophages [141, 142]. Thus, some LO products play key roles in inducing inflammation but others in initiating the resolution phase.

## **1.2 Macrophages**

Macrophages derive from haematopoietic stem cells (HSC) in the bone marrow, therefore belonging to the mononuclear phagocyte system (MPS), which further consists of blood monocytes, DC and the myeloid progenitor cells [143]. The bone marrow progenitors develop stepwise to monoblasts, pro-monocytes and monocytes before they are released into the blood stream, where they circulate or differentiate into macrophages by migration into tissues [144]. Macrophages are found in nearly all tissues [145]. The heterogeneity of blood monocytes due to their developmental state, and the tissue, entered by monocytes and providing different microenvironmental conditions, determine the development of different macrophage phenotypes [146]. Consequently, these distinct macrophage populations possess diverse functions, which reflects their ability to adapt in their physiological roles to the microenvironment, a property also known as macrophage plasticity. Host defense, wound healing and immune regulation are the three main features connected to macrophage functions [144]. Macrophages are prominent phagocytic cells and clearing the tissue from cell debris or apoptotic cells is vital for the host. However, whereas an immune response is absent in the case of phagocytosis of senescent cells occurring in a healthy state, the elimination of cells that have undergone necrosis is detected by macrophages due to necrosis-related danger signals, resulting in a change of macrophage physiology and therefore in the production and release of pro-inflammatory mediators. Thus, the innate immune response is activated [147]. Due to the recognition of such danger signals by PRRs as TLR on macrophages [148], these cells are one of the first immune cells detecting possible threats for the host and initiating countermeasures.

### 1.2.1 M1 and M2 polarization

Due to their marked plasticity, macrophages are able to polarize into specific phenotypes dependent on the microenvironmental conditions which demand distinct macrophage functions. The polarization state of M1 and M2 represents two opposing phenotypes, so called according to the T helper ( $T_H$ )1/ $T_H$ 2 classification and their distinct communication with macrophages [149]. M1 respond to stimuli originating from an IL-12-mediated  $T_H$ 1 response, such as IFN- $\gamma$ , or to microbial products, such as LPS. These stimuli lead to the classically activated macrophages [150] (Figure 1.2). M1 possess several characteristics which discriminate them from the M2 polarized macrophages. M1 are a source of pro-inflammatory cytokines, including TNF $\alpha$ , IL-1 $\beta$ , IL-6, IL-12, IL-15, and IL-18 [151, 152], as well as of chemokines (CCL15, CCL20, CXCL9, CXCL10, CXCL11) to regulate immune cell recruitment, especially of DC, neutral killer cells (NK), and T-cells [7, 144]. Elevated expression of major histocompatibility complex (MHC)-II antigens and CD80/CD86 as costimulatory factors, enabling the M1 for an efficient antigen presentation [151, 153, 154], enhanced endocytic functions, and the ability to effectively kill intracellular pathogens [151], are further specific qualities. The latter is attributable to the synthesis of ROS and NO by the inducible NO synthase (iNOS) [155], itself triggered by increased TNF $\alpha$  levels [152], as well as to the acidification of the phagosome and the impairment of nutrient provision for microorganisms [156]. By communication with T- and B-cells, M1 are strongly involved in triggering the immune response [150] and exhibit potential to destroy tumor cells [157].

M2, representing a more heterogeneous group than M1, are supposed to be subdivided dependent on the stimulus [150]: Whereas M2b are generated by stimulation with Fc $\gamma$  receptors plus a TLR stimulus, M2c are obtained in presence of glucocorticoids, IL-10 or TGF- $\beta$ . Alternatively activated macrophages, or M2a, are triggered by the  $T_H$ 2 cytokines IL-4 or IL-13, according to their cell-cell interaction. Characteristic properties of M2a are the upregulation of the mannose receptor (CD206) [158] and other C-type lectins [150] as well as scavenger receptors as CD163 [159], participating in hemoglobin clearance, adhesion to endothelial cells, and tissue regeneration [160]. M2a have an anti-inflammatory cytokine profile, including IL-10 and TGF- $\beta$ , whereas M1-related cytokines are downregulated [151]. Chemokines from M2a (CCL5, CCL16, CCL17, CCL18, CCL22, CCL24) recruit eosinophils, basophils and  $T_H$ 2 cells [7, 144, 150]. Besides other intracellular enzymes, arginase 1 is upregulated [159], leading, contrarily to M1 producing NO by

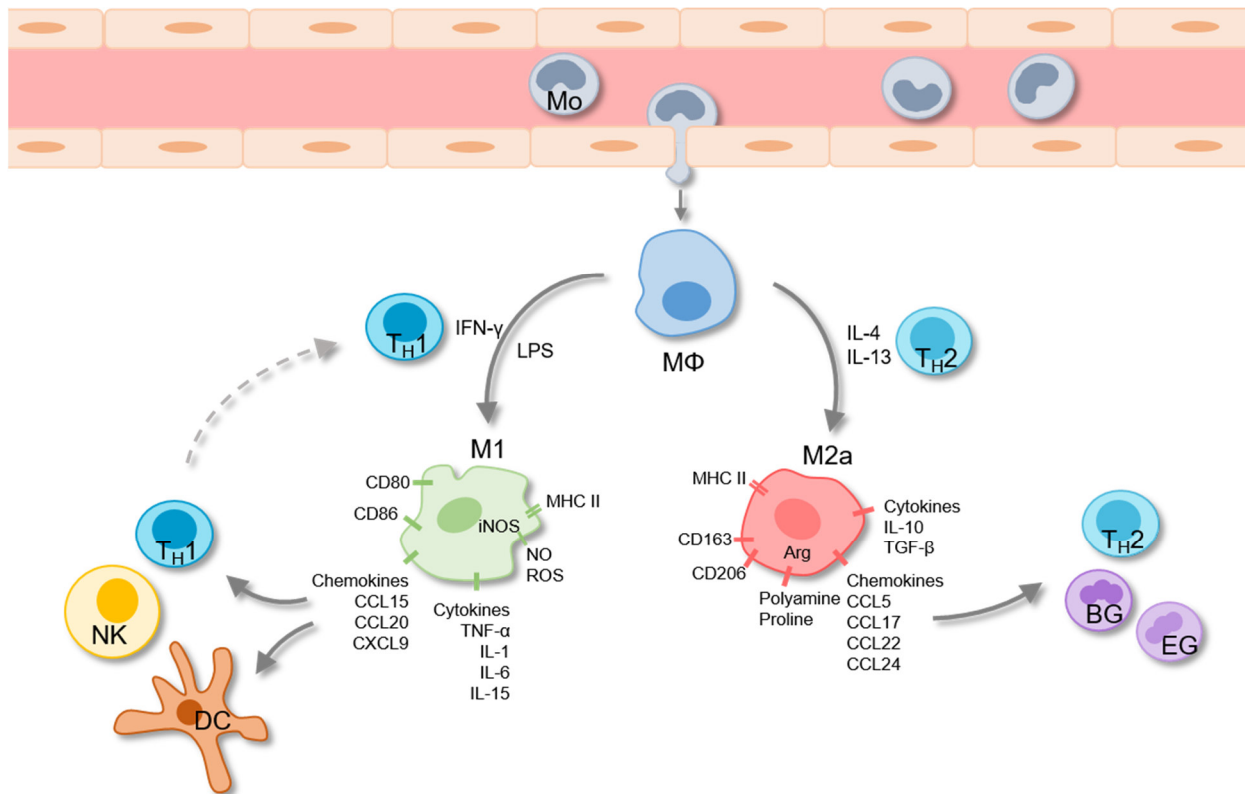


**Figure 1.2: Macrophage differentiation and polarization.** In presence of M-CSF, LPS, and the  $T_H1$ -cytokine IFN- $\gamma$ , monocytes differentiate and polarize into M1 which are characterized by high microbicidal and immune stimulating activity and potent tumor cell cytotoxicity. Contrarily, M2a develop in presence of M-CSF and the  $T_H2$ -cytokines IL-4 or IL-13. They possess anti-inflammatory and scavenging properties, enable tissue repair and promote tumor progression. Mo, monocytes;  $M\Phi$ , unpolarized macrophages; NK, neutral killer cells; DC, dendritic cells; BG, basophil granulocytes; EG, eosinophil granulocytes.

the arginine pathway, to the production of polyamine and proline implicated in cell growth and proliferation, collagen formation and tissue repair [161]. M2 are furthermore involved in tumor initiation, progression, and metastasis, due to malignant cells exploiting the M2 functions in favor of their own development [162].

### 1.2.2 Role of M1 and M2 in cancer occurrence

The role of macrophages in cancer is crucial but multifaceted due to their implication in tumor progression and metastasis [163] as “alternative activated” M2 on the one hand and the ability of M1 to eliminate tumor cells and metastases on the other [164]. However, both phenotypes cannot be separated completely regarding tumor development, since a phenotypic switch is central especially in inflammation-related cancer. Regarding different phases of tumor establishment, the

M1 phenotype may facilitate initiation and promotion [165], if the conditions of a chronic inflammation are present [163] or host immune reactivity remains unresolved [29]. Pro-inflammatory mediators, originally produced by M1 as a result of the immune response for microbial killing, facilitate the formation of mutations by oxygen and nitrogen species reacting with the DNA of epithelial cells [166] and even accumulation of mutations by the inhibition of the tumor suppressor p53 [167]. The cellular alterations lead to changes in the cellular cytokine expression profile [168]. Consequently, on the way to malignancy, the tumor affects the macrophage phenotype, educating it from M1 towards M2 [165], since the M1 related gene expression profile is obstructive or even destructive for the tumor's growth in this stage. The quantity of tumor-associated macrophages exhibiting an M2 phenotype in the tumor microenvironment is visible in many types of cancer, often correlated with poor prognosis [169]. Recruitment of M2 to the tumor occurs by colony-stimulating factor (CSF)-1, able to promote malignancy by facilitating infiltration and behavior of TAMs and therefore metastasis [170]. CSF-1 upregulates the expression of vascular endothelial growth factor (VEGF) in macrophages, which attracts those as well, and plays a key role in vascularization and angiogenic processes. Angiogenesis is an important feature for solid tumors concerning growth and metastasis, enabling the tumor's nourishment and therefore survival. Apart from VEGF, there are some more factors expressed by M2, directly or indirectly promoting angiogenesis, proliferation and viability, including hypoxia, hypoxia inducible factor (HIF)2 $\alpha$  [171], HIF1 $\alpha$ , and IL-1 [172], as well as several growth factors [173]. By suppression of immune functions, namely antigen presentation, DC maturation or cytotoxic activities, the tumor ensures its survival [173-175]. Inhibition of NF- $\kappa$ B signaling, therefore decreasing the levels of iNOS, TNF $\alpha$  and other cytokines represent such an immune modulating mechanism by promoting the M2 immune suppressing phenotype [176]. In fact, the tumor exploits physiological functions of M2 such as tissue repair, release of anti-inflammatory cytokines and growth factors, as well as immune-suppression, and redirects them for the own survival and progression. Nevertheless, the cytokines present in the microenvironment secreted during infection, inflammation, and immunity can likewise act as inhibitors of tumor development and progression [168], recruiting and activating immune cells and initiating an effective immune response against the malignant cells. Accordingly, the detection of tumor cells by the innate and adaptive immune system through recognition of antigens present on cancer cells [168, 177] is crucial for the coordinated activation of elimination mechanisms by M1, DC, NK cells, T- and B-cells; a mechanism also known as cancer immunosurveillance [178]. In fact, intra-

tumoral lymphocyte infiltrates have been linked to decreased metastasis and increased patient survival [179], whereas lymphocyte absence leads to higher tumor susceptibility [180]. Furthermore, IFN- $\gamma$ , released from T-cells and M1, functions anti-tumoral, whereas deficiencies in IFN- $\gamma$  or the IFN- $\gamma$  receptor result in deregulated target-cell growth and apoptosis, increased angiogenesis, and impaired upregulation of MHC I expression in the tumor [180-182]. Moreover, IFN- $\gamma$  has been shown to initiate a phenotypic switch from immunosuppressive M2 like TAMs into the immunostimulatory M1 phenotype, able to induce CD4<sup>+</sup> T-cell proliferation, CD8<sup>+</sup> T-cell cytotoxicity, accompanied by the reduction of pro-tumoral TAM mediators [183]. Initiating the phenotypic switch from M2 to M1, preventing the reverse case in the early phase of tumor development, as well as inhibiting monocytes/macrophages to develop towards M2 are promising concepts of anti-cancer therapy [157]. This is due to M1 being potent effector cells against cancer [184] by direct elimination through TNF $\alpha$  and NO as the main mediators [177]. Different methods targeting the immune cell function have been reported, all of them resulting in an induction of anti-tumoral immune responses [157]: Inhibition of STAT6 [185] or STAT3 [186] results in enhanced immune cell function and reduced tumor growth and metastasis. Inhibition of the TAM-related stress protein legumain leads to a CD8<sup>+</sup> T-cell mediated TAM reduction in the tumor microenvironment [187]. Src homology 2-containing inositol phosphatase-1 (SHIP1) expression was found to prevent M2 skewing [188], whereas conversely, treatment with the TLR9 ligand CpG combined with an IL-10 receptor antibody promotes the phenotypic switch from M2 to M1, triggering DC maturation and an anti-tumoral immune response [184, 189]. Restoring the host's immunity is additionally beneficial for anti-cancer immunotherapies, supporting their efficiency by recovered antigen presenting functions of immune cells [190].

## 1.3 Vacuolar-type H<sup>+</sup> -ATPase

### 1.3.1 Structure and function

The vacuolar H<sup>+</sup> -ATPases (v-ATPase) act as ATP driven proton pumps to acidify intracellular organelles and maintain pH homeostasis in all eukaryotic cells [191]. Operating by a rotary mechanism similar to other ATPases like the well-characterized F-ATPase [192], the v-ATPase was first identified as such in 1983 [193, 194]. The v-ATPase is composed of an ATP-hydrolytic domain (V<sub>1</sub>), oriented to the cytoplasmic membrane side, and a membrane-embedded proton-

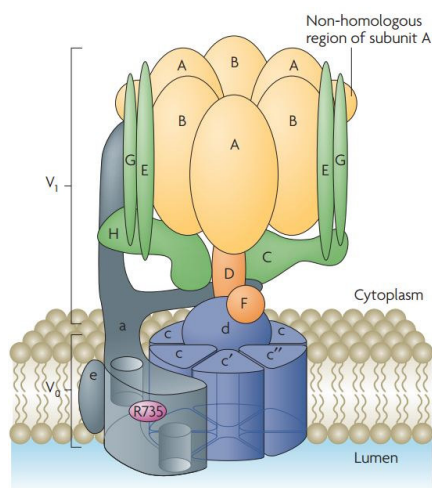


**Figure 1.3: Structure of the v-ATPase.** The activity of the v-ATPase depends on the assembly of two main domains, the peripheral and ATP hydrolyzing  $V_1$  domain, including the subunits A, B (yellow), D, F (orange), and the N-terminal part of a (grey), and the integral  $V_0$  domain, containing the subunits a, e (grey), c, c', c'', and d (blue). Subunits D, F, and d form the central stalk, which connects  $V_1$  to  $V_0$  and acts as a rotor by coupling the energy from ATP hydrolysis to the rotation of the proteolipid ring formed by the three c subunits. Subunits C, E, G, and H (green) have a stator function during rotation and proton translocation [1]. Reprinted by permission from Macmillan Publishers Ltd: *Nature Reviews Molecular Cell Biology* 8, 917-929 copyright 2007.

translocating domain ( $V_0$ ) (Figure 1.3).  $V_1$  contains eight subunits (A-H), where A and B, forming a hexamer, are responsible for ATP binding and hydrolysis, D and F belong to the central stalk that connects the  $V_1$  and  $V_0$  domain, and C, E, G, and H form the peripheral stalk.  $V_0$  consists of six proteolipid subunits (a, c, c', c'', d, e). Subunit d completes the central stalk, whereas subunit a is attributed to the peripheral stalk [1]. The three different c-subunits are hydrophobic proteins, arranged to a ring [195] that forms together with D, F, and d the rotary component of the pump, hereby causing an active proton transport. The peripheral stalk functions as a stator that fixes the ATP hydrolyzing hexamer and subunit a in their positions during rotation [1] (Figure 1.3).

Regulatory mechanisms include the reversible dissociation and assembly of the  $V_1$  and  $V_0$  domain, where subunit d is implicated due to its connective position between the rotary  $V_0$  ring and the central stalk of  $V_1$ . Furthermore, the regulation of efficiency of coupling the proton transport with ATP hydrolysis as well as the control of cellular localization and membrane expression of v-ATPase belong to these mechanisms [1]. In some cells, including macrophages, the v-ATPase is located at the membrane of intracellular compartments (such as lysosomes, endosomes, vacuoles, secretory granules, Golgi) and additionally at the plasma membrane [196]. Due to the diversity of effects that protons can have on many proteins concerning their charge, stability, or conformation, the concentration of protons (pH) in cellular compartments is of particular importance and explains the variety of v-ATPase functions [197]. The proton pumping enzyme contributes to cellular processes such as membrane trafficking, protein degradation [198], bone resorption [199], sperm maturation [200], renal acidification [2], receptor-mediated endocytosis, prohormone processing and uptake/transport of small molecules [1].

### 1.3.2 Inhibition of the v-ATPase by myxobacterial compounds

Implicated in such a variety of cellular processes, a malfunction of v-ATPase leads to the disturbance of several vital cell functions and therefore to diseases. An interference with the v-ATPase might thus be a possible intervention for the treatment of such diseases. In this field, bacteria were once found to be a source of metabolites able to selectively inhibit the v-ATPase, while other ATPases remain largely unaffected by these compounds. The first natural product in this context, named bafilomycin, was isolated in 1984 from *Streptomyces griseus* [201], a species belonging to the order actinomycetales that are aerobic and Gram-positive actinobacteria [202]. Bafilomycin was shown to have cytotoxic activity against fungi, yeast, and Gram-positive bacteria [201]. Bowman et al. [203] identified bafilomycin, a 16-membered lactone ring (Figure 1.4), as first and relatively specific inhibitor of the v-ATPase with an activity in the nanomolar range. The binding site of this plecomacrolide is supposed to be at the c subunit of the v-ATPase [204]. Later, also myxobacteria that have a very distinct secondary metabolism, were found to produce biologically active natural products inhibiting the v-ATPase [205]. Myxobacteria are Gram-negative  $\delta$ -proteobacteria [205], strictly aerobic and with relatively large rod-shaped cells. They live typically in soil but also related habitats [206]. The apicularens, isolated from the myxobacteria *Chondromyces robustus* in 1998 by Kunze et al [207] and also produced by other myxobacteria species, were structurally identified as 10-membered macrolactone with a highly unsaturated enamide side chain [208] (Figure 1.4). These compounds are inactive against Gram-negative and Gram-positive bacteria, as well as against several yeasts and fungi [207], but have cytotoxic activity in the nanomolar range against several human cancer cell lines [209]. Structurally related to the benzolactone enamides, the apicularens are v-ATPase inhibiting agents [210] with their binding site at the interface of subunit a and c of the v-ATPase [211]. Another group of myxobacterial products are the archazolids, isolated from *Archangium gephyra*, as the fourth group of compounds detected in these strains [4, 212]. The compounds have potent cytotoxic activity in the low nanomolar range against different cell lines [213]. Structurally characteristic for the archazolids is the 24-membered macrolactone ring with a thiazole side chain [212, 214] (Figure 1.4). Archazolid possesses high potency against isolated v-ATPase and does not influence F-ATPase or  $\text{Na}^+/\text{K}^+$ -ATPase by binding to the c subunit [210]. Today,

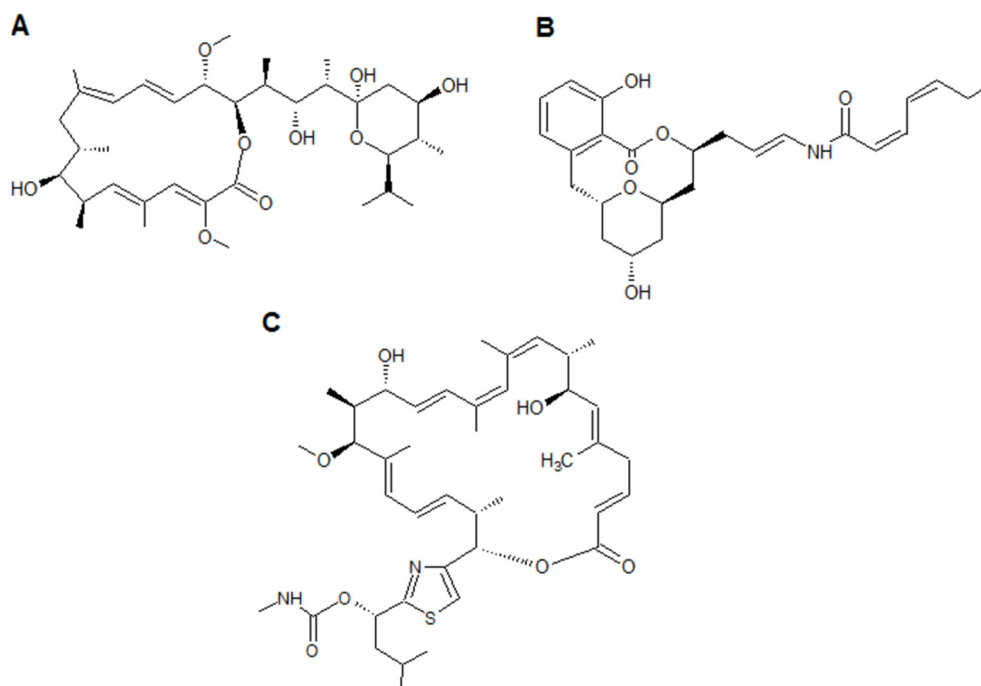


**Figure 1.4:** Chemical structure of bafilomycin A1 (A), apicularen A (B), and archazolid B (C)

bafilomycin A1, apicularen A, and archazolid B, used for the experiments in this thesis, are accessible by total chemical synthesis [208, 215-217].

### 1.3.3 Role of the v-ATPase in disease

Due to its broad physiological contributions, the v-ATPase is involved in several pathological processes. For example, the v-ATPase is implicated in the entry of several viruses and toxins by acidic compartments into cells, when low pH mediates fusion of endosomal and microbial membrane, thus releasing the pathogen's mRNA into the cytoplasm [218]. Deregulation of the v-ATPase due to genetic defects in the  $\alpha 4$  or B1 subunit can cause distal renal tubule acidosis by a dysfunction of the v-ATPase to secrete protons from the cytoplasm of intercalated cells into the lumen of the tubule [2]. Furthermore, osteoclasts need the  $H^+$ -pumping v-ATPase for bone resorption during bone remodeling. Genetic defects of the v-ATPase  $\alpha 3$  subunit followed by deficient proton provision lead to osteopetrosis [219]. Moreover, the v-ATPase is extensively involved in tumor promotion. Many types of cancer have been shown to overexpress v-ATPase [220, 221] since elevated cytoplasmic pH promotes tumor cell growth whereas low pH in the extracellular environment facilitates invasiveness of cancer cells [222]. An acidic tumor

environment increases the release and activity of lysosomal proteolytic enzymes such as cathepsins and the activation of matrix metalloproteinases (MMP), responsible for the degradation of the extracellular matrix that is a requirement for a tumor to metastasize [223]. Accordingly, it has been shown by Sennoune et al that highly metastatic cancer cell lines have a higher expression of plasma membrane v-ATPase compared to poorly metastatic cell lines [221]. Metastatic activity could be further decreased by treatment with the v-ATPase inhibitor archazolid [223]. The marked expression of the v-ATPase at the plasma membrane is also important for microvascular endothelial cells involved in angiogenesis because too acidic environment impairs the migratory activity of these cells, which use the v-ATPase to regulate their cytosolic pH [224]. Exposure of normal cells to a persistent acidic environment usually induces apoptosis but tumor cells exploit an acidic pH for the survival mechanisms described above. Due to the common ability of cancer cells to circumvent apoptosis, the induction of programmed cell death of tumor cells by v-ATPase inhibition is a useful strategy to reduce tumor growth [5, 225, 226]. The use of v-ATPase inhibitors has also been beneficial in drug-resistant tumor cells that overexpress this proton pump [220, 225, 227].

## **2 AIM OF THE THESIS**

Persistent inflammatory processes have been identified to increase the risk for the development of solid tumors [29]. One of the main properties of the tumor microenvironment is an acidic pH for optimal activity of many tumor promoting factors, maintained by the activity of an overexpressed v-ATPase, pumping protons into cellular organelles and the extracellular space [228]. By specific inhibition of the v-ATPase, the myxobacterial compound archazolid B exhibits potent cytotoxic activity against several cancer cell lines [5, 222, 229]. However, only little is known about the effects of v-ATPase inhibitors on primary human cells, even though this constitutes a stringently required knowledge with respect to the treatment of cancer patients. Since the v-ATPase supports various vital physiological processes, it is important to investigate if v-ATPase inhibition impairs the viability of primary human cells. Immune cells, representing an essential part of the innate and adaptive immune system, are important effectors in cancer immunosurveillance [230, 231]. Nevertheless, immune cells possess different faces in regard to cancer development depending on the stimuli they are exposed to [230]. The polarization of macrophages into M1 and M2 represents such an opposing phenotypic development, since M1 exhibit cancer cell cytotoxicity while M2 which predominate in tumor infiltrates (TAM) promote malignant cell growth [157]. Concerning inflammation-related cancer, several key elements have been identified to contribute to cancer occurrence in a multifaceted manner [26]. On this basis, it was the aim of this study to investigate whether or not archazolid B affects human monocyte-derived macrophages and if the polarization state of macrophages is of importance in this connection. Regarding this, the focus of investigation was on some of the reported key functionalities as enzyme regulation, cytokine release and transcription factor expression. It was further of relevance to reveal the biochemical mechanisms underlying the interference of archazolid B with these key factors.

## 3 MATERIALS AND METHODS

### 3.1 Materials

#### Chemicals

---

|                                    |   |
|------------------------------------|---|
| [ <sup>3</sup> H]-arachidonic acid | BIOTREND Chemikalien GmbH, Köln, Germany            |
| Acetic acid                        | Carl Roth GmbH + Co. KG, Karlsruhe, Germany         |
| Acetonitrile                       | Thermo Fisher Scientific Inc., MA                   |
| Ammonium chloride                  | Carl Roth GmbH + Co. KG, Karlsruhe, Germany         |
| Arachidonic acid                   | Cayman Chemical, MI                                 |
| BCECF-AM                           | Life Technologies/Thermo Fisher Scientific Inc., MA |
| Biotase                            | Biochrom GmbH, Berlin, Germany                      |
| Bromphenol blue                    | Merck KGaA, Darmstadt, Germany                      |
| BSA                                | Applichem GmbH, Darmstadt, Germany                  |
| BSA, fatty acid free               | Sigma-Aldrich Inc., Deisenhofen, Germany            |
| Ca <sup>2+</sup> -Ionophor A23187  | Cayman Chemical, MI                                 |
| CaCl <sub>2</sub>                  | Applichem GmbH, Darmstadt, Germany                  |
| D'PBS                              | SERVA Electrophoresis GmbH, Heidelberg, Germany     |
| DAPI                               | Sigma-Aldrich Inc., Deisenhofen, Germany            |
| DCFH-DA                            | Sigma-Aldrich Inc., Deisenhofen, Germany            |
| Dextran                            | Sigma-Aldrich Inc., Deisenhofen, Germany            |
| DMEM (high glucose)                | Biochrom GmbH, Berlin, Germany                      |
| DMSO                               | Merck KGaA, Darmstadt, Germany                      |
| EDTA                               | Applichem GmbH, Darmstadt, Germany                  |
| FCS                                | PAA/GE Healthcare Europe GmbH, Freiburg, Germany    |
| FITC                               | Thermo Fisher Scientific Inc., MA                   |
| FITC-dextran                       | Sigma-Aldrich Inc., Deisenhofen, Germany            |
| Formic acid                        | Sigma-Aldrich Inc., Deisenhofen, Germany            |
| Glucose                            | Applichem GmbH, Darmstadt, Germany                  |
| Glycerole                          | Caesar & Loretz GmbH, Hilden, Germany               |
| Glycine                            | Carl Roth GmbH + Co. KG, Karlsruhe, Germany         |
| HBSS                               | Life Technologies/Thermo Fisher Scientific Inc., MA |
| HCl                                | Grüssing GmbH, Filsum, Germany                      |
| HEPES                              | Thermo Fisher Scientific Inc., MA                   |
| Human serum                        | Lonza Group AG, Basel, Switzerland                  |
| IFN- $\gamma$                      | PeproTech GmbH, Hamburg, Germany                    |
| IL-4                               | PeproTech GmbH, Hamburg, Germany                    |

|   |   |
|---|---|
| KCl   | Carl Roth GmbH + Co. KG, Karlsruhe, Germany         |
| KH <sub>2</sub> PO <sub>4</sub>               | Sigma-Aldrich Inc., Deisenhofen, Germany            |
| Leupeptin                                     | Sigma-Aldrich Inc., Deisenhofen, Germany            |
| L-glutamine                                   | Biochrom GmbH, Berlin, Germany                      |
| Low fat powdered milk                         | Carl Roth GmbH + Co. KG, Karlsruhe, Germany         |
| LPS   | Sigma-Aldrich Inc., Deisenhofen, Germany            |
| LSC fluid Rotiszint® eco plus                 | Carl Roth GmbH + Co. KG, Karlsruhe, Germany         |
| LSM 1077                                      | PAA/GE Healthcare Europe GmbH, Freiburg, Germany    |
| LysoTracker Red DND-99                        | Life Technologies/Thermo Fisher Scientific Inc., MA |
| Methanol HPLC grade                           | Merck KGaA, Darmstadt, Germany                      |
| MgCl <sub>2</sub>                             | Merck KGaA, Darmstadt, Germany                      |
| MgSO <sub>4</sub>                             | Applichem GmbH, Darmstadt, Germany                  |
| Mowiol  | Life Technologies/Thermo Fisher Scientific Inc., MA |
| MTT   | Sigma-Aldrich Inc., Deisenhofen, Germany            |
| Na <sub>2</sub> HCO <sub>3</sub>              | Applichem GmbH, Darmstadt, Germany                  |
| Na <sub>3</sub> VO <sub>4</sub>               | Applichem GmbH, Darmstadt, Germany                  |
| Na <sub>4</sub> P <sub>2</sub> O <sub>7</sub> | Sigma-Aldrich Inc., Deisenhofen, Germany            |
| NaCl  | Carl Roth GmbH + Co. KG, Karlsruhe, Germany         |
| NaF   | Applichem GmbH, Darmstadt, Germany                  |
| NaH <sub>2</sub> PO <sub>4</sub>              | Sigma-Aldrich Inc., Deisenhofen, Germany            |
| Nigericin                                     | Enzo Life Sciences Inc., NY                         |
| Non-immune goat serum                         | Life Technologies/Thermo Fisher Scientific Inc., MA |
| Nonidet P40                                   | Applichem GmbH, Darmstadt, Germany                  |
| n-propyl gallate                              | Sigma-Aldrich Inc., Deisenhofen, Germany            |
| Paraformaldehyde                              | Carl Roth GmbH + Co. KG, Karlsruhe, Germany         |
| Penicillin-streptomycin solution              | Biochrom GmbH, Berlin, Germany                      |
| peqGOLD IV protein marker                     | peqLab Biotechnology GmbH, Erlangen, Germany        |
| PGB <sub>1</sub>                              | Biomol GmbH, Hamburg, Germany                       |
| PMSF  | Sigma-Aldrich Inc., Deisenhofen, Germany            |
| Ponceau                                       | Sigma-Aldrich Inc., Deisenhofen, Germany            |
| rhM-CSF                                       | Cell Guidance Systems Ltd, Cambridge, UK            |
| RPMI 1640                                     | Sigma-Aldrich Inc., Deisenhofen, Germany            |
| SDS   | Carl Roth GmbH + Co. KG, Karlsruhe, Germany         |
| Staurosporine                                 | Merck KGaA, Darmstadt, Germany                      |
| STI   | Sigma-Aldrich Inc., Deisenhofen, Germany            |
| sucrose                                       | Applichem GmbH, Darmstadt, Germany                  |
| Thiomersal                                    | Sigma-Aldrich Inc., Deisenhofen, Germany            |

|                       |   |
|-----------------------|---|
| Trifluoro acetic acid | Applichem GmbH, Darmstadt, Germany          |
| Tris                  | Carl Roth GmbH + Co. KG, Karlsruhe, Germany |
| TritonX100            | Carl Roth GmbH + Co. KG, Karlsruhe, Germany |
| Trypan blue           | Sigma-Aldrich Inc., Deisenhofen, Germany    |
| Trypsin-EDTA          | Thermo Fisher Scientific Inc., MA           |
| Tween®20              | Carl Roth GmbH + Co. KG, Karlsruhe, Germany |
| Zymosan A             | Sigma-Aldrich Inc., Deisenhofen, Germany    |
| β-glycerophosphate    | Sigma-Aldrich Inc., Deisenhofen, Germany    |
| β-mercaptoethanol     | Carl Roth GmbH + Co. KG, Karlsruhe, Germany |

### Compounds

---

|                   |  |
|-------------------|--|
| Actinomycin D     | Cayman Chemical, MI  |
| Ammonium chloride | Carl Roth GmbH + Co. KG, Karlsruhe, Germany                            |
| Apicularen A      | Prof. Menche, Rheinische Friedrich-Wilhelms-Universität, Bonn, Germany |
| Archazolid B      | Prof. Menche, Rheinische Friedrich-Wilhelms-Universität, Bonn, Germany |
| Bafilomycin A1    | Sigma-Aldrich Inc., Deisenhofen, Germany                               |
| BWA4C             | Sigma-Aldrich Inc., Deisenhofen, Germany                               |
| Chloroquine       | Sigma-Aldrich Inc., Deisenhofen, Germany                               |
| Cytochalasin B    | Enzo Life Sciences Inc., NY  |
| Dexamethasone     | Sigma-Aldrich Inc., Deisenhofen, Germany                               |
| DPI               | Sigma-Aldrich Inc., Deisenhofen, Germany                               |
| Indometacin       | Sigma-Aldrich Inc., Deisenhofen, Germany                               |
| LY294002          | BIOZOL Diagnostica Vertrieb GmbH, Eching, Germany                      |
| Parthenolide      | Sigma-Aldrich Inc., Deisenhofen, Germany                               |
| RSC-3388          | Merck KGaA, Darmstadt, Germany   |
| SB203580          | Enzo Life Sciences Inc., NY  |
| SP600125          | Enzo Life Sciences Inc., NY  |
| U0126             | Enzo Life Sciences Inc., NY  |

### Primer

---

|                             |   |
|-----------------------------|---|
| B2M (forward and reverse)   | TIB MOLBIOL Syntheselabor GmbH, Berlin, Germany |
| COX-2 (forward and reverse) | TIB MOLBIOL Syntheselabor GmbH, Berlin, Germany |
| IL-1β (forward and reverse) | TIB MOLBIOL Syntheselabor GmbH, Berlin, Germany |
| TNFα (forward and reverse)  | TIB MOLBIOL Syntheselabor GmbH, Berlin, Germany |

**Primary antibodies**


---

|                                  |   |
|----------------------------------|---|
| ATP6V0A2                         | Abcam plc, Cambridge, UK                                      |
| $\beta$ -actin                   | Santa Cruz Biotechnology Inc., Heidelberg, Germany            |
| COX-2                            | Enzo Life Sciences Inc., NY                                   |
| GAPDH                            | Santa Cruz Biotechnology, Heidelberg, Germany                 |
| FLAP                             | Abcam plc, Cambridge, UK                                      |
| 5-LO                             | Prof. Steinhilber, Goethe University, Frankfurt/Main, Germany |
| I $\kappa$ B $\alpha$            | Cell Signaling Technology Inc., MA                            |
| phosphorylated I $\kappa$ B      | Cell Signaling Technology Inc., MA                            |
| NF- $\kappa$ B p65               | Cell Signaling Technology Inc., MA                            |
| phosphorylated NF $\kappa$ B p65 | Cell Signaling Technology Inc., MA                            |
| Akt                              | Cell Signaling Technology Inc., MA                            |
| phosphorylated Akt               | Cell Signaling Technology Inc., MA                            |
| MEK1/2                           | Cell Signaling Technology Inc., MA                            |
| phosphorylated MEK1/2            | Cell Signaling Technology Inc., MA                            |
| phosphorylated MEK3/6            | Cell Signaling Technology Inc., MA                            |
| p38                              | Cell Signaling Technology Inc., MA                            |
| phosphorylated p38               | Cell Signaling Technology Inc., MA                            |
| p44/42                           | Cell Signaling Technology Inc., MA                            |
| phosphorylated p44/42            | Cell Signaling Technology Inc., MA                            |
| phosphorylated SAPK/JNK          | Cell Signaling Technology Inc., MA                            |
| phosphorylated STAT1             | Cell Signaling Technology Inc., MA                            |
| phosphorylated STAT3             | Cell Signaling Technology Inc., MA                            |

**Secondary antibodies**


---

|  |   |
|--|---|
| Alexa Fluor® 488<br>goat anti-rabbit IgG | Life Technologies/Thermo Fisher Scientific Inc., MA |
| Alexa Fluor® 555<br>goat anti-mouse IgG  | Life Technologies/Thermo Fisher Scientific Inc., MA |
| IRDye 800CW                              | LI-COR Biosciences Inc., Bad Homburg, Germany       |
| IRDye 680LT                              | LI-COR Biosciences Inc., Bad Homburg, Germany       |

**Antibodies for ELISA**


---

|                              |  |
|------------------------------|--|
| Capture/detection antibodies | R&D Systems GmbH, Wiesbaden-Nordenstadt, Germany |
|------------------------------|--|

**Consumables**

---

|                          |   |
|--------------------------|---|
| Clean-Up® C18 columns    | United Chemical Technologies Inc., PA                 |
| Glass bottom dishes      | MatTek Corporation, MA                                |
| Glass coverslips         | Carl Roth GmbH + Co. KG, Karlsruhe, Germany           |
| Microscope slides        | Carl Roth GmbH + Co. KG, Karlsruhe, Germany           |
| Nitrocellulose membranes | Amersham/GE Healthcare Europe GmbH, Freiburg, Germany |

## 3.2 Methods

### 3.2.1 Cell isolation and cell culture

#### 3.2.1.1 Monocyte isolation from leukocyte concentrates

Leukocyte concentrates from peripheral blood of healthy female human donors without an anti-inflammatory medication for the last ten days were obtained from the Institute of Transfusion Medicine, University Hospital Jena, and prepared by centrifugation ( $4000 \times g$ , 20 min, 20 °C). Buffy coat cell isolation was achieved by dextran sedimentation (5% dextran from *Leukonostoc* spp. ( $M_r = 500,000$  g/mol) (w/v) in dulbecco's phosphate buffered saline (D'PBS)) at room temperature. Different cell fractions from buffy coats were obtained by density centrifugation at  $400 \times g/10$  min/20 °C on lymphocyte separation medium (LSM) 1077 without brake (Heraeus Multifuge X3R Centrifuge, Thermo Scientific, MA). Peripheral blood mononuclear cells (PBMC), containing monocytes, T-, and B-lymphocytes, were isolated by two further centrifugation steps at  $150 \times g/10$  min/4 °C and were resuspended in ice-cold D'PBS. Monocytes from PBMC fraction were isolated by adherence to culture flasks ( $2 \times 10^7$  cells/mL RPMI 1640 medium supplemented with 10% (v/v) heat-inactivated fetal calf serum (FCS), L-glutamine (2 mM), penicillin (100 U/mL), and streptomycin (100 µg/mL)) for 1 h at 37 °C/5% CO<sub>2</sub> as described [232].

#### 3.2.1.2 Macrophage differentiation and polarization

For differentiation towards macrophages freshly isolated monocytes were incubated in RPMI 1640 (supplemented with 5% (v/v) FCS, L-glutamine (2 mM), penicillin (100 U/mL), and streptomycin (100 µg/mL)) and recombinant human macrophage colony stimulating factor (rhM-CSF) (25 ng/mL) for 6 d as reported [233]. After 6 d incubation unpolarized macrophages were activated and polarized by supplementing the medium for further 24 h with either LPS (100 ng/mL) alone or in combination with recombinant human IFN- $\gamma$  (100 ng/mL) for M1 polarized macrophages or with recombinant human IL-4 (20 ng/mL) for M2 polarized macrophages [150, 233].

#### 3.2.1.3 MDA-MB-231

MDA-MB-231 cells (human gland/breast epithelial cancer cell line) were cultured in Dulbecco's modified eagle medium (DMEM) supplemented with 10% (v/v) heat-inactivated FCS, penicillin

(100 U/mL), and streptomycin (100 µg/mL) at 37 °C/5% CO<sub>2</sub>. Cells were detached by trypsin-EDTA for 10 min at 37 °C/5% CO<sub>2</sub> three times per week, resuspended in DMEM and seeded at a concentration of  $0.15 \times 10^6$ /mL at 37°C/5% CO<sub>2</sub>.

### 3.2.2 Determination of cell viability

The viability of macrophages and MDA-MB-231 cells was assessed by 3-(4,5-dimethylthiazol-2-yl)-2,5-diphenyltetrazolium bromide (MTT) assay as described [234]. Thus, cells were resuspended in the appropriate medium and seeded into 96 well plates ( $10^6$ /mL; 100 µL/well) for 1 h at 37 °C/5% CO<sub>2</sub>. Cells were then preincubated with compounds or vehicle (0.3% DMSO) for 30 min, MDA-MB-231 stimulated with LPS (100 ng/mL) and macrophages with LPS (100 ng/mL) with or without IFN- $\gamma$  (100 ng/mL), with IL-4 (20 ng/mL), or left untreated for 24 h and 48 h, respectively, at 37 °C/5% CO<sub>2</sub>. MDA-MB-231 were additionally incubated with cell culture supernatants of macrophages which had been treated with archazolid at indicated concentrations or vehicle (DMSO) before (in detail described in 3.2.7). MTT (5 mg/mL) was added, cells were further incubated for four hours until blue formazan crystals due to reduction of MTT by viable cells were visible, and lysed in a sodium dodecyl sulfate (SDS)-lysis buffer (10% (w/v) SDS, HCl (20 mM); pH 4.5) with shaking at room temperature in the dark. After 20 h absorption was measured at 570 nm with a microplate reader (Thermo Fisher Scientific Inc., MA).

Exclusion of trypan blue was used to control cell viability of macrophages after differentiation. Thus, the macrophage suspension was added to a trypan blue solution and cells counted by a Vi-cell counter (Beckman Coulter GmbH, Krefeld, Germany). Successful plasma membrane destruction after sonification for cell homogenates was visualized by exclusion of trypan blue as well.

### 3.2.3 Analysis of vesicular pH

The pH measurements were performed as reported [235] and sodium buffer (NaCl (135 mM), KCl (5 mM), CaCl<sub>2</sub> (1 mM), MgSO<sub>4</sub> (1 mM), KH<sub>2</sub>PO<sub>4</sub> (2 mM), glucose (5 mM), HEPES (6 mM)) and potassium buffer ((NaCl (10 mM), KCl (130 mM), CaCl<sub>2</sub> (1 mM), MgSO<sub>4</sub> (1 mM), NaH<sub>2</sub>PO<sub>4</sub> (2 mM), glucose (5 mM), HEPES (6 mM)) were used as described [236]. For measurements of vesicular pH, monocytes ( $10^6$ /mL) were differentiated into macrophages. At day 6, macrophages were incubated with fluorescein isothiocyanate (FITC)-labelled dextran (0.5 mg/mL; 70,000 Da)

for 1 h at 37°/5% CO<sub>2</sub>. Cells were washed with D'PBS, preincubated with compounds or vehicle (0.1% DMSO) for 30 min and stimulated with LPS (100 ng/mL) for 24 h at 37 °C/5% CO<sub>2</sub>. The pH values were calculated from the ratio of fluorescence intensities at the excitation wavelengths of 480 nm and 450 nm and emission at 520 nm, measured with a NOVOstar microplate reader (BMG Labtech, Ortenberg, Germany). In situ fluorescence calibration was performed with the ionophore nigericin (10 μM) in potassium buffer at pH values between 4.5 and 7.5.

Imaging of FITC-dextran uptake was performed with macrophages ( $0.25 \times 10^6$ /mL) seeded onto glass bottom dishes and apart from that as described for analysis of vesicular pH. After washing, uptake of FITC-dextran into acidic organelles was imaged using an Axio Observer.Z1 inverted microscope and a LCI Plan-Neofluar 63x/1.3 Imm Corr DIC M27 objective (Carl Zeiss, Jena, Germany).

For imaging of acidic organelles by LysoTracker staining, macrophages ( $0.25 \times 10^6$ /mL) were resuspended in RPMI 1640 without phenol red and plated onto glass bottom dishes. After adherence, cells were treated with compounds or vehicle (0.1% DMSO) for 30 min and stimulated with LPS (100 ng/mL) for 24 h. Macrophages were then stained with a fluorescent LysoTracker dye (50 nM) for 1 h. After washing, red fluorescence of the protonated and accumulated probe in acidic cell organelles was imaged microscopically (Axio Observer.Z1, LCI Plan-Neofluar 63x/1.3 Imm Corr DIC M27 objective; Carl Zeiss, Jena, Germany).

### 3.2.4 Investigation of phagocytic activity

For determination of phagocytic activity, opsonized zymosan was prepared as reported [237]. Briefly, zymosan (20 mg/mL) was pre-treated by heating in a boiling water bath for 20 min, sonificated (SFX250, Branson, CT), washed and resuspended in Hank's balanced salt solution (HBSS) buffer. Opsonization was obtained by incubation with human serum (65% (v/v)) at a concentration of 20 mg/mL for 60 min at 37 °C. For assessing phagocytosis in living cells, macrophages ( $0.25 \times 10^6$ /mL) were resuspended in HBSS and plated onto glass bottom dishes. After adherence, cells were pre-treated with compounds or vehicle (0.1% DMSO) for 30 min and stimulated with LPS (100 ng/mL) for 24 h. Phagocytosis was started by adding the particle suspension (1 mg/mL) at 37 °C/5% CO<sub>2</sub> and microscopic live cell imaging was started immediately (see 3.2.6).

### 3.2.5 Immunofluorescence microscopy

Macrophages ( $0.25 \times 10^6/\text{mL}$ ) were resuspended in RPMI 1640 (supplemented with 5% (v/v) FCS, L-glutamine (2 mM), penicillin (100 U/mL), and streptomycin (100  $\mu\text{g}/\text{mL}$ )), seeded in 12 well plates containing glass coverslips and incubated for 1 h at 37 °C/5% CO<sub>2</sub> to ensure cell attachment. For immunofluorescence analysis of v-ATPase, macrophages were pre-incubated with compounds or vehicle (0.1% DMSO) for 30 min and stimulated with LPS (100 ng/mL), LPS (100 ng/mL)/IFN- $\gamma$  (100 ng/mL) for M1, or with IL-4 (20 ng/mL) for M2 for 24 h at 37 °C/5% CO<sub>2</sub>. For microscopic analysis of I $\kappa$ B and NF- $\kappa$ B, macrophages were pre-incubated with compounds or vehicle for 16 h and stimulated with LPS (100 ng/mL) for 15 min at 37 °C/5% CO<sub>2</sub>. Cells were fixed with paraformaldehyde (PFA) solution (4% (w/v)) and autofluorescence of free formaldehyde was quenched with ammonium chloride (50 mM). For visualization of 5-LO translocation and FLAP co-localization, macrophages were pre-incubated with compounds or vehicle for 16 h and stimulated with Ca<sup>2+</sup>-ionophore A23187 (2.5  $\mu\text{M}$ ) for 3 min. Cells were fixed with ice-cold methanol (100%) for 20 min at -20 °C. Permeabilization was achieved by treatment with Triton X-100 (0.2% (v/v)). After blocking with non-immune goat serum (10% (v/v)), samples were incubated with antibodies over night at 4 °C as indicated (Table 3.1). The samples were extensively washed and then stained with the fluorophore-labeled secondary antibodies Alexa Fluor 488 goat anti-rabbit IgG (1:500) and Alexa Fluor 555 goat anti-mouse IgG (1:500) for 10 min at room temperature in the dark. DNA was stained using 4',6-diamidino-2-phenylindole (DAPI) (0.7  $\mu\text{g}/\text{mL}$ ) for 3 min at room temperature. Samples were placed on microscope slides using Mowiol containing n-propyl gallate (0.25%). The slides were stored at 4 °C in the dark until microscopic analysis.

**Table 3.1: Primary antibodies for immunofluorescence.** Antibodies were diluted with BSA (5% (w/v)) in sterile PBS

| <b>antibody</b>       | <b>source</b>      | <b>dilution</b> |
|-----------------------|--------------------|-----------------|
| I $\kappa$ B $\alpha$ | mouse, monoclonal  | 1:125           |
| NF- $\kappa$ B p65    | rabbit, monoclonal | 1:100           |
| 5-LO                  | mouse, monoclonal  | 1:100           |
| FLAP                  | rabbit, polyclonal | 1:150           |
| ATP6V0A2              | rabbit, polyclonal | 1:250           |

The fluorescence was visualized with an Axio Observer.Z1 inverted microscope and a LCI Plan-Neofluar 63x/1.3 Imm Corr DIC M27 objective. Images were taken with an AxioCam MR3 camera and acquisition was done with AxioVision 4.8 software (All components Carl Zeiss, Jena, Germany).

### 3.2.6 Live cell imaging

For imaging of living cells, macrophages ( $0.25 \times 10^6/\text{mL}$ ) were resuspended in RPMI without phenol red and plated into glass bottom dishes. After treatments, macrophages were imaged at 37 °C/5% CO<sub>2</sub> using the incubator unit XLmulti S1 including the heater unit XL S1 and the CO<sub>2</sub> module S1 for the Axio Observer.Z1 inverted microscope and a Plan-Apochromat 40x/1,3 Oil DIC M27 objective or a LCI Plan-Neofluar 63x/1.3 Imm Corr DIC M27 objective. If necessary, definite focus for Axio Observer.Z1 was used for focussing macrophages automatically over a pre-set timespan. Images were taken with an AxioCam MR3 camera and acquisition was done with AxioVision 4.8 software.

### 3.2.7 Determination of extracellular cytokine levels

Monocytes ( $10^6/\text{mL}$ ), resuspended in RPMI 1640 (supplemented with 5% (v/v) FCS, L-glutamine (2 mM), penicillin (100 U/mL), and streptomycin (100 µg/mL)), were plated into 24-well plates and incubated for 1-2 hours before rhM-CSF (25 ng/mL) was added, and cells further incubated for 6 d at 37 °C/5% CO<sub>2</sub>. At day 6, unpolarized macrophages were pre-incubated with compounds or vehicle for 30 min and polarized with LPS (100 ng/mL) alone or with INF-γ (100 ng/mL) for M1 or with IL-4 (20 ng/mL) for M2 at 37 °C/5% CO<sub>2</sub>. After 24 h, supernatants were collected, centrifuged ( $400 \times g/10 \text{ min}/4 \text{ °C}$ ) (Centrifuge 5424 R, Eppendorf, Hamburg, Germany), and stored at -20 °C. Cytokines (IL-1β, IL-6, IL-8, IL-10, TNFα, MCP-1) in supernatants were analyzed by in-house made ELISA.

### 3.2.8 Determination of extracellular PGE<sub>2</sub> levels

Supernatants of macrophages were obtained as described in 3.2.7. PGE<sub>2</sub> was either analyzed by a commercially available ELISA kit (Biotrend Chemikalien GmbH, Köln, Germany) or by ultra

performance liquid chromatography (UPLC)-coupled ESI tandem mass spectrometry (MS/MS) as described in chapter 3.2.11.

### 3.2.9 Determination of eicosanoid release

Monocytes ( $1.5 \times 10^6$ /mL) were resuspended in RPMI 1640 (supplemented with 5% (v/v) FCS, L-glutamine (2 mM), penicillin (100 U/mL), and streptomycin (100  $\mu$ g/mL)), plated into 12-well plates and incubated with rhM-CSF (25 ng/mL) for 6 days at 37 °C/5%CO<sub>2</sub> to obtain differentiated macrophages. For long-term incubations (24 h), macrophages were pre-incubated with compounds or vehicle (0.1% DMSO) for 30 min and then stimulated with either LPS (100 ng/mL), LPS (100 ng/mL)/IFN- $\gamma$  (100 ng/mL) for M1, or IL-4 (20 ng/mL) for M2 for 24 h at 37 °C/5% CO<sub>2</sub>. Then, eicosanoid formation was stimulated by addition of Ca<sup>2+</sup>-ionophore A23187 (2.5  $\mu$ M) for 10 min at 37 °C and cells were placed on ice to stop the reaction. For analysis of effects of compounds on short-term prostanoid formation (30 min), macrophages were stimulated with LPS (100 ng/mL) or LPS (100 ng/mL)/IFN- $\gamma$  (100 ng/mL) for 24 h at 37 °C/5% CO<sub>2</sub>. Fresh RPMI 1640 (supplemented with 0.5% (v/v) FCS, L-glutamine (2 mM), penicillin (100 U/mL), and streptomycin (100  $\mu$ g/mL)) was added and cells incubated for 30 min at 37 °C/5% CO<sub>2</sub> before they were pre-incubated with compounds or vehicle (0.1% DMSO) for 15 min at 37 °C and subsequently stimulated with Ca<sup>2+</sup>-ionophore A23187 (2.5  $\mu$ M) plus AA (5  $\mu$ M) for 30 min at 37 °C to induce product formation. Incubations were terminated by placing the cells on ice. HCl (30  $\mu$ L/mL; 1 M) for protonation of lipid mediators and PGB<sub>1</sub> (60 ng) as internal standard was added before samples were extracted by solid phase extraction (SPE) (3.2.10).

### 3.2.10 Solid phase extraction

For the preparation of the samples for eicosanoid analysis, the samples were centrifuged ( $400 \times g/10 \text{ min}/4 \text{ }^\circ\text{C}$ ) and transferred to C18 SPE columns, which were conditioned before with 1 mL methanol (100%) and 1 mL water. Samples were washed twice with 0.5 mL water and eluted with 300  $\mu$ L methanol (100%). After centrifugation ( $15,000 \times g/5 \text{ min}/4 \text{ }^\circ\text{C}$ ) eicosanoids were analyzed by UPLC-MS/MS analysis as described in chapter 3.2.11.

### 3.2.11 UPLC-MS/MS analysis

UPLC-MS/MS analysis was performed with an Acquity UPLC BEH C18 column (1.7  $\mu\text{m}$ , 2.1  $\times$  50 mm, Waters, Milford, MA) using an Acquity<sup>TM</sup> UPLC system (Waters, Milford, MA). Chromatography was performed at a flow rate of 0.8 mL/min and a column temperature of 45 °C. The solvents for the mobile phase were water/acetonitrile (90/10; A) and acetonitrile (B) both acidified with 0.07% (v/v) formic acid. Isocratic elution at A/B = 70/30 was performed for 2 min and followed by a linear gradient to A/B = 30/70 within 5 min. The chromatography system was coupled to a QTRAP 5500 mass spectrometer (AB Sciex, Darmstadt, Germany) equipped with a Turbo V<sup>TM</sup> source and electrospray ionization (ESI) probe. Eicosanoid identification is based on the detection of specific fragment ions (listed in Table 3.2) through multiple reaction monitoring (MRM) using the negative ion mode in combination with retention times.

**Table 3.2: metabolite fragment ions and conditions used in MRM.** Q1, first quadrupole; Q3, third quadrupole; CE, collision energy

| metabolite                                | transition I |          |         | transition II |          |         | retention time [min] |
|---|--------------|----------|---------|---------------|----------|---------|----------------------|
|   | Q1 [m/z]     | Q3 [m/z] | CE [eV] | Q1 [m/z]      | Q3 [m/z] | CE [eV] |                      |
| <b>PGB<sub>1</sub></b>                    | 335          | 113      | -31     | 335           | 221      | -28     | 1,69                 |
| <b>PGE<sub>2</sub></b>                    | 351          | 189      | -22     | 351           | 271      | -20     | 0,62                 |
| <b>TxB<sub>2</sub></b>                    | 369          | 195      | -18     | 369           | 169      | -25     | 0,45                 |
| <b>12-HHT</b>                             | 279          | 163      | -30     | -             | -        | -       | 3,30                 |
| <b>11-HETE</b>                            | 319          | 167      | -21     | -             | -        | -       | 4,70                 |
| <b>PGF<sub>2<math>\alpha</math></sub></b> | 353          | 193      | -35     | -             | -        | -       | 0,56                 |
| <b>LTB<sub>4</sub></b>                    | 335          | 129      | -26     | 335           | 195      | -22     | 2,68                 |
| <b>Epi/trans LTB<sub>4</sub></b>          | 335          | 195      | -22     | -             | -        | -       | 2,58                 |
| <b>5-HETE</b>                             | 319          | 115      | -20     | 319           | 203      | -20     | 5,04                 |
| <b>12-HETE</b>                            | 319          | 179      | -18     | -             | -        | -       | 4,81                 |
| <b>15-HETE</b>                            | 319          | 219      | -18     | -             | -        | -       | 4,54                 |
| <b>5-HETrE</b>                            | 321          | 115      | -19     | -             | -        | -       | 5,71                 |
| <b>5-HEPE</b>                             | 317          | 115      | -17     | -             | -        | -       | 4,37                 |

Parameters were set as follows: The ion spray voltage was -4500 V, the heater temperature 500 °C, the declustering potential -30 to -120 eV, the entrance potential -5 to -10 eV, the cell exit potential -11 to -17 eV, the curtain gas pressure 35 psi, the nebulizer gas pressure 50 psi, the Turbo

V gas pressure 80 psi. Analyst 1.6 software (AB Sciex, Darmstadt, Germany) was used for automatic peak integration using IntelliQuan default settings. Data were normalized on the internal standard PGB<sub>1</sub>, and are given as relative intensities.

### 3.2.12 Determination of kinase activation, STAT1/3- and IκB phosphorylation, and NF-κB activity

Monocytes ( $2 \times 10^6$ /mL) were resuspended in RPMI 1640 (supplemented with 5% (v/v) FCS, L-glutamine (2 mM), penicillin (100 U/mL), and streptomycin (100 μg/mL)), and incubated with rhM-CSF (25 ng/mL) for 6 d at 37 °C/5% CO<sub>2</sub>. After differentiation, macrophages were first starved for 6 h (AKT, ERK, p38, MEK1/2, SAPK/JNK, MEK3/6) or directly pre-incubated (NFκB, IκB, STAT1, STAT3) with compounds or vehicle (0.1% DMSO) for 16 h at 37 °C/5% CO<sub>2</sub>. 5% (v/v) FCS was added to starved cells prior to stimulation with LPS (100 ng/mL) for 15 min. After stimulation, macrophages were immediately placed on ice, washed once with D'PBS and lysed as described in 3.2.15. Lysates were finally used for protein separation by SDS-PAGE and subsequent Western blot analysis as described in 3.2.16.

### 3.2.13 Determination of v-ATPase, COX-2, and 5-LO expression

Monocytes ( $2 \times 10^6$ /mL) were resuspended in RPMI 1640 (supplemented with 5% (v/v) FCS, L-glutamine (2 mM), penicillin (100 U/mL), and streptomycin (100 μg/mL)), and differentiated with rhM-CSF (25 ng/mL) for 6 d at 37 °C/5% CO<sub>2</sub>. Macrophages were pre-incubated with compounds or vehicle (0.1% DMSO) for 30 min and activated with LPS (100ng/mL), LPS (100 ng/mL) plus INF-γ (100 ng/mL) or IL-4 (20 ng/mL) for 24 h at 37 °C/5% CO<sub>2</sub>. Then, cells were immediately placed on ice, washed once with D'PBS and lysed as described in 3.2.15 before they were used for protein separation by SDS-PAGE and subsequent Western blot analysis (3.2.16).

### 3.2.14 Subcellular fractionation

Monocytes ( $2 \times 10^6$ /mL) were resuspended in RPMI 1640 (supplemented with 5% (v/v) FCS, L-glutamine (2 mM), penicillin (100 U/mL), and streptomycin (100 μg/mL)), and differentiated with rhM-CSF (25 ng/mL) for 6 d at 37 °C/5% CO<sub>2</sub>. Macrophages were pre-treated with compounds for 30 min at 37 °C/5% CO<sub>2</sub> and stimulated with LPS (100 ng/mL) for 24 h. Cells were detached

with biotase, collected by centrifugation ( $400 \times g/10 \text{ min}/4 \text{ }^\circ\text{C}$ ), and lysed with 200  $\mu\text{L}$  TKM buffer (Tris (50 mM), sucrose (250 mM), KCl (25 mM),  $\text{MgCl}_2$  (5 mM), EDTA (1 mM), and freshly added leupeptin hemisulfate salt (10  $\mu\text{g}/\text{mL}$ ), trypsin inhibitor from soybean (STI) (60  $\mu\text{g}/\text{mL}$ ), phenylmethylsulfonyl fluoride (PMSF) (1 mM)) with subsequent sonification (output 3, cycle 10%, 10 cycles) (SFX250, Branson, CT) on ice. Cell disruption was checked microscopically by trypan blue exclusion. Except for 20  $\mu\text{L}$  which were saved for Western blot analysis, the total lysate was centrifuged at  $13,000 \times g/15 \text{ min}/4 \text{ }^\circ\text{C}$ . The supernatant contained the cytoplasmic fraction (S13), the pellet was lysed in 200  $\mu\text{L}$  TKM buffer yielding the P13 fraction, representing the nucleus, rough ER, DNA. The P13 lysate was transferred into ultracentrifuge tubes and centrifuged at  $100,000 \times g/1.5 \text{ h}/4 \text{ }^\circ\text{C}$  (LE-80 ultracentrifuge, Beckman Coulter, Krefeld, Germany). The pellet was again lysed in 200  $\mu\text{L}$  TKM buffer and sonicated until solubilization. 10  $\mu\text{L}$  of each fraction was retained for determination of protein concentration by a protein assay (Bio-Rad Laboratories, CA). To each fraction 4  $\times$  loading buffer (Tris/HCl (40 mM) pH 8, EDTA (4 mM), 10% (w/v) SDS, 10% (v/v)  $\beta$ -mercaptoethanol) and bromphenol blue (0.05% (w/v) in 50% (v/v) glycerol) was added and the samples boiled for 5 min at  $96 \text{ }^\circ\text{C}$ . The samples were collected by centrifugation and stored at  $-20 \text{ }^\circ\text{C}$  before protein separation by SDS-PAGE and Western blotting for v-ATPase (3.2.16).

### 3.2.15 Generation of whole cell lysates for Western blot

Macrophages were lysed with a NP-40 lysis buffer (1% (v/v) NP-40, sodium vanadate (1 mM), sodium fluoride (10 mM), sodium pyrophosphate (5 mM),  $\beta$ -glycerophosphate (25 mM), EDTA (5 mM), and freshly added leupeptin hemisulfate salt (10  $\mu\text{g}/\text{mL}$ ), STI (60  $\mu\text{g}/\text{mL}$ ), PMSF (1 mM) in Tris-buffered saline (TBS: Tris/HCl (50 mM), NaCl (100 mM)); pH 7.4) for 30 min on ice with occasional vortexing. Lysates were centrifuged ( $10,000 \times g/4 \text{ }^\circ\text{C}/5 \text{ min}$ ) and protein concentration in the supernatants were determined using a Protein Assay (Bio-Rad Laboratories, CA). After addition of 4  $\times$  SDS loading buffer (Tris/HCl (50 mM; pH 6.8), SDS (2% (w/v)), glycerol (10% (v/v)),  $\beta$ -mercaptoethanol (1% (v/v)), EDTA (12.5 mM), bromphenol blue (0.02% (w/v))), samples were boiled for 5 min at  $96 \text{ }^\circ\text{C}$ , lysates collected by centrifugation and stored at  $-20 \text{ }^\circ\text{C}$  before protein separation by SDS-PAGE (3.2.16).

### 3.2.16 SDS-PAGE and Western blot

Proteins from cell lysates were separated by vertical SDS-polyacrylamide gel electrophoresis (SDS-PAGE) using a Mini-Protean electrophoresis system (Mini-PROTEAN® Tetra Cell, Bio-Rad Laboratories Inc., Hercules, CA) and a running buffer (glycine (192 mM), Tris (25 mM), SDS (3.5 mM)). The applied pre-stained marker peqGOLD allowed to analyze proteins in the range of 10 to 170 kDa. Proteins were transferred from polyacrylamide gels on nitrocellulose membranes (Amersham Biosciences, Little Chalfont, UK) with a tank blotting method (Mini Trans-Blot® cell and PowerPac™ Basic power supply, Bio-Rad Laboratories Inc., Hercules, CA) in transfer buffer (glycine (39 mM), Tris (48 mM), 20% (v/v) methanol) at 90 V for 90 min. Protein transfer was controlled by Ponceau staining (5% (w/v) Ponceau S in 5% (v/v) acetic acid). Membranes were washed, blocked with 5% (w/v) BSA or 5% (w/v) low fat powdered milk in TBS-Tween (TBS, 0.1% (v/v) Tween®20) for 1 h at room temperature and incubated with primary antibodies (Table 3.3) overnight at 4 °C. Membranes were washed twice in TBS-Tween and incubated with fluorescently-labeled secondary antibodies IRDye 800CW (dilution 1:10,000) and IRDye 680LT (dilution 1:80,000) for 1 h at room temperature in the dark. Membranes were washed again twice in TBS-Tween and further twice in TBS before drying for 30 min at 37 °C in the dark. Proteins were detected using the Odyssey Infrared Imaging System (LI-COR Biosciences, Bad Homburg, Germany) and analyzed with the Odyssey application software.

**Table 3.3: Primary antibodies used for Western blot analysis.** Antibodies were diluted in 5% BSA/TBS-Tween or 5% low fat powdered milk in TBS-Tween.

| <b>antibody (and phosphorylation site)</b> | <b>source</b>      | <b>dilution</b> |
|--|--------------------|-----------------|
| IκBα                                       | mouse, monoclonal  | 1:1000          |
| phospho-IκBα (Ser32)                       | rabbit, monoclonal | 1:500           |
| NF-κB p65                                  | rabbit, monoclonal | 1:500           |
| phospho-NF-κB p65 (Ser536)                 | mouse, monoclonal  | 1:500           |
| phospho-STAT1 (Tyr701)                     | rabbit, polyclonal | 1:1000          |
| phospho-STAT3 (Tyr705)                     | rabbit, monoclonal | 1:1000          |
| MEK1/2                                     | rabbit, polyclonal | 1:1000          |
| phospho-MEK1/2 (Ser217/221)                | rabbit, polyclonal | 1:1000          |
| p44/42 (ERK1/2)                            | rabbit, polyclonal | 1:1000          |
| phospho-p44/42 (ERK1/2) (Thr202/Tyr204)    | mouse, monoclonal  | 1:1000          |

**Table 3.3 (continued): Primary antibodies used for Western blot analysis.**

| <b>antibody (and phosphorylation site)</b> | <b>source</b>      | <b>dilution</b> |
|--|--------------------|-----------------|
| phospho-MEK3/6 (Ser189) (Ser207)           | rabbit, monoclonal | 1:1000          |
| p38  | rabbit, monoclonal | 1:1000          |
| phospho-p38 (Thr180/Tyr182)                | rabbit, polyclonal | 1:1000          |
| phospho-SAPK/JNK (Thr183/Tyr185)           | mouse, monoclonal  | 1:1000          |
| AKT  | mouse, monoclonal  | 1:1000          |
| phospho-AKT (Ser473)                       | rabbit, polyclonal | 1:1000          |
| GAPDH                                      | mouse, monoclonal  | 1:1000          |
| $\beta$ -actin                             | mouse, monoclonal  | 1:1000          |

### 3.2.17 Generation of cell homogenates

To generate cell homogenates, macrophages ( $10^6/\text{mL}$ ) were resuspended in RPMI 1640 (supplemented with 5% (v/v) FCS, L-glutamine (2 mM), penicillin (100 U/mL), and streptomycin (100  $\mu\text{g}/\text{mL}$ )), pre-incubated with compounds for 30 min and polarized with LPS (100 ng/mL) plus  $\text{INF-}\gamma$  (100 ng/mL) for M1 or with IL-4 (20 ng/mL) for M2 for 24 h at 37 °C/5% $\text{CO}_2$ . Macrophages were detached with biotase and collected by centrifugation ( $400 \times \text{g}/10 \text{ min}/4 \text{ }^\circ\text{C}$ ). Cells were then washed with D'PBS-EDTA (1 mM) and sonicated on ice (output 1, cycle 40%, 12 cycles) (SFX250, Branson, CT). Cell disruption was proved by trypan blue exclusion and microscopic analysis. Sonification was repeated if necessary. Lysates were distributed according to  $3.5 \times 10^6$  cells/sample and product formation stimulated with  $\text{CaCl}_2$  (2 mM) and AA (20  $\mu\text{M}$ ) for 15 min at 37 °C. Finally, the reaction was stopped by placing the cells on ice, HCl (30  $\mu\text{L}/\text{mL}$ ; 1 M) and  $\text{PGB}_1$  (60 ng) were added, the samples were centrifuged ( $2000 \times \text{g}/10 \text{ min}/4 \text{ }^\circ\text{C}$ ) and used for SPE (3.2.10) before analysis by UPLC-MS/MS (3.2.11).

### 3.2.18 Analysis of mRNA expression and degradation

Monocytes ( $2 \times 10^6/\text{mL}$ ) were resuspended in RPMI 1640 (supplemented with 5% (v/v) FCS, L-glutamine (2 mM), penicillin (100 U/mL), and streptomycin (100  $\mu\text{g}/\text{mL}$ )). After 6 d of differentiation with rhM-CSF (25 ng/mL), macrophages were pre-incubated with compounds or vehicle (0.1% DMSO) for 30 min or 16 h, respectively, and stimulated with LPS (100 ng/mL) for indicated times at 37 °C/5%  $\text{CO}_2$ . For measurement of  $\text{TNF}\alpha$  mRNA degradation, macrophages

were stimulated with LPS (100 ng/mL) for 24 h and incubated with compound or vehicle (0.1% DMSO) for 1 h. Then, transcription was stopped by addition of actinomycin (5 µg/mL) and cells were incubated for the indicated times. Total RNA from macrophages was isolated using the E.Z.N.A.® Total RNA Kit I (Omega Biotek, GA, ). Total mRNA amount was determined by photometric analysis at 230 nm, 260 nm, 280 nm, and 320 nm measured by Nanodrop (Thermo Fisher Scientific Inc., MA) and calculation of the ratios A260 nm/A280 nm and A260 nm/A230 nm confirmed the quality of the mRNA. cDNA was generated by reverse transcription by SuperScript® III First-Strand Synthesis SuperMix (Life technologies, CA) with random hexamers and a thermal cycling protocol as follows: 5-10 min at 25 °C, 50 min at 50 °C, 5 min at 85 °C. The cDNA was amplified by PCR (Mx3005P qPCR system, Agilent Technologies, CA) using the primers listed in Table 3.4 and according to the PCR conditions described in Table 3.5.

**Table 3.4: Primers for qRT-PCR.** Primers were diluted in nuclease-free water to 0.3 µM

| <b>name</b>                | <b>strand</b> | <b>nucleotide sequence</b>     |
|----------------------------|---------------|--------------------------------|
| beta-2-microglobulin (B2M) | forward       | 5'- CTCCGTGGCCTTAGCTGTG -3'    |
|                            | reverse       | 5'- TTTGGAGTACGCTGGATAGCCT -3' |
| TNF $\alpha$               | forward       | 5'- CCCAGGGACCTCTCTCTAATC -3'  |
|                            | reverse       | 5'- ATGGGCTACAGGCTTGTCCT -3'   |
| IL-1 $\beta$               | forward       | 5'- ACAGATGAAGTGCTCCTTCCA -3'  |
|                            | reverse       | 5'- GTCGGAGATTCGTAGCTGGAT -3'  |
| COX-2                      | forward       | 5'- TGCATTCTTTGCCAGCACT -3'    |
|                            | reverse       | 5'- AAAGGCGCAGTTTACGCTGTC -3'  |

**Table 3.5: Three-step cycling protocol for thermal cycler.**

| <b>step</b>          | <b>temperature</b> | <b>time</b> | <b>number of cycles</b> |
|----------------------|--------------------|-------------|-------------------------|
| initial denaturation | 95 °C              | 10 min      | 1                       |
| denaturation         | 95 °C              | 15 sec      | 45                      |
| annealing            | 60 °C              | 30 sec      |                         |
| extension            | 72 °C              | 30 sec      |                         |
| termination          | 95 °C              | 60 sec      | 1                       |
|                      | 55 °C              | 30 sec      |                         |
|                      | 95 °C              | 30 sec      |                         |

For quantification Maxima SYBR Green/ROX qPCR Master Mix (Fermentas, Darmstadt, Germany) was used. To calculate the relative TNF $\alpha$  mRNA expression (normalized to B2M) the  $2^{(-\Delta\Delta C(T))}$  method was used [238]. Data acquisition was done by the MxPro software (Mx3005P®/version 4.10, Agilent Technologies, CA).

### 3.2.19 Determination of [ $^3\text{H}$ ]-AA release

Tritium-labeled AA was used to determine cPLA $_2$  activity by measuring AA release from macrophages. Thus, macrophages ( $0.5 \times 10^6/\text{mL}$ ) were incubated with 2.5 nM [ $^3\text{H}$ ]-AA (corresponding to 0.25  $\mu\text{Ci}/\text{mL}$ ; specific activity 100 Ci/mmol) in RPMI 1640 without additives for 24 h at 37 °C/5% CO $_2$ . Cells were collected by centrifugation ( $400 \times \text{g}/10 \text{ min}/4 \text{ }^\circ\text{C}$ ) and washed twice with PG buffer (D'PBS plus 0.1% (w/v) glucose) containing fatty acid-free bovine serum albumin (BSA) (2 mg/mL) to remove unincorporated [ $^3\text{H}$ ]AA. Macrophages were resuspended in buffer containing CaCl $_2$  (1 mM) and distributed to 0.5 mL each in Eppendorf cups at a concentration of  $2 \times 10^6/\text{mL}$ . The samples were pre-incubated with compounds or vehicle (0.1% DMSO) for 10 min, then thiomersal (50  $\mu\text{M}$ ) was added to avoid re-acylation of unconverted AA into membranes and after 5 min, cells were stimulated with Ca $^{2+}$ -ionophore A23187 (2.5  $\mu\text{M}$ ) for 30 min at 37 °C. The reaction was stopped on ice for 10 min and cells were centrifuged ( $500 \times \text{g}/15 \text{ min}/20 \text{ }^\circ\text{C}$ ). 300  $\mu\text{L}$  of the supernatant was combined with 2 mL liquid scintillation counting (LSC) fluid and assayed for radioactivity by scintillation counting (Micro Beta Trilux, Perkin Elmer, MA).

### 3.2.20 Determination of reactive oxygen species (ROS)

The measurement of ROS levels was performed as reported [239]. Briefly, monocytes ( $0.5 \times 10^6/\text{mL}$ ), resuspended in RPMI 1640 (supplemented with 5% (v/v) FCS, L-glutamine (2 mM), penicillin (100 U/mL), and streptomycin (100  $\mu\text{g}/\text{mL}$ )), were incubated with rhM-CSF (25 ng/mL) for 6 d. Macrophages were incubated with compounds or vehicle (0.1% DMSO) for 30 min and stimulated with LPS (100 ng/mL) for 24 h or left untreated. Cells were washed and incubated in HBSS buffer containing 2'-7'-dichlorofluorescein diacetate (DCFH-DA) (10  $\mu\text{M}$ ) for 30 min at 37 °C/5% CO $_2$ . To detect and quantify intracellular formation of H $_2$ O $_2$ , fluorescence of the deacetylated dye (2'-7'-dichlorofluorescein) was measured at an excitation wavelength of 485 nm

and an emission wavelength of 535 nm using a NOVOstar microplate reader (BMG Labtechnologies GmbH, Offenburg, Germany).

### 3.2.21 Statistics

The data are presented as mean + standard error of the mean (SEM) of n experiments, where n represents the number of experiments. Statistical data was analyzed using the GraphPad InStat software (GraphPad Software, CA), and was performed by Student's t test for paired groups and by one-way ANOVA for independent or correlated samples followed by a Bonferroni (< 5 groups) or Tukey-Kramer (> 5 groups) post hoc test for multiple comparisons [240]. A P value of < 0.05 (\*) was considered significant.

## 4 RESULTS

### 4.1 Influence of archazolid on macrophage function

#### 4.1.1 v-ATPase expression and functionality

For the investigation of the v-ATPase inhibitor archazolid and its effects on macrophages, the expression and localization of the v-ATPase in LPS-stimulated (M), LPS/INF- $\gamma$  (M1), and IL-4 (M2) polarized macrophages was examined by immunofluorescence microscopy and Western blot analysis (Figure 4.1; A and B).

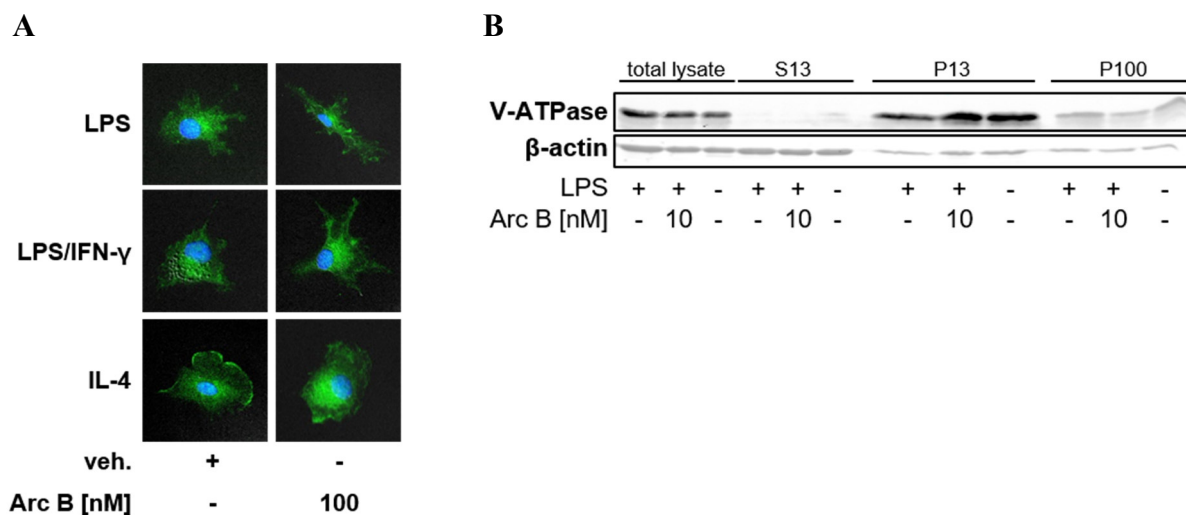


**Figure 4.1: Expression and localization of the v-ATPase in macrophages.** (A) Macrophages were pre-treated with archazolid (Arc B) at indicated concentrations or vehicle (0.1% DMSO) for 30 min and stimulated with LPS (100 ng/mL)/INF- $\gamma$  (100 ng/mL) or with IL-4 (20 ng/mL) for 24 h. Cells were fixed, permeabilized, and incubated with an antibody against v-ATPase (green), followed by Alexa Fluor 488 goat anti-rabbit IgG. Nuclei were stained with DAPI (blue). Results are representative of three independent experiments. (B) Macrophages were pre-treated and stimulated as described in Fig. 4.1 (A). Cells were lysed with TKM buffer followed by sonification and fractions were obtained by centrifugation at  $13,000 \times g$  (S13, P13) and  $100,000 \times g$  (P100). Samples were analyzed by Western blotting.  $\beta$ -Actin was used as control. Representative Western blots of two independent experiments are shown.

In agreement with other studies [241-243] the expression of the v-ATPase could be confirmed for macrophages and was further shown to be independent of the stimulation with LPS, LPS/INF- $\gamma$ , or IL-4, since immunolabeling and microscopic analysis did not reveal visible differences of the enzyme's localization between the macrophage subtypes. Western blot analysis confirmed that the

v-ATPase is primarily expressed in the P13 fraction which represents mainly membranes of ER and nucleus, whereas P100 contains partly microsomal membranes and plasma membranes where the v-ATPase was found, too, but in a lower amount. Archazolid did not have an effect on expression or localization of the v-ATPase in any of the macrophage subtypes. Next, the functionality of the v-ATPase in macrophages, namely their main role to acidify lysosomal compartments, was ensured. Consistent with other inhibitors of the v-ATPase which have been shown to elevate the lysosomal pH in various cell types [210, 244], archazolid caused significantly increased vesicular pH in LPS-activated macrophages as evidenced by the pH-dependent internalization of FITC-labeled dextran (Figure 4.2, A). The successful uptake of FITC-dextran was confirmed by microscopic analysis (Figure 4.2, B). The pH elevation by archazolid occurred at least at 100 nM but only slightly at 10 nM. Chloroquine (CQ; 100  $\mu$ M) and  $\text{NH}_4\text{Cl}$  (50 mM) also moderately elevated lysosomal pH (Figure 4.2, A) in agreement with the literature [235, 245-247]. These findings were also supported by the results obtained by staining of acidic organelles

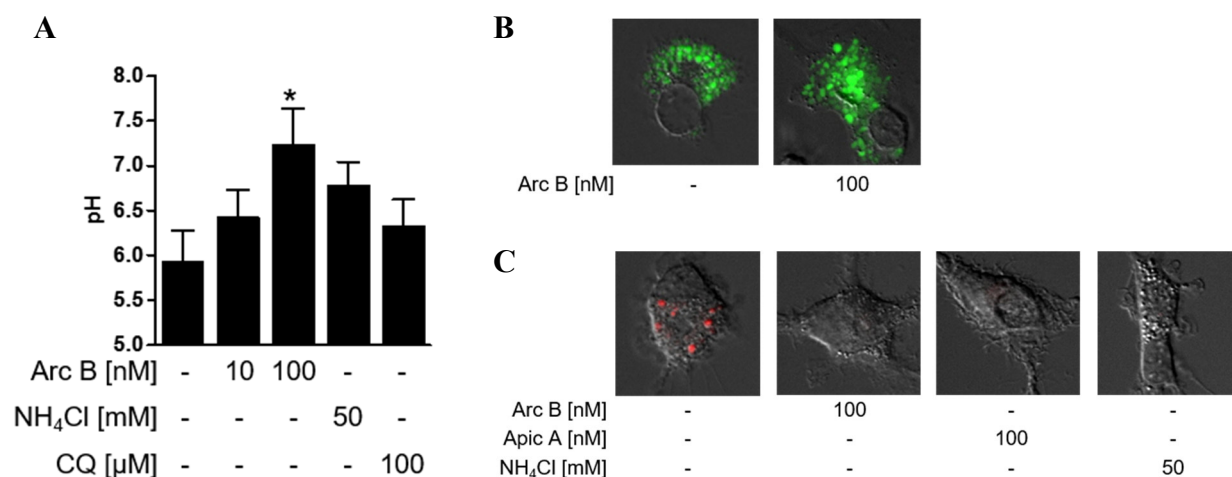


**Figure 4.2: Effects of v-ATPase inhibition on lysosomal pH of human macrophages.** (A, B) Macrophages were incubated with FITC-Dextran (0.5 mg/mL) for 60 min, pre-incubated with archazolid (Arc B) at indicated concentrations,  $\text{NH}_4\text{Cl}$  (50 mM), chloroquine (CQ; 100  $\mu$ M), or vehicle (0.1% DMSO) for 30 min and stimulated with LPS (100 ng/mL) for 24 h. FITC-Dextran uptake into lysosomes was determined by measurement of emission at 520 nm (A) or by analysis of immunofluorescence pictures (FITC-dextran: green; differential interference contrast) (B). (C) Macrophages were pre-incubated with archazolid (Arc B; 100 nM), apicularen (Apic A; 100 nM),  $\text{NH}_4\text{Cl}$  (50 mM) or vehicle (0.1% DMSO) for 30 min and stimulated with LPS (100 ng/mL) for 24 h, followed by incubation with LysoTracker (50 nM; red) for 60 min. Values shown are percentages of vehicle control, means + SEM; n=8 (A). \* $P < 0.05$ , \*\* $P < 0.01$ , \*\*\* $P < 0.001$  vs. the LPS-stimulated vehicle (DMSO). ANOVA + Bonferroni post-hoc test. Pictures shown are representative of three independent experiments.

with the pH sensitive LysoTracker probe and fluorescence microscopy (Figure 4.2, C). Here, the structurally different v-ATPase inhibitor apicurenen also caused the alkalization of acidic organelles as well as the alkalizing control  $\text{NH}_4\text{Cl}$ .

#### 4.1.2 Viability of M, M1, and M2

Since v-ATPase inhibitors have been in the focus of investigation particularly concerning their ability to induce apoptosis causing cancer cell death [5], the effect of archazolid on macrophage

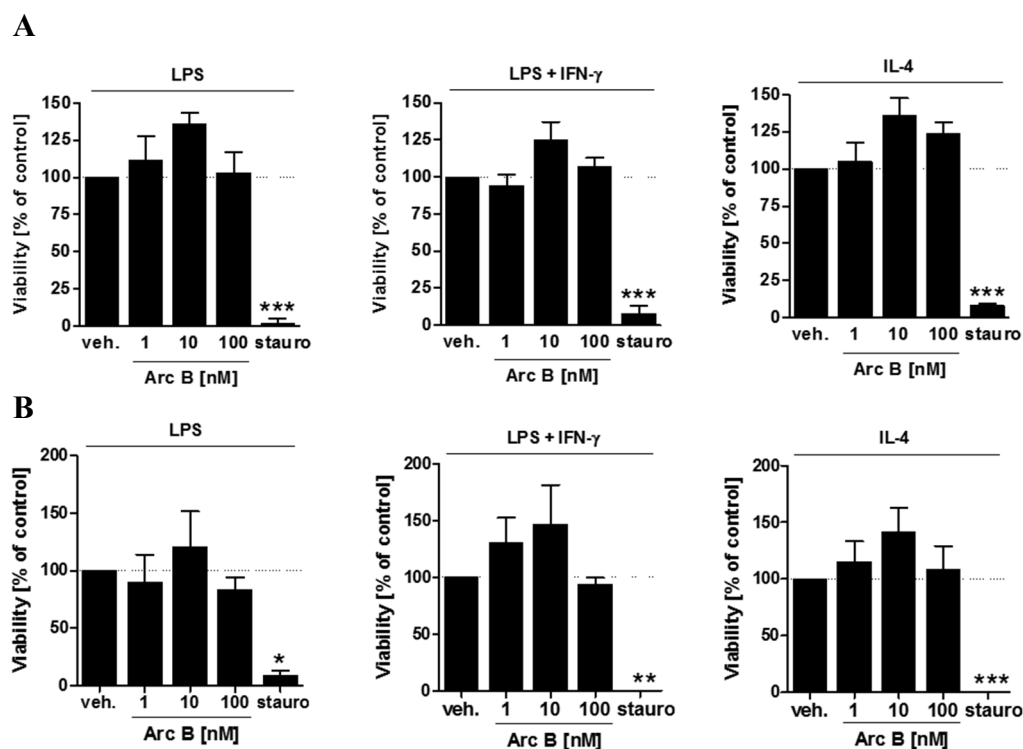


**Figure 4.3: Viability of macrophages.** Macrophages were pre-incubated with archazolid (Arc B) at indicated concentrations, staurosporine (stauro;  $3 \mu\text{M}$ ) or vehicle (0.3% DMSO) for 30 min and stimulated with LPS (100 ng/mL), with LPS (100 ng/mL)/IFN  $\gamma$  (100 ng/mL) or with IL-4 (20 ng/mL) for 24 h (A) and 48 h (B). Cell viability was determined by MTT assay. Values shown are percentages of vehicle control, means + SEM;  $n = 3$ . \*\*\* $P < 0.001$  vs. the LPS, LPS/IFN- $\gamma$  or the IL-4-treated vehicle (DMSO). ANOVA + Bonferroni post-hoc test.

viability was examined by MTT assay. Pre-treatment of LPS, LPS/INF- $\gamma$ , or IL-4 activated macrophages with archazolid (1 – 10 – 100 nM) for 24 h and 48 h, respectively, revealed no loss of cell viability, whereas the protein kinase inhibitor and apoptosis inducer staurosporine ( $3 \mu\text{M}$ ) completely abolished cell viability (Figure 4.3).

### 4.1.3 Morphology of M, M1, and M2

Microscopic analysis additionally confirmed cellular integrity of macrophages upon archazolid treatment for 24 h and revealed significant alterations of the cell shape for LPS- and LPS/IFN- $\gamma$ -treated cells which was not evident for M2 for which the morphology was obviously not affected.

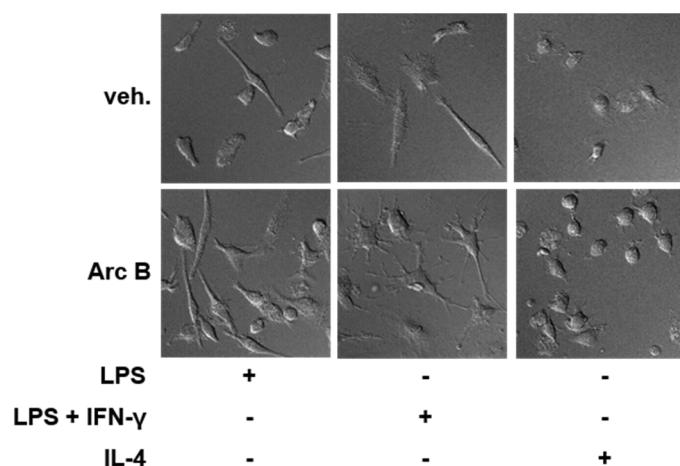


**Figure 4.4: Morphological changes of stimulated macrophages by archazolid.** Macrophages were pre-incubated with archazolid (Arc B; 100 nM) or vehicle (0.1% DMSO) for 30 min and stimulated with LPS (100 ng/mL), LPS (100 ng/mL)/IFN- $\gamma$  (100 ng/mL), or IL-4 (20 ng/mL) for 24 h. Images are shown as differential interference contrast. Results are representative of three independent experiments.

### 4.1.4 Phagocytosis

Since macrophages are typical members of the phagocyte system, we examined if archazolid affects this cell specific functionality. Successful engulfment of serum-opsonized zymosan particles after archazolid treatment revealed that phagocytosis of LPS-stimulated macrophages is

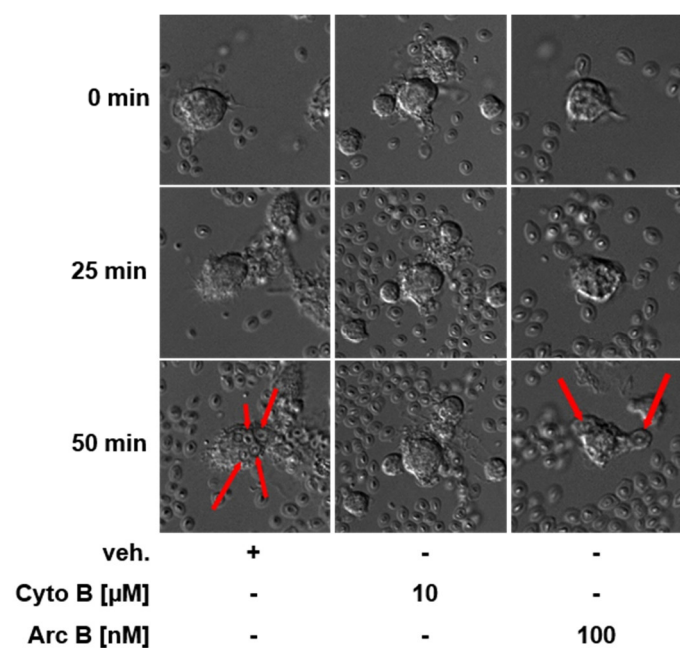


**Figure 4.5: Phagocytosis of serum-opsonized zymosan by LPS-stimulated macrophages.** Macrophages were pre-treated with archazolid (Arc B; 100 nM), cytochalasin (Cyto B; 10  $\mu$ M) or vehicle (0.1% DMSO) for 30 min and stimulated with LPS (100 ng/mL) for 24 h. Phagocytosis was initiated by addition of serum-opsonized zymosan suspension (1 mg/mL) (0 min), pictures were taken every 30 sec. Images are shown as differential interference contrast. Results are representative of two independent experiments. Red arrows indicate ingested zymosan particles at indicated time points.

not impaired in comparison to cytochalasin B which was used as reference control since this compound is known to suppress phagocytosis [248].

## 4.2 Effects of archazolid on macrophages

### 4.2.1 Cytokine release

After excluding that archazolid exhibits cytotoxicity against macrophages or detrimental impact on cellular integrity, viability, or phagocytic activity, the v-ATPase inhibitor was analyzed in view of its possible modulation of cytokine release from macrophages since these mediators play an important role in inflammatory events and inflammation-triggered cancer. After differentiation of freshly isolated monocytes for 6 d with rhM-CSF (25 ng/mL), macrophages were pre-treated with compounds for 30 min and then either activated by LPS, or polarized using LPS/INF- $\gamma$  towards M1 or using IL-4 towards M2 within 24 h. Analysis of MCP-1, IL-1 $\beta$ , IL-6, IL-8 and IL-10 in the medium revealed no significant modulation of the release of these proteins by archazolid, neither in M1 nor M2 polarized macrophages (Figure 4.6). However, the levels of TNF $\alpha$  were significantly

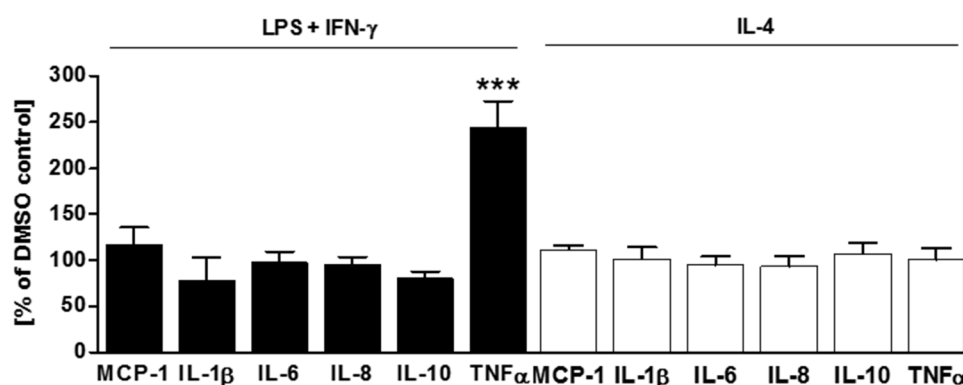


**Figure 4.6: Effects of v-ATPase inhibition on cytokine release from M1 and M2 polarized macrophages.** Macrophages were preincubated with archazolid B (100 nM) for 30 min and stimulated with LPS (100 ng/mL)/IFN- $\gamma$  (100 ng/mL) or with IL-4 (20 ng/mL) for 24 h. Levels of cytokines in supernatants were analyzed by ELISA. Values shown are percentages of vehicle control, means + SEM. \* $P < 0.05$ , \*\* $P < 0.01$ , \*\*\* $P < 0.001$  vs. the LPS/IFN- $\gamma$  stimulated vehicle (DMSO) or the IL-4-stimulated vehicle (DMSO), respectively. Paired *t*-test. Absolute values of LPS/IFN- $\gamma$  stimulated 100% controls: MCP-1:  $98 \pm 43$  ng/mL, IL-1 $\beta$ :  $1710 \pm 1465$  pg/mL, IL-6:  $31 \pm 9$  ng/mL, IL-8:  $52 \pm 5$  ng/mL, IL-10:  $1212 \pm 256$  pg/mL, TNF $\alpha$ :  $1992 \pm 653$  pg/mL. Absolute values of IL-4-stimulated 100% controls: MCP-1:  $86 \pm 35$  ng/mL, IL-1 $\beta$ :  $601 \pm 403$  pg/mL, IL-6:  $11 \pm 2$  ng/mL, IL-8:  $45 \pm 5$  ng/mL, IL-10:  $819 \pm 240$  pg/mL, TNF $\alpha$ :  $259 \pm 87$  pg/mL.  $n=3-7$ .

upregulated by 100 nM archazolid about 2.5-fold in M1, whereas the compound completely failed to alter TNF $\alpha$  levels in M2 (Figure 4.6).

More detailed concentration response experiments for TNF $\alpha$  release showed that for macrophages activated with LPS or LPS/INF- $\gamma$  the maximal effect was obtained at 30 nM archazolid (upregulation LPS: 338%  $\pm$  48%; LPS/INF- $\gamma$ : 277%  $\pm$  22%) and slightly declined at 100 nM (upregulation LPS: 219%  $\pm$  39%; LPS/INF- $\gamma$ : 243%  $\pm$  59%) (Figure 4.7, A). It should be noted

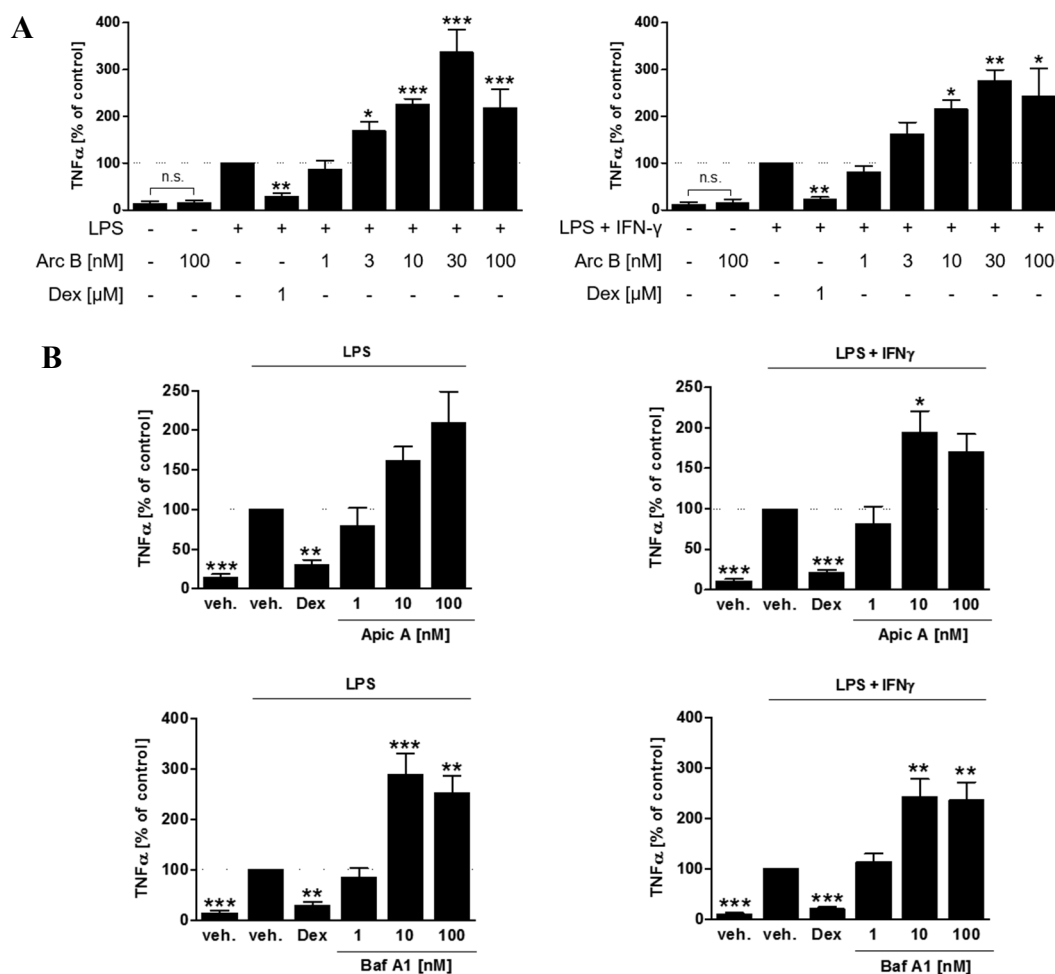


**Figure 4.7: Effects of v-ATPase inhibition on TNF $\alpha$  release.** Macrophages were pre-incubated with archazolid (Arc B), apicularen (Apic A), bafilomycin (Baf A1) at indicated concentrations, with dexamethasone (Dex; 1  $\mu$ M) or with vehicle (0.1% DMSO) for 30 min and stimulated with LPS (100 ng/mL) or with LPS (100 ng/mL)/IFN- $\gamma$  (100 ng/mL) for 24 h. Levels of cytokines in supernatants were analyzed by ELISA. Values shown are percentages of vehicle control, means + SEM. \* $P$  < 0.05, \*\* $P$  < 0.01, \*\*\* $P$  < 0.001 vs. the LPS-stimulated vehicle (DMSO) or the LPS/IFN- $\gamma$  stimulated vehicle (DMSO), respectively. ANOVA + Tukey post-hoc test. Absolute value of LPS-stimulated 100% control: 1383  $\pm$  229 pg/mL ( $n$  = 6), absolute value of LPS/IFN- $\gamma$  stimulated 100% control: 1906  $\pm$  273 pg/mL (A,  $n$  = 3) and 2347  $\pm$  632 pg/mL (B,  $n$  = 6).

that in unstimulated macrophages (no LPS, INF- $\gamma$ , or IL-4) archazolid was not effective in this manner. In contrast to archazolid, dexamethasone repressed TNF $\alpha$  levels both in LPS- (30%  $\pm$  7%) and LPS/INF- $\gamma$ -stimulated macrophages (24%  $\pm$  4%) (Figure 4.7, A).

In order to investigate if the effect of archazolid is related to suppression of v-ATPase activity, the v-ATPase inhibitors bafilomycin A1 and apicularen A were tested in the same experimental settings. For both compounds, upregulation of TNF $\alpha$  levels was evident with maximal effects at 10 nM (Figure 4.7, B).

## 4.2.2 pH elevation and TNF $\alpha$ release

As shown in 4.1.1/Figure 4.2, v-ATPase inhibition as well as the control substances chloroquine and NH<sub>4</sub>Cl led to elevated pH in lysosomal compartments. Furthermore, all tested v-ATPase inhibitors increased TNF $\alpha$  levels in LPS- and LPS/INF- $\gamma$ -stimulated macrophages (Figure 4.7). Thus, chloroquine and NH<sub>4</sub>Cl were investigated for their effects on TNF $\alpha$  release from macrophages to see if pH elevation may elevate TNF $\alpha$  levels. In contrast to archazolid, chloroquine (100  $\mu$ M) and NH<sub>4</sub>Cl (50 mM) markedly repressed TNF $\alpha$  release from LPS-activated and LPS/INF- $\gamma$  polarized macrophages (Figure 4.8) suggesting that other mechanism than solely elevation of lysosomal pH due to inhibition of v-ATPase is responsible for the TNF $\alpha$ -upregulatory effects of archazolid.

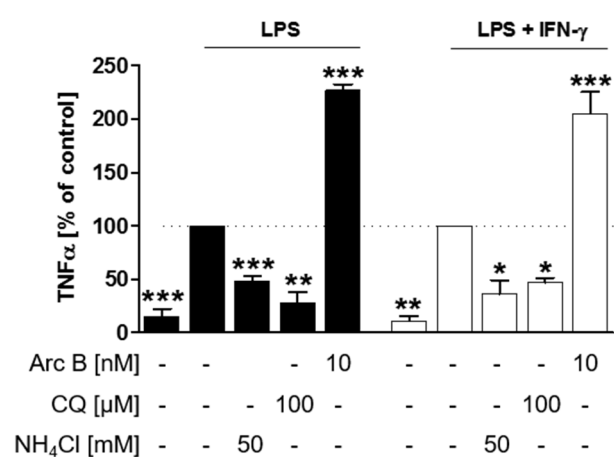


**Figure 4.8: Effect of pH-elevating agents on TNF $\alpha$  release from macrophages.** Macrophages were pre-incubated with archazolid (Arc B; 10 nM), NH<sub>4</sub>Cl (50 mM), chloroquine (CQ; 100  $\mu$ M) or vehicle (0.1% DMSO) for 30 min and stimulated with LPS (100 ng/mL) or LPS (100 ng/mL)/INF- $\gamma$  (100 ng/mL) for 24 h. TNF $\alpha$  levels in supernatants were analyzed by ELISA. Values shown are percentages of vehicle control, means  $\pm$  SEM; n=3. \*P < 0.05, \*\*P < 0.01, \*\*\*P < 0.001 vs. the LPS-stimulated vehicle (DMSO) or the LPS/INF- $\gamma$  stimulated vehicle (DMSO), respectively. ANOVA + Bonferroni post-hoc test.

### 4.2.3 TNF $\alpha$ mRNA expression and degradation

The stimulatory effect of archazolid on TNF $\alpha$  release from LPS-activated macrophages was abrogated by co-incubation with dexamethasone (Figure 4.9, A). This led to the assumption that archazolid may affect the expression of TNF $\alpha$  at the transcriptional level. To determine mRNA levels, macrophages were pre-treated with or without 100 nM archazolid in the presence or absence of 1  $\mu$ M dexamethasone 30 min or 16 h prior to stimulation with LPS. TNF $\alpha$  mRNA levels after 4 h and after 8 h were significantly higher in the presence of archazolid versus cells treated with LPS alone, and also after 1 h and after 16 h, 20 h and 24 h, archazolid led to elevated amounts of TNF $\alpha$  mRNA (Figure 4.9, B). Note that dexamethasone effectively repressed the stimulatory effects of archazolid. mRNA of IL-1 $\beta$  which was used as control due to the lack of archazolid affecting IL-1 $\beta$  protein levels, was not increased by archazolid (Figure 4.9, B). Experiments using

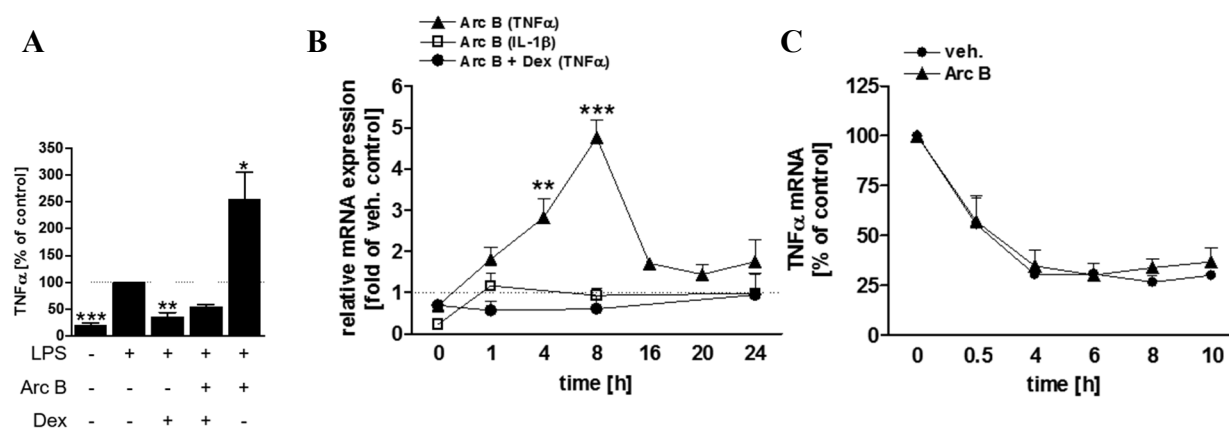


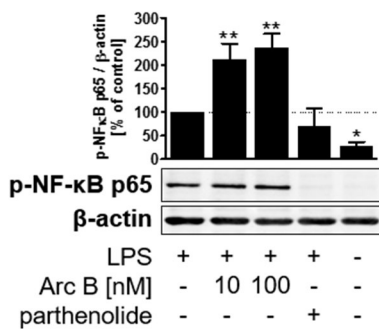
**Figure 4.9: Effects of archazolid on TNF $\alpha$  mRNA and degradation.** (A) Macrophages were pre-incubated with archazolid (Arc B; 100 nM), with or without dexamethasone (Dex; 1  $\mu$ M), or with vehicle (0.1% DMSO) for 16 h and stimulated with LPS (100 ng/mL) for 8 h. Levels of TNF $\alpha$  in supernatants were analyzed by ELISA. Values shown are percentages of vehicle control, means + SEM; n = 3. \*P < 0.05, \*\*P < 0.01, \*\*\*P < 0.001 vs. the LPS-stimulated vehicle (DMSO). ANOVA + Bonferroni post-hoc test. (B) Macrophages were pre-incubated with archazolid (Arc B; 100 nM) for 30 min or with archazolid (Arc B; 100 nM) plus dexamethasone (Dex; 1  $\mu$ M) for 16 h or with vehicle (0.1% DMSO) and stimulated with LPS (100 ng/mL) for indicated times. mRNA was extracted and determined by RT-qPCR. mRNA levels were normalized against B2M. Values shown are fold of control, means + SEM; n = 3-5. \*\*P < 0.01, \*\*\*P < 0.001 vs. the unstimulated archazolid B treated sample. ANOVA + Tukey post-hoc test. (C) Macrophages were stimulated with LPS (100 ng/mL) for 24 h and incubated with archazolid (Arc B; 10 nM) or vehicle (0.1% DMSO) for 60 min. Transcription was stopped by addition of actinomycin D (5  $\mu$ g/mL) and macrophages incubated for indicated times. RNA was extracted and determined by RT-qPCR. Values shown are percentages of control, means + SEM; n=3-4.

actinomycin D that blocks mRNA transcription [249] indicated that archazolid did not prevent TNF $\alpha$  mRNA degradation (Fig. 4C).

#### 4.2.4 Transcription factors

Having revealed that archazolid affects TNF $\alpha$  at the mRNA level and that dexamethasone abrogates these effects, the transcription factors NF- $\kappa$ B and I $\kappa$ B became interesting to investigate whether they are involved in elevating TNF $\alpha$  levels of macrophages. As analyzed by Western blotting, archazolid (10 and 100 nM) elevated the activation and phosphorylation of the p65 subunit of NF- $\kappa$ B in LPS-activated macrophages (Figure 4.10, A), whereas it did not alter I $\kappa$ B phosphorylation (Figure 4.10, B).

A



B

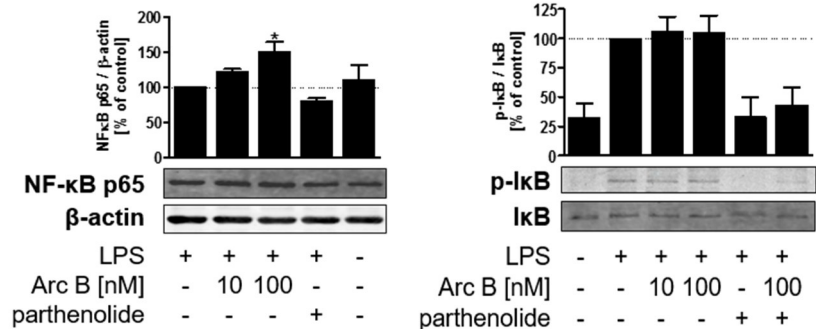


**Figure 4.10: Effects of archazolid on NF- $\kappa$ B (A) and I $\kappa$ B (B).** Macrophages were pre-incubated with archazolid (Arc B) at the indicated concentrations, with parthenolide (10  $\mu$ M) with or without archazolid B or with vehicle (0.1% DMSO) for 16 h and stimulated with LPS (100 ng/mL) for 15 min or left unstimulated. Protein phosphorylation or expression in cell lysates were analyzed by Western blotting. Representative Western blots of three to six independent experiments are shown.  $\beta$ -Actin or the appropriate unphosphorylated protein were used as control. Values shown are percentages of vehicle control, means + SEM;  $n = 4$  (A, left panel);  $n = 3$  (A, right panel);  $n = 3-6$  (B). \* $P < 0.05$ , \*\* $P < 0.01$ , vs. the LPS-stimulated vehicle (DMSO). ANOVA + Bonferroni post-hoc test.

This NF- $\kappa$ B-stimulatory effect of archazolid could be confirmed by analysis of the translocation of activated NF- $\kappa$ B from the cytosol into the nucleus in LPS-stimulated macrophages by immunofluorescence microscopy. 10 nM archazolid increased the amount of the p65 subunit of NF- $\kappa$ B in the nucleus (stained with DAPI) of LPS-stimulated cells (Figure 4.11, lower series) whereas I $\kappa$ B was detectable in unstimulated but not verifiable in LPS-stimulated macrophages (Figure 4.11, upper series) probably due to its degradation upon LPS treatment.

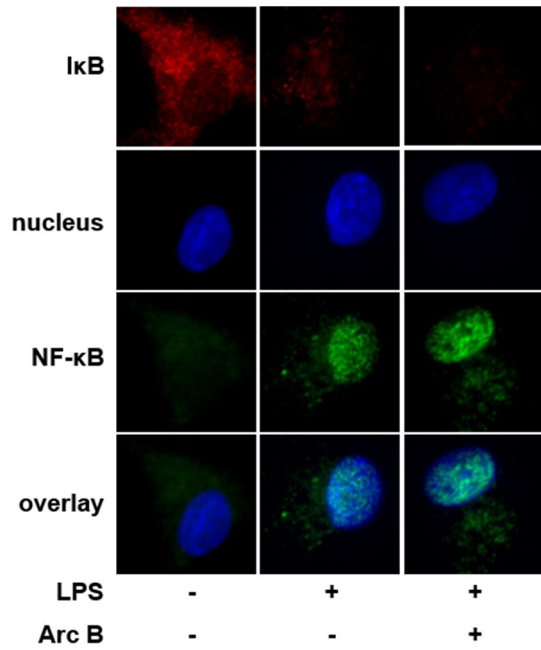


**Figure 4.11:** Macrophages were pre-incubated with archazolid (Arc B; 10 nM), or vehicle (0.1% DMSO) for 16 h and stimulated with LPS (100 ng/mL) for 15 min or left unstimulated. Fixed and permeabilized cells were stained with antibodies against IκB and NF-κB p65, followed by Alexa Fluor 555 goat anti-mouse IgG and Alexa Fluor 488 goat anti-rabbit IgG. Nuclei were stained with DAPI (blue). Red, IκB; green, NF-κB. Immunofluorescence pictures of two independent experiments are shown.

Further transcription factors like STAT1 and STAT3 were observed as differently activated by archazolid regarding stimulation of macrophages with LPS/IFN-γ or IL-4. Whereas archazolid at

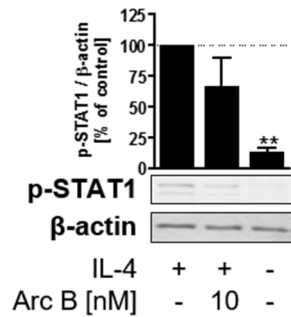
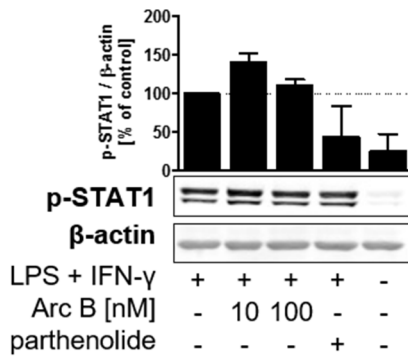
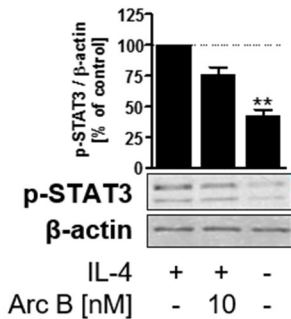
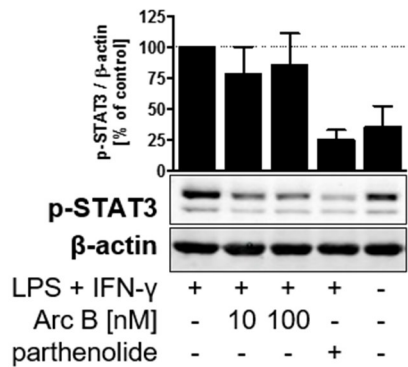


**Figure 4.12: Effects of archazolid B on transcription factors STAT1 and STAT3.**

Macrophages were pre-incubated with archazolid (Arc B) at the indicated concentrations, with parthenolide (10 μM) or with vehicle (0.1% DMSO) for 16 h and stimulated with LPS (100 ng/mL) for 15 min or left untreated. Protein phosphorylation or expression in cell lysates were analyzed by Western blotting. Representative Western blots of two to four independent experiments are shown. β-Actin was used as control. Values shown are percentages of vehicle control, means + SEM; n = 2-4 (upper left panel); n = 3 (upper right panel); n = 3-4 (lower left panel); n = 3 (lower right panel). \*\*P < 0.01, vs. the LPS-stimulated vehicle (DMSO). ANOVA + Bonferroni post-hoc test.



10 nM elevated phosphorylation of STAT1 in LPS/IFN- $\gamma$ -stimulated macrophages it did not strongly affect STAT3 in M1 and decreased both transcription factors in IL-4-stimulated cells slightly (Figure 4.12).

#### 4.2.5 Kinases involved in LPS signal transduction

Because archazolid obviously stimulated the LPS-induced increase of TNF $\alpha$  levels, it seemed possible that archazolid may enhance the involved signal transduction. Thus, the phosphorylation of typical protein kinases (PK) that are integrated in the signal transduction was analyzed by Western blotting. Macrophages, starved for 6 h by serum depletion prior to LPS activation, were treated with or without archazolid and then stimulated with LPS for 15 min. Reference PK inhibitors were used to control kinase-specific protein phosphorylation. Archazolid (10 and 100 nM) did not affect the phosphorylation/activation of Akt, ERK, p38 MAPK, and MEK1/2 (Figure 4.13). Though, SAPK/JNK was increased by archazolid as well as MEK-3/6, which was, however,

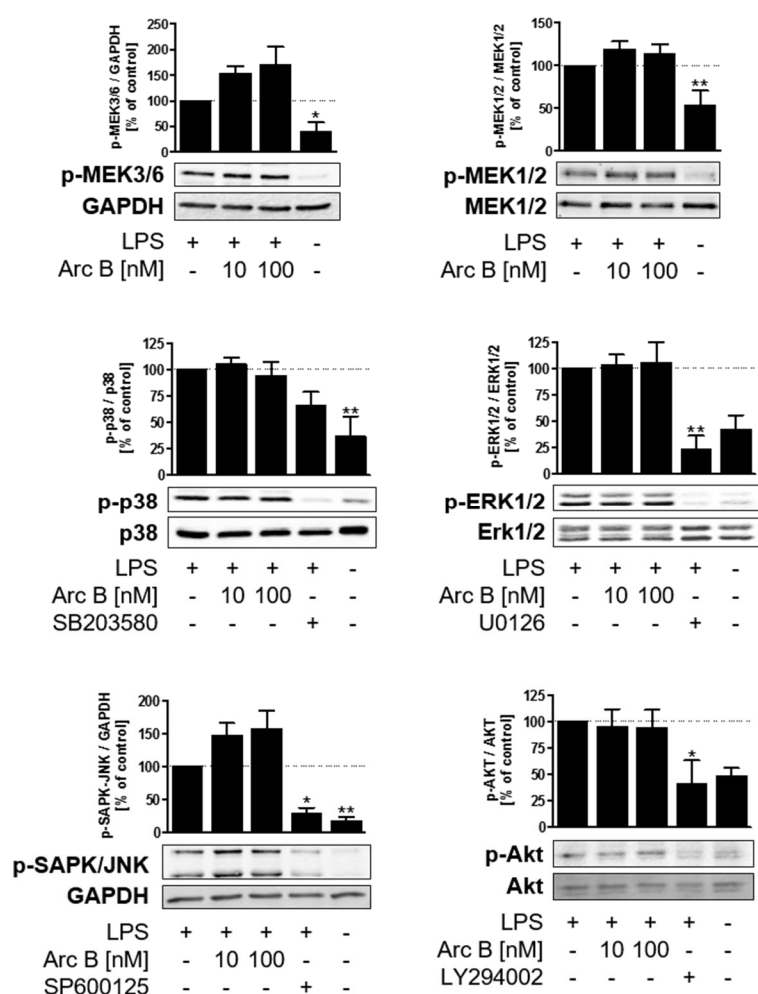


**Figure 4.13:** Macrophages, starved for 6 h prior to LPS-stimulation, were pre-incubated with archazolid (Arc B) at indicated concentrations, with reference inhibitors (LY294002 (10  $\mu$ M), U0126 (3  $\mu$ M), SB203580 (10  $\mu$ M), SP600125 (10  $\mu$ M)) or with vehicle (0.1% DMSO) for 16 h and stimulated with LPS (100 ng/mL) for 15 min or left untreated. Protein phosphorylation or expression in cell lysates were analyzed by Western blotting. Representative Western blots of three to five independent experiments are shown. The respective unphosphorylated protein or GAPDH were used as control. Values shown are percentages of vehicle control, means + SEM;  $n = 3$  (MEK3/6, ERK, SAPK/JNK, Akt);  $n = 5$  (p38, MEK1/2). \* $P < 0.05$ , \*\* $P < 0.01$ , vs. the LPS-stimulated vehicle (DMSO). ANOVA + Bonferroni post-hoc test.

not elevated as strong as this resulted in an induction of its downstream kinase p38. The reference inhibitors (LY294002 for Akt, U0126 for ERK, SB203580 for p38 and SP600125 for SAPK/JNK) blocked phosphorylation as expected (Figure 4.13).

#### 4.2.6 ROS levels

Production of ROS represents a characteristic property of M1 phenotypes due to their important role as phagocytic cells as an important step in innate immunity defending the host against invading pathogens. After revealing archazolid as compound elevating NF- $\kappa$ B activity therefore increasing TNF $\alpha$  levels in LPS and LPS/INF- $\gamma$  stimulated macrophages, it was further examined if archazolid contributes to elevated ROS levels in LPS-stimulated macrophages. At concentrations of 10 and 30 nM archazolid increased ROS levels significantly (Figure 4.14) whereas the NADPH oxidase inhibitor DPI [250] diminished ROS formation.

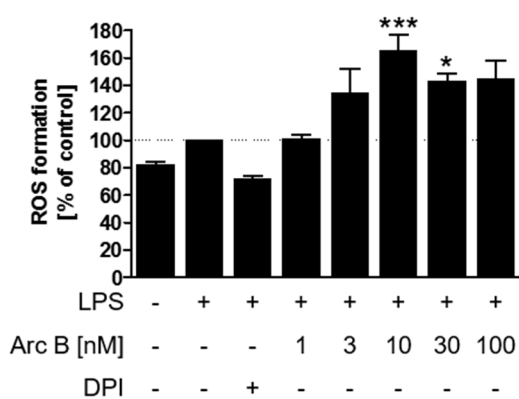


**Figure 4.14: ROS levels in LPS-stimulated macrophages.** Macrophages were pre-incubated with archazolid (Arc B) at the indicated concentrations, DPI (5  $\mu$ M), or with vehicle (0.1% DMSO) for 30 min and stimulated with LPS (100 ng/mL) for 24 h. Fluorescence of oxidized DCFH-DA (5  $\mu$ g/mL) was measured (excitation wavelength: 485 nm, emission wavelength: 535 nm). Values shown are percentages of vehicle control, means + SEM; n = 4. \*P < 0.05, \*\*\*P < 0.001 vs. the LPS-stimulated vehicle (DMSO). ANOVA + Tukey post-hoc test.

#### 4.2.7 Viability of MDA-MB-231

Although archazolid exhibits potent cytotoxic activity against cancer cells, we demonstrated that the viability of monocyte-derived macrophages, regardless of their polarization state, is not impaired by archazolid (4.1.2, Figure 4.3). There is evidence that high TNF $\alpha$  levels contribute to elimination of tumor cells [9]. After we had revealed that archazolid increases TNF $\alpha$  release from LPS- and LPS/IFN- $\gamma$ -activated macrophages, it was interesting to investigate whether supernatants of archazolid treated macrophages decrease the viability of the cancer cell line MDA-MB-231 due to high content of TNF $\alpha$ . Macrophages were pre-treated with archazolid (10 nM and 100 nM) for 30 min and stimulated with LPS for 4 h. In order to avoid that archazolid directly decreases viability of the cancer cell line, the medium was changed to wash out archazolid and macrophages

were further incubated for 20 h. The viability of MDA-MB-231 after treatment with prepared supernatants for 48 h was determined by MTT assay. Indeed, supernatants of macrophages treated with 100 nM archazolid reduced the viability of MDA-MB-231 significantly (10 nM:  $80\% \pm 3\%$ ; 100 nM:  $42\% \pm 6\%$ ) (Figure 4.15). However, abolishing the effects of supernatants of archazolid-treated cells by a TNF $\alpha$  antibody could not be achieved, supposing that decreased viability of MDA-MB-231 is not only due to elevated TNF $\alpha$  levels.

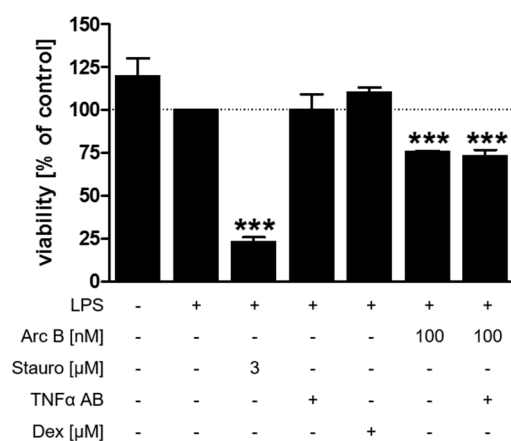


**Figure 4.15: Viability of MDA-MB-231 after incubation with archazolid-treated macrophage supernatants.** MDA-MB-231 were pre-incubated with staurosporine (stauro; 3  $\mu$ M) for 30 min and stimulated with LPS (100 ng/mL) or incubated with macrophage supernatants (pre-treated with archazolid (Arc B; 100 nM), dexamethasone (Dex; 1  $\mu$ M), TNF $\alpha$  antibody (1  $\mu$ g/mL) with or without archazolid (Arc B; 100 nM) or vehicle (0.1% DMSO)) for 48 h. Cell viability determined by MTT assay. Values shown are percentages of vehicle control, means + SEM; n = 3-5. \*\*\*P < 0.001 vs. the LPS treated vehicle (DMSO). ANOVA + Bonferroni post-hoc test.

## 4.3 Influence of archazolid on eicosanoid metabolism

### 4.3.1 COX-2 products

Besides cytokines, the eicosanoids are prominent mediators linked to inflammation and ITC. Thus, archazolid was investigated to see if it also modulates lipid mediator formation. Macrophages were pre-incubated with archazolid and stimulated with LPS, LPS/IFN- $\gamma$ , or with IL-4 for 24 h and PGE $_2$  release into the medium was assessed by ELISA. Dexamethasone, a potent anti-inflammatory drug that was shown to suppress PGE $_2$  release in activated macrophages [251, 252] was used as reference compound. Surprisingly, archazolid (1 to 100 nM) affected PGE $_2$  in the different macrophage phenotypes in a distinct manner, depending on the polarization. Thus, in LPS- and LPS/INF- $\gamma$ -stimulated macrophages, archazolid concentration-dependently increased PGE $_2$  up to 2.3-fold (Figure 4.16, a and b) whereas in M2 cells, PGE $_2$  levels were not altered (Figure 4.16, c). A similar pattern was observed for the v-ATPase inhibitors bafilomycin and apicularene that also significantly upregulated PGE $_2$  levels at 10 to 100 nM in M and M1 but not in M2 cells (Figure 4.16, d-f).

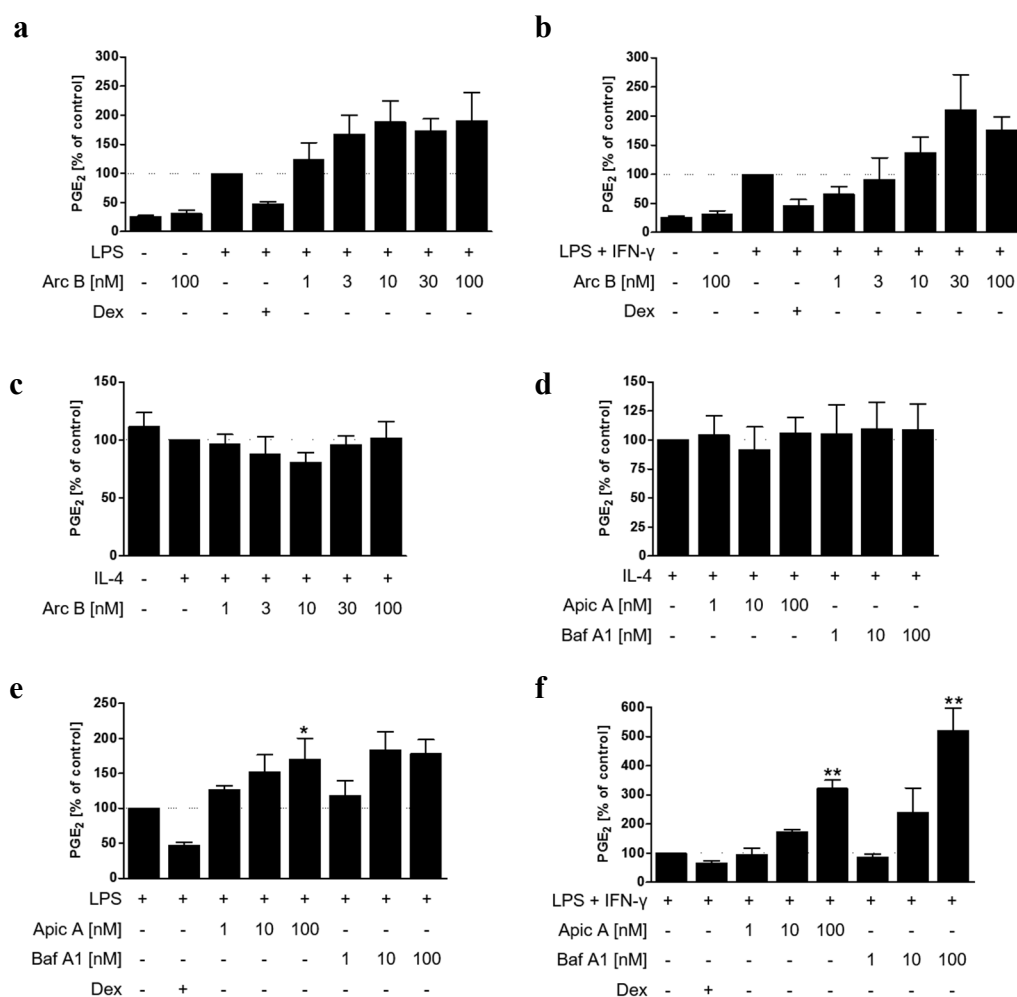


**Figure 4.16: Effects of v-ATPase inhibitors on PGE<sub>2</sub> levels.** Macrophages were pre-incubated with archazolid (Arc B), apicularen (Apic A), bafilomycin (Baf A1) at indicated concentrations, dexamethasone (Dex; 1  $\mu$ M), or with vehicle (0.1% DMSO) for 30 min and stimulated with LPS (100 ng/mL), LPS (100 ng/mL)/IFN- $\gamma$  (100 ng/mL) or IL-4 (20 ng/mL) or left unstimulated for 24 h. PGE<sub>2</sub> release into supernatants of macrophages was analyzed by ELISA. (a) Absolute value of 100% control: 1248  $\pm$  451 pg/mL, (b) absolute value of 100% control: 767  $\pm$  391 pg/mL, (c) absolute value of 100% control: 732  $\pm$  246 pg/mL. (d) absolute value of 100% control: 1366  $\pm$  503 pg/mL, (e) Absolute value of 100% control: 1248  $\pm$  451 pg/mL, (f) absolute value of 100% control: 1563  $\pm$  167 pg/mL. Values shown are percentages of vehicle control, means  $\pm$  SEM; n = 3-4. \*P < 0.05, \*\*P < 0.01, \*\*\*P < 0.001 vs. the LPS, LPS/IFN- $\gamma$  or the IL-4-stimulated vehicle (DMSO), respectively. ANOVA + Tukey post hoc test (a-c), ANOVA + Bonferroni post hoc test (d-f).

Besides PGE<sub>2</sub>, other prostanoids are produced by the COX pathway in macrophages [253]. In order to investigate whether v-ATPase inhibition is attributable to COX-2 induction the formation of other prostanoids (PGF<sub>2 $\alpha$</sub> , TxB<sub>2</sub>, 12-HHT and 11-HETE) was examined using UPLC-MS/MS analysis. Though the magnitudes of all these produced prostanoids were different, the enhancing

effect of archazolid (100 nM) on prostanoid mediators was obvious (Figure 4.17).  $\text{PGF}_{2\alpha}$  and  $\text{TxB}_2$  were increased by about 1.5-fold whereas 12-HHT and 11-HETE were increased about 2.2- and 3.3-fold, respectively. The differences between LPS and LPS/IFN- $\gamma$  stimulation were only small but surprisingly, except for 12-HHT, LPS stimulation led to higher product formation than its combination with IFN- $\gamma$ .

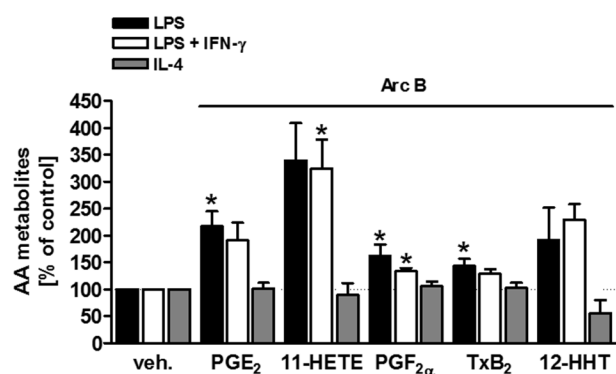


**Figure 4.17: Effect of archazolid on COX-2 product formation.** Macrophages were pre-incubated with archazolid (Arc B; 100 nM) or with vehicle (0.1% DMSO) for 30 min and stimulated with LPS (100 ng/mL), LPS (100 ng/mL)/IFN- $\gamma$  (100 ng/mL) or IL-4 (20 ng/mL) for 24 h. Levels of COX-2 products were analyzed by UPLC-MS/MS. Values shown are percentages of vehicle control, means + SEM; n = 3-4. \* $P < 0.05$ , \*\* $P < 0.01$ , \*\*\* $P < 0.001$  vs. the LPS, LPS/IFN- $\gamma$  or the IL-4-stimulated vehicle (DMSO), respectively. Paired  $t$ -test.

### 4.3.2 pH-elevating drugs

Blocking the acidification of vesicles and certain organelles [254, 255], it appeared possible that alterations in the vesicular pH by v-ATPase inhibitors, especially an elevation, may underlie the upregulation of PGE<sub>2</sub> in M1. Macrophages pre-incubated with archazolid or agents that also elevate the vesicular pH by other mechanisms such as chloroquine or NH<sub>4</sub>Cl were stimulated with either LPS or LPS/IFN- $\gamma$  for 24 h. The release of PGE<sub>2</sub> into supernatants was examined by ELISA. However, contrarily to archazolid the pH elevating drugs chloroquine and NH<sub>4</sub>Cl did not increase but markedly reduced PGE<sub>2</sub> synthesis in M and M1 (Figure 4.18).

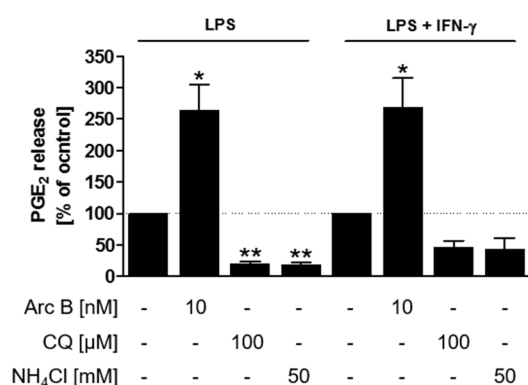


**Figure 4.18: Effect of pH elevation on PGE<sub>2</sub> release.** Macrophages were pre-incubated with archazolid (Arc B; 10 nM), chloroquine (CQ; 100  $\mu$ M), NH<sub>4</sub>Cl (50 mM) or vehicle (0.1% DMSO) for 30 min and stimulated with LPS (100 ng/mL)/IFN- $\gamma$  (100 ng/mL) or left unstimulated for 24 h. PGE<sub>2</sub> release into supernatants of macrophages was analyzed by ELISA. Values are shown as percentages of vehicle control, means + SEM; n = 3. \* $p < 0.05$ , \*\* $p < 0.01$ , \*\*\* $p < 0.001$  vs. the LPS or LPS/IFN- $\gamma$  stimulated vehicle (DMSO), respectively. ANOVA + Bonferroni post-hoc test.

### 4.3.3 Arachidonic acid release

v-ATPase inhibitors may directly interact with the enzymes involved in PG synthesis including cPLA<sub>2</sub>. Although there is no direct stimulatory effect of archazolid on cPLA<sub>2</sub> in cell-free assays [256], it appeared possible that v-ATPase inhibitors could activate the enzymes by direct interference in the cellular environment. Macrophages were first stimulated with LPS for 24 h and then labeled with [<sup>3</sup>H]-AA for 24 h. Macrophages were pre-incubated with archazolid or the cPLA<sub>2</sub> inhibitor RSC-3388 for 10 min before thiomersal was added for 5 min to reduce re-acylation of unconverted AA into membranes. Then, cells were stimulated with Ca<sup>2+</sup>-ionophore A23187 for AA release by cPLA<sub>2</sub> for 30 min. In such short-term incubation, archazolid (up to 100 nM) failed to modulate AA release, and RSC-3388 suppressed AA liberation as expected (Figure 4.19).

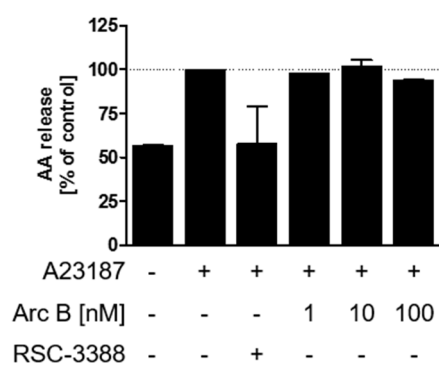


**Figure 4.19: Effect of archazolid on AA release.** Macrophages were stimulated with LPS (100 ng/mL) for 24 h before labeling with [<sup>3</sup>H]AA for 24 h. Cells were pre-incubated with archazolid (Arc B) at indicated concentrations, RSC-3388 (1 μM) or vehicle (0.1% DMSO) for 10 min, thiomersal (50 μM) was added for 5 min and cells were stimulated with A23187 (2.5 μM) for 30 min. [<sup>3</sup>H]AA release was analyzed by scintillation counting. Values are shown as percentages of vehicle control, means + SEM; n = 2.

### 4.3.4 COX-2 activity, protein-, and mRNA expression

Having determined that cPLA<sub>2</sub> activity and thus substrate supply is not influenced by archazolid the possibility remained that the v-ATPase inhibitor affects enzymes downstream of cPLA<sub>2</sub> as COX-2 directly. To analyze COX-2 activity by short term incubation, macrophages were first stimulated with LPS or LPS/IFN-γ for 24 h to induce enzyme expression. Then, cells were pre-incubated with archazolid (100 nM) or the COX inhibitor indomethacin (10 μM) for 15 min and stimulated with Ca<sup>2+</sup>-ionophore A23187 plus AA for 30 min. The short-term PGE<sub>2</sub> synthesis was increased only marginal in LPS-stimulated but was rather slightly reduced in LPS/IFN-γ-stimulated macrophages by archazolid whereas indomethacin reduced PGE<sub>2</sub> synthesis as expected (Figure 4.20). This finding rather excludes direct stimulatory effects of archazolid on COX and PGE synthases.

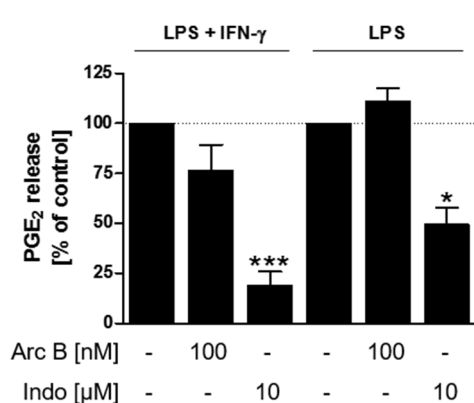


**Figure 4.20: Effect of archazolid on COX-2 activity.** Expression of COX-2 in macrophages was initiated by stimulation of the cells with LPS (100 ng/mL) or LPS (100 ng/mL)/IFN- $\gamma$  (100 ng/mL) for 24 h. Macrophages were pre-incubated with archazolid (Arc B; 100 nM), indomethacin (Indo; 10  $\mu$ M) or vehicle (0.1% DMSO) for 15 min and stimulated with A23187 (2.5  $\mu$ M) plus AA (5  $\mu$ M) for 30 min. PGE<sub>2</sub> in supernatants was measured by ELISA. Data in is shown as percentages of vehicle control, means + SEM; n = 3. \* $p$  < 0.05, \*\* $p$  < 0.01, \*\*\* $p$  < 0.001 vs. the LPS or LPS/IFN- $\gamma$  stimulated vehicle (DMSO), respectively. ANOVA + Bonferroni post-hoc test.

Next, the protein expression of COX-2 in LPS-stimulated macrophages with respect to its influence by archazolid was investigated. Macrophages were pre-treated with archazolid (10 and 100 nM) or dexamethasone, activated by LPS, and COX-2 protein was assessed by Western blot. As depicted in Figure 4.21, the amounts of COX-2 protein were increased by archazolid at 100 nM. Dexamethasone (1  $\mu$ M) repressed COX-2 expression as expected and also prevented the increased levels of COX-2 due to archazolid (Figure 4.21) shown by co-incubation of both substances.

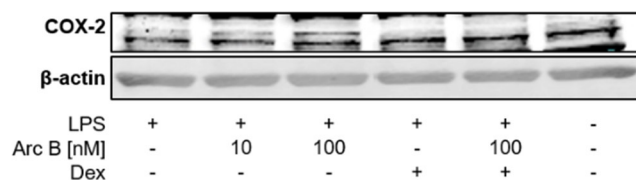


**Figure 4.21:** Cells were pre-incubated with archazolid (Arc B) at indicated concentrations with or without dexamethasone (Dex; 1  $\mu$ M) or vehicle (0.1% DMSO) for 30 min and stimulated with LPS (100 ng/mL) for 24 h. COX-2 protein in macrophage lysates was analyzed by Western blotting. Representative Western blots of three independent experiments are shown.  $\beta$ -Actin was used as control.

Since dexamethasone blocks COX-2 induction on the transcriptional level [257, 258], it appeared reasonable to study the effects of archazolid on the COX-2 mRNA level. Macrophages were pre-incubated with archazolid with or without dexamethasone and stimulated with LPS for 1, 4, 8, 16, 20, and 24 h. In fact, archazolid (100 nM) caused a continuous elevation of COX-2 mRNA relative to B2M and  $\beta$ -actin as housekeeping genes with a maximum at 20 h and an 7-fold elevation (Figure 4.22, A). Of interest, this upregulatory effect of archazolid was completely repressed by dexamethasone (Figure 4.22, A) in agreement with PGE<sub>2</sub> release (Figure 4.22, B).

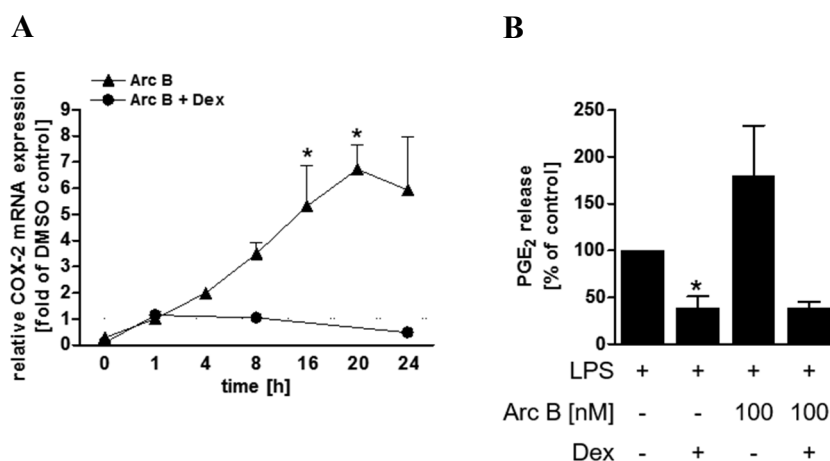


**Figure 4.22: Effect of archazolid on COX-2 mRNA expression.** Macrophages were pre-incubated with archazolid (Arc B; 100 nM) for 30 min or with archazolid (Arc B; 100 nM) plus dexamethasone (Dex; 1  $\mu$ M) for 16 h or with vehicle (0.1% DMSO) and stimulated with LPS (100 ng/mL) for indicated times. mRNA was extracted and determined by RT-qPCR. mRNA levels were normalized against geometric mean of B2M and  $\beta$ -Actin. PGE<sub>2</sub> in supernatants after 16 h pre-incubation and 24 h stimulation with LPS (100 ng/mL) were analyzed by ELISA. Values shown are given as fold increase of LPS-treated cells (no archazolid) (A) or as percentages of vehicle control (B), means + SEM; n = 3. \* $p$  < 0.05, \*\* $p$  < 0.01, \*\*\* $p$  < 0.001 vs. the unstimulated archazolid B treated sample (A) or vs. the LPS-stimulated vehicle control (B). ANOVA + Tukey post-hoc test.

### 4.3.5 Lipoygenase product formation

Macrophages express various LOs (5-LO, 12-LO and 15-LO) that in analogy to COX enzymes convert AA via dioxygenation to bioactive lipid mediators (e.g., LTs, 5/12-DiHETEs, 5-HETE, 12-HETE and 15-HETE) [89, 105]. Thus, the supernatants of M, M1 and M2 were also analyzed for LO-derived mediators using a UPLC-MS/MS technique. Similar to the prostanoids, the 15-LO-derived product 15-HETE was strongly upregulated by 10 and 100 nM archazolid in M and M1 cells, but not in M2 (Figure 4.23, A). 12-LO product synthesis was not altered by the v-ATPase inhibitor (Figure 4.23, B). In contrast to the prostanoids and 15-HETE, the synthesis of 5-LO-derived products (5-HETE, LTB<sub>4</sub> and its two trans-isomers) were clearly reduced by 10 nM archazolid in all three types of macrophages (M, M1, M2) with prominent effects in M1 and M2 and less pronounced suppression in M (Figure 4.23, C). BWA4C, a well-known iron ligand-type 5-LO inhibitor [259], was used as reference substance which blocked 5-LO product formation as expected almost at the level of macrophages lacking stimulation with Ca<sup>2+</sup>-ionophore A23187.

Beyond this, v-ATPase inhibition by apicularen and bafilomycin was also shown to impair 5-LO product formation (Figure 4.23, D).

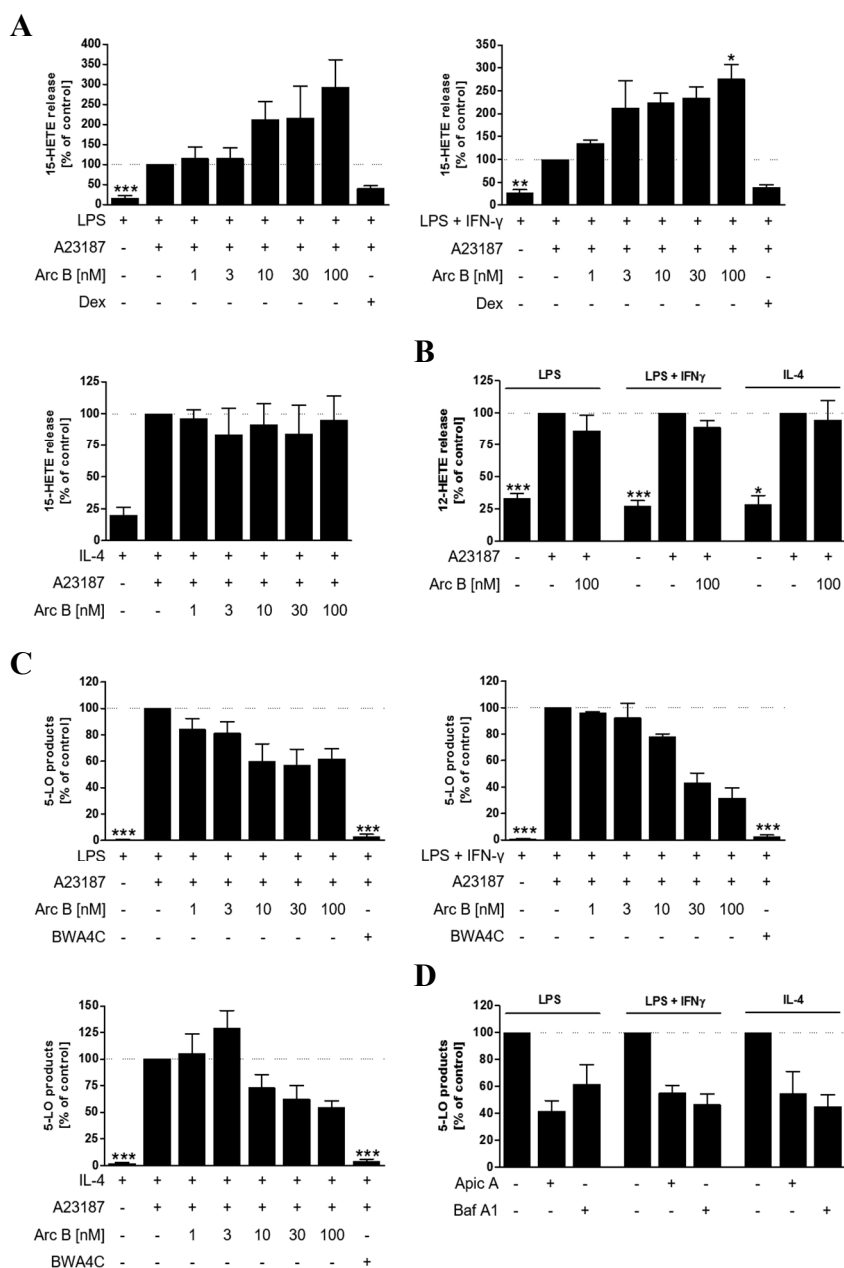


**Figure 4.23: Effect of v-ATPase inhibition on lipoxygenase product formation.** Macrophages were pre-incubated with archazolid (Arc B) at indicated concentrations, apicularen (Apic A; 100 nM), bafilomycin (Baf A1; 100 nM), BWA4C (100 nM), or vehicle (0.1% DMSO) for 30 min and stimulated with either LPS (100 ng/mL), LPS (100 ng/mL)/IFN- $\gamma$  (100 ng/mL) or IL-4 (20 ng/mL) for 24 h. Cells were stimulated with A23187 (2.5  $\mu$ M) for 10 min. Levels of 5-LO products (5-HETE, LTB<sub>4</sub>, epi/trans-LTB<sub>4</sub>), 12-HETE and 15-HETE were analyzed by UPLC-MS/MS. Values shown are percentages of vehicle control, means + SEM.  $n = 3-8$ . \* $P < 0.05$ , \*\* $P < 0.01$ , \*\*\* $P < 0.001$  vs. the LPS, LPS/IFN- $\gamma$  or the IL-4-treated vehicle (DMSO). ANOVA + Tukey (archazolid B) or Bonferroni (apicularen A, bafilomycin A1) post-hoc test.

By analysis of 5-LO products derived from other fatty acids than AA, such as EPA-derived 5-HEPE and DGLH-derived 5-HETrE, it should be emphasized that their formation was inhibited by archazolid (10 and 100 nM), too (Figure 4.24)

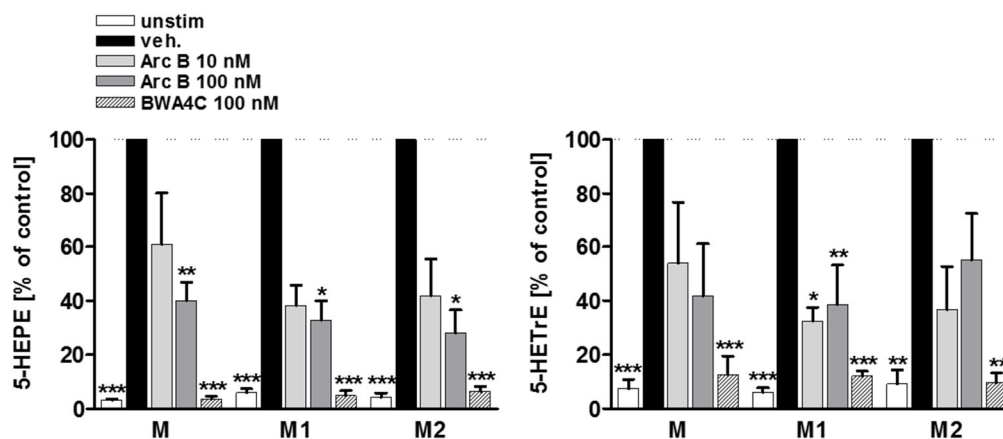


**Figure 4.24: Effect of archazolid on ETA- and EPA-derived 5-LO products.** Macrophages were pre-incubated with archazolid (Arc B) at indicated concentrations, BWA4C (100 nM), or vehicle (0.1% DMSO) for 30 min and stimulated with either LPS (100 ng/mL), LPS (100 ng/mL)/IFN- $\gamma$  (100 ng/mL) or IL-4 (20 ng/mL) for 24 h. Cells were stimulated with A23187 (2.5  $\mu$ M) for 10 min. Levels of 5-HEPE and 5-HETrE were analyzed by UPLC-MS/MS. Values shown are percentages of vehicle control, means + SEM.  $n = 4$ . \* $P < 0.05$ , \*\* $P < 0.01$ , \*\*\* $P < 0.001$  vs. the LPS, LPS/IFN- $\gamma$  or the IL-4-treated vehicle (DMSO). ANOVA + Tukey post-hoc test.

#### 4.3.5.1 5-LO translocation

To investigate whether an impaired 5-LO translocation or deficient colocalization of 5-LO with FLAP is the reason for inhibited 5-LO product synthesis immunofluorescence microscopy experiments were conducted. 5-LO predominated in the nucleoplasm in unstimulated macrophages (Figure 4.25, upper series) and translocated to the nuclear envelope upon  $\text{Ca}^{2+}$ -ionophore stimulation (Figure 4.25, middle series) whereas FLAP did not change its localization at the nuclear membrane upon stimulation. The overlay of 5-LO and FLAP in  $\text{Ca}^{2+}$ -ionophore stimulated- and archazolid-treated macrophages (Figure 4.25, lower panel) shows that the v-ATPase inhibitor does not disturb 5-LO translocation to the nuclear membrane.

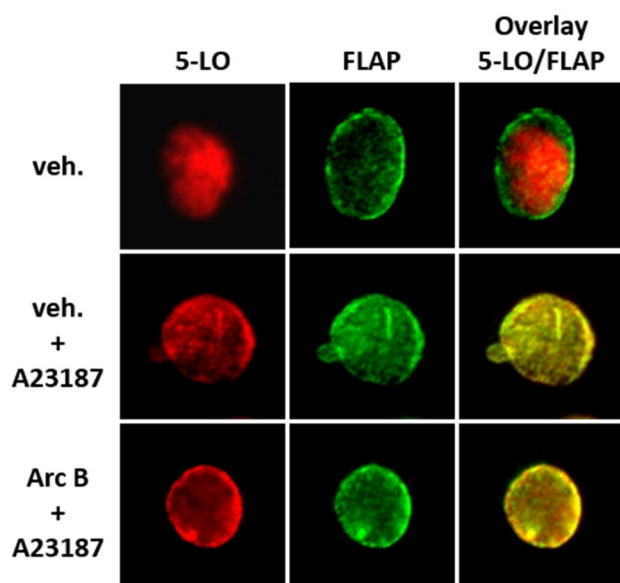


**Figure 4.25: Effect of archazolid on 5-LO translocation.** Macrophages were pre-incubated with archazolid (Arc B; 100 nM) or vehicle (0.1% DMSO) for 16 h and stimulated with A23187 (2.5  $\mu$ M) for 3 min. Macrophages were fixed, permeabilized and incubated with antibodies against 5-LO and FLAP, followed by Alexa Fluor 488 goat anti-rabbit IgG and Alexa Fluor 555 goat anti-mouse IgG. Red, 5-LO; green, FLAP. Immunofluorescence pictures of two independent experiments are shown.

#### 4.3.6 5- and 15-LO product formation in cell homogenates

Since archazolid obviously affected 5- and 15-LO product formation quite differently it was investigated whether archazolid influences 5- or 15-LO product formation also in homogenates of M1 and M2 macrophages. Archazolid inhibited 5-LO product formation in homogenates of M1 and M2 (Figure 4.26). These results regarding 5-LO product synthesis are in agreement with the finding that archazolid directly inhibits 5-LO in a cell-free assay [256]. 15-HETE derived from 15-LO was increased in M1 in accordance with the increased product levels in the supernatants of

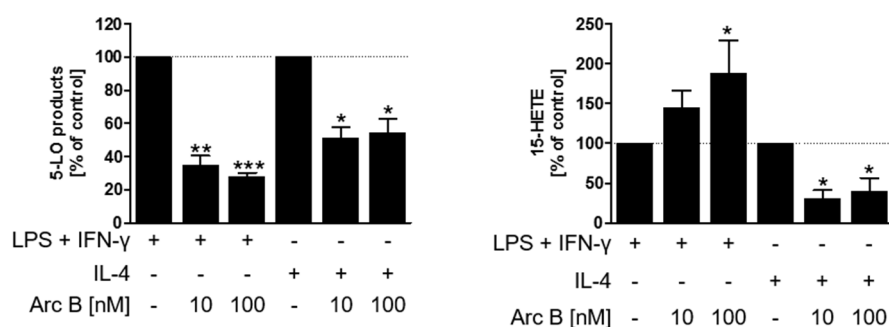


**Figure 4.26: Effects of archazolid on 5- and 15-LO product formation of M1 and M2 homogenates.** Macrophages were pre-incubated with archazolid (Arc B) at indicated concentrations for 30 min and polarized with LPS (100 ng/mL)/IFN- $\gamma$  (100 ng/mL) or with IL-4 (20 ng/mL) for 24 h. Cells were disrupted by sonification and CaCl<sub>2</sub> (2 mM) and AA (20  $\mu$ M) were added for 15 min. Product formation was analyzed by UPLC-MS/MS. Values shown are percentages of vehicle control, means + SEM. n = 3-4. \*P < 0.05, \*\*P < 0.01, \*\*\*P < 0.001 vs. the LPS/IFN- $\gamma$  or the IL-4-treated vehicle (DMSO). ANOVA + Bonferroni post-hoc test.

archazolid-treated intact cells. However, 15-HETE formation was decreased in homogenates of M2 macrophages (Figure 4.26) whereas 15-HETE release from intact M2 was not affected (Figure 4.23, A, lower panel).

### 4.3.7 5-LO protein expression

Having revealed that archazolid exhibits a direct inhibitory action on 5-LO, it was analyzed by Western blotting if archazolid influences the protein expression levels of this enzyme leading to decreased 5-LO product formation. As depicted in Figure 4.27 archazolid neither had an effect on 5-LO protein expression in M1 nor in M2.

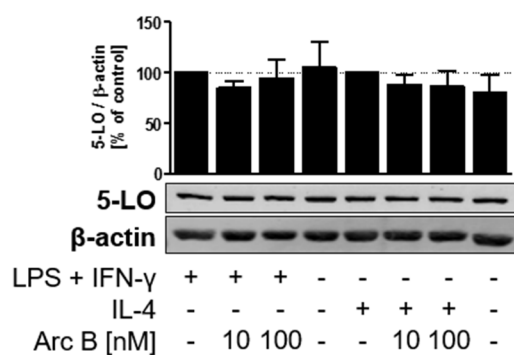


**Figure 4.27: Effect of archazolid on 5-LO protein expression.**

Macrophages were pre-incubated with archazolid (Arc B) at indicated concentrations or vehicle (0.1% DMSO) for 30 min and stimulated with LPS (100 ng/mL)/IFN- $\gamma$  (100 ng/mL) or IL-4 (20 ng/mL) for 24 h. Protein expression in cell lysates were analyzed by Western blotting. Representative Western blots of four independent experiments are shown.  $\beta$ -Actin was used as control. Values shown are percentages of vehicle control, means + SEM;  $n = 2-4$ .

## 5 DISCUSSION

The inflammatory status after infection or tissue injury is determined by the immune cells present at the inflammatory site as well as by their mediators responsible for the progression or resolution of inflammation [17]. Cytokines, chemokines and AA metabolites are among the most important molecules in this context [17, 260]. The failure of initiating the resolution phase and consequent progression of chronic inflammatory processes facilitate many secondary diseases, including cardiovascular and renal diseases, rheumatoid arthritis, atherosclerosis, and cancer [28, 261]. In this study, the focus was placed on inflammation-triggered cancer (ITC), where the decisive implication of the above-mentioned mediators has been reported before [26]. Among the innate immune cells involved in regulating the inflammatory environment, macrophages play a key role in ITC due to their marked plasticity occurring as M1 or M2 phenotype that suppress or promote tumor cells by modulating the immune response, respectively [157]. Affecting the synthesis or release of mediators from innate immune cells involved in inflammation and related diseases by pharmaceutical intervention might thus constitute a valuable therapeutic approach. Moreover, targeting TAMs or the specific modulation of mediator release from macrophage phenotypes might offer additional perspectives in anti-cancer therapy. Thus, it is not surprising that several approaches exist with this aim [184, 262-264].

Several types of tumors overexpress the v-ATPase [220, 221] that maintains a low pH in the tumor microenvironment for an optimal activity of tumor promoting enzymes [223]. For this reason, the v-ATPase is a potential target in the treatment of cancer and the potency of selective v-ATPase inhibitors against several cancer cell lines has previously been reported [5, 222, 229]. Nevertheless, there is only little knowledge about v-ATPase inhibition in human primary cells [265, 266]. Thus, the question was raised whether and how the v-ATPase inhibitor archazolid B affects human monocyte-derived macrophages. In this respect it was of particular interest if the polarization state of macrophages is of relevance. Furthermore, it was important to reveal whether the promising effects of archazolid B on cancer cells might be supported by effects of archazolid B on polarized macrophages. This thesis gives insights into the effects of the v-ATPase inhibitor archazolid B on inflammatory cytokine release from M1 and M2, and the possible underlying biochemical mechanisms are discussed. Furthermore, the involvement of archazolid B in

eicosanoid metabolism of M1 and M2 was addressed. The relevance of these effects in view of ITC and possible benefits is discussed.

## **5.1 Archazolid B inhibits the v-ATPase functionality by simultaneous unimpaired macrophage integrity**

Archazolid B is known to inhibit the v-ATPase [210] and to exhibit potent cytotoxic activity against several cancer cell lines [5, 267]. Thus, it was obvious and, with respect to future applications of the compound in anti-cancer therapies, even necessary to investigate if archazolid shows analogous cytotoxicity against primary human cells, especially against macrophages since they are important immune cells that play an essential, though diverse role in inflammation and ITC. The viability of macrophages differentiated from freshly isolated peripheral blood monocytes, stimulated with LPS alone (M), in combination with IFN- $\gamma$  (M1) or with IL-4 (M2) was not impaired by archazolid. Also microscopic analysis supported macrophage integrity. Even the polarization revealed morphological differences between M/M1 and M2 since the latter were rather round shaped cells, whereas M/M1 exhibited a DC-like appearance, clearly intensified by archazolid. Whereas the morphological distinctions between M1 and M2 have already been observed before [268, 269], the potentiation of M1 appearance by archazolid supposes a polarization enhancement of the M1 phenotype. Morphological changes of activated macrophages is closely connected to their phagocytic activity [270] since this constitutes one of the main features of M1 clearing the environment both from pathogens as well as from apoptotic cells or cell debris. The proper engulfment of foreign particles is thus an essential event for the host's health. Therefore, an unimpaired phagocytic activity after archazolid treatment further confirmed that the compound preserves the cellular integrity. Measuring the pH of archazolid-treated and LPS-stimulated macrophages as well as their microscopic analysis after FITC-Dextran or LysoTracker incubation revealed that archazolid inhibits the v-ATPase and elevates vesicular pH as reported [210]. However, the impact of archazolid on cellular pH homeostasis did not impair the viability of M, M1 and M2 which was the indispensable basis for further investigations.

## 5.2 Archazolid elevates TNF $\alpha$ levels in M and M1 due to increased transcription

Cytokines are intensively involved in inflammatory processes and in the communication between host/immune cells and neoplastic cells [8, 29]. Changes in this mediator system can result in the modulation of cell functionality. M1 and M2 exhibit a completely different pattern of cytokine expression due to distinct regulatory mechanisms according to their opposing roles in inflammation and cancer [150]. Different impacts of compounds on protein expression in M1 and M2 were therefore basically conceivable. Indeed, treatment of M1 and M2 with archazolid differed between the two subtypes in regard to their cytokine release. Pro-inflammatory IL-1, IL-6, IL-8, MCP-1, TNF $\alpha$ , and anti-inflammatory IL-10 release from M2 were not affected by archazolid but a selective elevation of TNF $\alpha$  release from M1 was achieved at nanomolar concentrations. TNF $\alpha$  release from M was increased with similarly intensity, supposing a specific effect of archazolid on the pro-inflammatory macrophage phenotype. The increase of TNF $\alpha$  levels was furthermore revealed as a class effect of v-ATPase inhibiting agents since apicularen and bafilomycin affected M and M1 in the same manner, whereas they did not influence M2 cytokine levels. The v-ATPase functions mainly in regulating organellar pH, an essential requirement of the cell [191]. In fact, vesicular acidification is an important procedure for intracellular trafficking due to the pH gradient along the endo- and exocytic pathway that determines the cargo's way in the cell [271]. v-ATPase inhibition by archazolid was therefore reasonable to be involved in elevating TNF $\alpha$  levels in M and M1. However, opposite data with other pH elevating drugs such as ammonium chloride and chloroquine, which did not increase TNF $\alpha$  levels but rather decreased TNF $\alpha$  release from M and M1 excluded pH increases as a major cause. Apart from the fact that the cytokine profile of M1 includes TNF $\alpha$ , this cytokine further belongs, next to LPS and INF- $\gamma$ , to the cytokines which induce the polarization of macrophages towards M1 [151]. Therefore, the strong increase of TNF $\alpha$  levels from M1 by archazolid might affect phenotypic development of macrophages in the sense of a positive feedback.

Tracing back the increased release of TNF $\alpha$ , modifications in transcriptional or translational processes are possible, particularly since transcription is a prominent step in gene regulation, controlled by a variety of transcription factors [272]. TNF $\alpha$  mRNA expression was found to be significantly increased by archazolid, apparently leading to elevated protein levels. In contrast, IL-

$l\beta$  mRNA expression was not affected in accordance with protein levels after archazolid treatment, affirming a specific effect of archazolid on TNF $\alpha$  mRNA. The assumption of transcription factors being involved in elevating TNF $\alpha$  mRNA by archazolid was further supported by the result of the co-incubation of archazolid with dexamethasone, which showed that elevated TNF $\alpha$  mRNA by archazolid can be repressed by dexamethasone. The ability of dexamethasone to regulate gene transcription has been attributed to the interference of its glucocorticoid receptor with different transcription factors, such as NF- $\kappa$ B [258]. Members of the “ $\kappa$ B”-family seem to be the most prominent enhancers for transcriptional activation of the TNF $\alpha$  gene [273, 274]. NF- $\kappa$ B mediates its effects by binding specific elements in the promoter region of the DNA, for instance of the TNF $\alpha$  gene, to regulate transcription. Therefore, it has to be transported from the cytoplasm into the nucleus when released from its inhibitory I $\kappa$ B proteins [50]. The proper translocation of NF- $\kappa$ B p65 upon stimulation by simultaneous degradation of I $\kappa$ B, also after archazolid treatment, was shown by immunofluorescence microscopy. Immunoblotting revealed an elevated activation of NF- $\kappa$ B p65 by archazolid. Unexpectedly, however, I $\kappa$ B phosphorylation remained unaffected. A possible explanation for this might base on the finding that phosphorylation at serine 536 of p65 can occur I $\kappa$ B-independent [275] and the antibody used in this study for immunoblotting detected phosphorylated p65 at Ser536. Additionally, it was found that full activity of NF- $\kappa$ B does not necessarily need degradation of I $\kappa$ B, but instead post-translational modifications such as phosphorylation at specific residues [53]. Phosphorylation at Ser536, located in the transactivation domain (TAD) of p65, usually takes place by IKK ( $\alpha$ ,  $\beta$  or  $\epsilon$ ), that are also activated by LPS, TNF $\alpha$ , AKT, p38, or directly by the NF- $\kappa$ B-activating kinase (NAK) [53]. Alternatively, phosphorylation at Ser536 is achieved by the ribosomal subunit kinase (RSK)-1. The latter acts through signaling by the tumor suppressor p53 which represents the pathway independent from I $\kappa$ B degradation and increases NF- $\kappa$ B binding to the target DNA due to decreased I $\kappa$ B affinity [276] (Figure 5.1). An activation of NF- $\kappa$ B via TNF $\alpha$  as stimulatory agent is also possible [277]. However, it could be excluded that elevation of TNF $\alpha$  levels by archazolid caused the increase of NF- $\kappa$ B activity, since NF- $\kappa$ B phosphorylation was already elevated by archazolid after 15 min whereas increased TNF $\alpha$  release by the compound was first obtained between four and eight hours, further increasing up to 24 hours. Thus, the exact mechanisms of NF- $\kappa$ B induction by archazolid could not be fully elucidated but an involvement of the pathways of IKK, or RSK-1 seem to be reasonable.

Upon transcription, the RNA transcripts have to be transported from the nucleus to the cytoplasm for translation and post-translational modifications in the ribosomes at the ER and the Golgi. Concerning this, the stability of the transcribed mRNA is a further crucial step within de novo protein biosynthesis since stabilizing mechanisms might lead to a higher translation rate, resulting in elevated protein levels. Archazolid, however, did not impair degradative processes, and enhanced stability was thus not implicated in the elevation of TNF $\alpha$  levels.

The activation of transcription factors is regulated by upstream signaling pathways, where three prominent MAPK pathways are intensively involved in the regulation of TNF $\alpha$  release from human cells, namely the ERK, the p38 MAPK, and the SAPK/JNK pathway [38, 40, 41, 278], therefore, representing possible targets for archazolid. The activation of the three MAPKs is induced by LPS in accordance with the effect of archazolid on TNF $\alpha$  release. However, phosphorylation of MEK1/2 as well as its downstream target ERK1/2 were not affected by archazolid. Activation of MEK3/6 was slightly elevated by the compound but did not result in further activation of p38 MAPK. Accordingly, it is unlikely that MEK3/6 activation causes increased TNF $\alpha$  levels. Phosphorylation of SAPK/JNK was elevated by archazolid and might

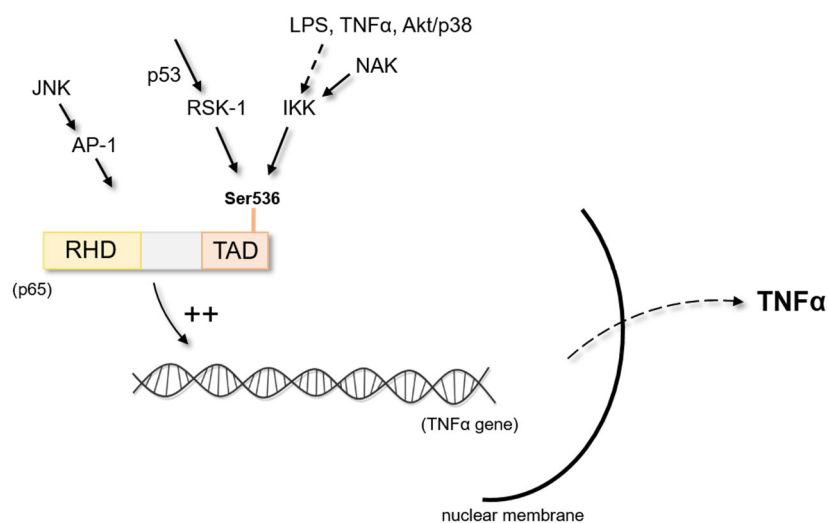


**Figure 5.1: Simplified schematic depiction of induction of NF- $\kappa$ B activity resulting in elevated TNF $\alpha$  gene transcription.** NF- $\kappa$ B activity is elevated by phosphorylation of Ser536 in the TAD of p65 achieved by p53-dependent RSK-1 or IKK that are activated by NAK or signaling through LPS, TNF $\alpha$  or Akt/p38. Transcriptional activity of NF- $\kappa$ B can additionally be induced by interference of JNK-activated AP-1. NAK, NF- $\kappa$ B-activating kinase; IKK, I $\kappa$ B kinase; RSK-1, ribosomal subunit kinase-1; AP-1, activator protein-1; RHD, Rel homology domain; TAD, transactivation domain.

therefore contribute to elevated TNF $\alpha$  levels in LPS-stimulated macrophages particularly since this kinase has been reported to regulate TNF $\alpha$  synthesis [38]. However, SAPK/JNK phosphorylation results rather in transcriptional activation of its main target activator protein (AP)-1 or members of the ATF, Ets, or Jun transcription factor families [279]. Though, phosphorylation of AP-1 positively regulates NF- $\kappa$ B's transcriptional activity [51] and might therefore indeed contribute to elevated TNF $\alpha$  levels via transcriptional interaction with NF- $\kappa$ B (Figure 5.1).

The kinase Akt has been found to be an oncogenic kinase in many cancers supporting survival mechanisms of tumor cells [49]. Furthermore, it is also implicated in cytokine synthesis [36] and contributes to an elevated NF- $\kappa$ B activity by phosphorylation of IKK in a p38 MAPK-dependent manner [280]. Since archazolid did not increase p38 MAPK activation it was not surprising that also Akt phosphorylation remained completely unaffected, supposing that elevated NF- $\kappa$ B phosphorylation as well as increased TNF $\alpha$  levels result from another pathway.

Apart from their pro-inflammatory properties, or even due to them, respectively, M1 are effective in building immune responses against pathogens but also exhibit tumor cell killing properties [157]. Responsible for this is the cytokine profile, high antigen presenting activity, and the production of toxic intermediates, as well as all factors that affect those indirectly via diverse signaling pathways. By selectively increasing TNF $\alpha$  release from M1, archazolid becomes an interesting compound in the strategy of promoting M1 functions to support anti-cancer treatments. Even more, since archazolid itself is known to exhibit potent cytotoxic effects on tumor cells [213] while not decreasing viability of human primary macrophages. Promotion of polarization of host macrophages towards M1 might thus be a promising strategy to further potentiate the efficiency of archazolid against cancer cells. To substantiate the assumption that archazolid promotes M1-related functionalities, the next step of this thesis was to investigate whether further relevant factors are affected by archazolid. Thus, the STAT proteins STAT1 and STAT3 were interesting proteins in this context due to their different roles in tumor interference [281]. As transcription factors that mediate cytokine and growth factor receptor signals to the nucleus they are relevant to M1/M2 polarization. An overexpression of STAT3 has been correlated to some types of tumors, promoting proliferation and survival, consistent with the properties of the tumor-infiltrating M2 phenotype [282]. Moreover, STAT3 inhibits anti-tumor immune responses, partly mediated by NF- $\kappa$ B [281]. Contrarily, activity of STAT1 has been rather attributed to an inhibition of cancer cell growth by enhancing the anti-tumor immunity [281, 282] that is typical for the M1 phenotype [7]. The activity

of STAT1 was elevated by archazolid in M1, whereas phosphorylation of STAT3 was slightly repressed. In M2, the activity of both transcription factors was slightly decreased by the compound. Thus, at least increased activity of STAT1 in M1 by archazolid further supports the hypothesis of its M1-promoting activity.

ROS are an effective tool of macrophages to defend the host against infectious pathogens [155]. Regarding tumor cells, the role of ROS is much more complicated, similar to the complex role of macrophages in cancer occurrence. There is evidence, that the presence of ROS can have tumor promoting effects but likewise, oxidative stress can also help to destroy cancer cells and is thus used in anti-cancer therapies [283]. This is due to the ability of the tumor to develop regulatory mechanisms which shield cancer cells from the destructive properties of ROS. However, if this sensitive balance is disturbed, for instance due to an excessive elevation of ROS, tumor cells will become sensitive to ROS and undergo ROS-induced apoptotic cell death [284] because of cell damage as a result of oxidized cellular proteins, lipids and nucleic acids [285]. ROS further cause DNA damage and participate in several signaling pathways leading to programmed cell death [270]. Generally, basal ROS levels of M1 exceed those of M2 [286]. Archazolid additionally increased ROS levels of LPS-activated macrophages which further supports the presumption of a promoted M1 phenotype by the v-ATPase inhibitor. ROS are produced from at least three different sources: during respiration in the mitochondria [287], by NADPH oxidases [288], and by several other enzymes, including lipoxygenases and cyclooxygenases [289]. Since TNF $\alpha$  activates NADPH-oxidases by different mechanisms [289], increased ROS levels might result from elevated TNF $\alpha$  levels after archazolid treatment.

There are several indicators for archazolid promoting an M1 phenotype by enhancing individual functionalities of this macrophage subtype with respect to its immunological properties that help to fight against host-destructing factors like cancer cells. In view of the reported ability of archazolid to directly eliminate tumor cells, this additional and beneficial effect on primary macrophages of the M1 phenotype has to be taken into account when using v-ATPase inhibiting agents as anti-cancer drugs.

To verify if elevated TNF $\alpha$  levels by archazolid would be able to decrease viability of cancer cells as assumed, a wash-out experiment was performed. Due to the compound's property to kill tumor cells it had to be washed out in order to avoid that remaining archazolid falsify the result. For the viability test, the cancer cell line MDA-MB-231 was used. In fact, the viability of MDA-MB-231

was reduced by the archazolid-pre-treated samples. However, using a TNF $\alpha$  antibody, these effects could not be revoked, supposing that besides TNF $\alpha$  the viability of MDA-MB-231 was reduced by additional mechanisms.

### **5.3 Enzymes of the eicosanoid metabolism are differently affected by archazolid**

The arachidonic acid-derived eicosanoids play a similar diverse role in inflammation as the cytokines since they contribute to the initiation of acute inflammation as well as to the resolution phase [290], therefore playing a key role in ITC. Although the v-ATPase is well-known to promote tumor development and inhibitors of this enzyme have been investigated in several tumor cell lines, studies about a possible benefit of v-ATPase inhibition in primary cells through interaction with the AA pathways are missing. A strong interference of archazolid with the eicosanoid pathway at different sites could be revealed but with completely different outcomes. PGE<sub>2</sub> as well as the other COX-2-derived products PGF<sub>2 $\alpha$</sub> , TxB<sub>2</sub>, 11-HETE and 12-HHT were elevated selectively in LPS- and LPS/INF- $\gamma$  stimulated macrophages by archazolid, while M2 were not affected. This was further independent of the used v-ATPase inhibitor since the incubation with apicularen and bafilomycin led to comparable results. Concerning the COX-2 products, 11-HETE was the metabolite with the largest increase by archazolid, but the differences between LPS and LPS/INF- $\gamma$  stimulation are only marginal for the most metabolites. Since not only PGE<sub>2</sub> but also other COX-2 products are elevated by archazolid, it can be assumed that COX-2 itself, but not necessarily the downstream prostanoid synthases are affected. Different intensities of increase might result from diverse kinetics of these terminal enzymes converting PGH<sub>2</sub> into their products. COX-2 related products have long been considered only as pro-inflammatory mediators that need to be suppressed by potent inhibitors [291]. Nevertheless, there is increasing evidence that these prostanoids also mediate pro-resolving events [109] decreasing disease severity in some cases and that inhibition may prevent the initiation of the resolution phase [110, 114]. In view of their physiological diversity it is not surprising that there is more than just the role as “bad guys” in inflammation. Although the undisputable pro-inflammatory properties of prostanoids must not be disregarded, their potency in stimulating the resolution of inflammation might be exploited by drug intervention. With regard to M1 and the assumption that archazolid might promote this

phenotype in various ways as described above, the stimulation of COX-2 products further supports this hypothesis.

Even though the v-ATPase has rather been related to an implication in vesicular trafficking since an intact pH homeostasis is relevant for the secretory pathway and PGE<sub>2</sub> is instead released by passive diffusion or through the active multidrug resistance protein (MRP)-4 transporter [292], the contribution of pH elevation by archazolid to increased PGE<sub>2</sub> release had to be taken into account. Thus, the PGE<sub>2</sub> levels of LPS- and LPS/IFN- $\gamma$ -stimulated macrophages pre-treated with chloroquine and ammonium chloride were measured, which emphasized an inhibition by the two pH elevating compounds, in contrast to the elevated PGE<sub>2</sub> release by archazolid. Since cPLA<sub>2</sub> activity is pH dependent [293], a higher catalytic activity due to vesicular pH elevation resulting in an increased substrate supply for COX-2 may determine PGE<sub>2</sub> synthesis. However, whereas the cPLA<sub>2</sub> $\alpha$  inhibitor RSC-3388 inhibited the release of [<sup>3</sup>H]-AA, archazolid had no effect. Equally, the activity of COX-2 itself was not affected by archazolid in agreement with the finding of Reker et al, where archazolid had only negligible effects on this enzyme at high concentrations in a cell-free assay [256]. For this reason, protein levels in LPS-stimulated macrophages were analyzed by immunoblotting. COX-2 levels seemed to be relatively low compared to primary monocytes and were therefore hard to detect, probably attributable to a loss during the seven days lasting differentiation time of monocytes to macrophages. An elevation of COX-2 protein by archazolid at 100 nM could be shown. COX-2 expression was repressed by dexamethasone as reported [257] and counteracted archazolid-induced COX-2 expression. The investigation of COX-2 transcription further supported these results since an elevation of COX-2 mRNA was detectable after four hours with a maximum at 20 hours and a nearly 7-fold increase of mRNA levels. Similar to the results achieved for the COX-2 protein levels, dexamethasone reversed this effect completely. NF- $\kappa$ B targets COX-2 and induces COX-2 expression in macrophages in a LPS-dependent manner [294]. This leads to the suggestion that elevated COX-2 transcription by archazolid is the result of the increased activity of NF- $\kappa$ B by this compound. The abrogation of archazolid's effect on COX-2 protein and mRNA levels by dexamethasone additionally supports the involvement of NF- $\kappa$ B (see also 5.2, p. 69).

Besides COX-2, the lipoxygenases (LOs) are prominent AA-metabolizing enzymes. However, the impact of archazolid on LOs was intriguingly totally different. Thus, the formation of 5-LO products (LTB<sub>4</sub>, epi/trans- LTB<sub>4</sub>, 5-HETE) were inhibited by archazolid in a concentration-

dependent manner but independent of the stimulation with LPS, LPS/INF- $\gamma$  or IL-4, whereby the strongest effect was achieved in M1. The impairment of product synthesis also in M2 was quite interesting since TNF $\alpha$  and PGE<sub>2</sub> were only affected in the M1-like phenotypes. This was also found for 15-HETE, which was, in contrast to 5-LO products, increased by archazolid, but only in M and M1, while M2 remained unaffected. 12-LO product formation did not change by the influence of archazolid, neither in M and M1, nor in M2. Shifting the AA metabolism in favor of the COX pathway by inhibiting 5-LO as it has been reported for the reverse case [295] seems to be unlikely since the difference of COX-2 effects between M1 and M2 are not explainable in this way. Since sufficient substrate supply by cPLA<sub>2</sub> for AA-converting enzymes was already investigated in the context of PGE<sub>2</sub> formation, an impact of archazolid on cPLA<sub>2</sub> activity could be excluded. Contrarily to other LOs, FLAP is only essential for the product synthesis by 5-LO, which requires the interaction with FLAP for full activity converting AA [126]. This is also supported by the finding that inhibition of FLAP by MK886 prevents leukotriene synthesis [296]. Therefore, the translocation of 5-LO and subsequent co-localization with FLAP was examined by immunofluorescence microscopy. As expected, FLAP and 5-LO did not co-localize in unstimulated macrophages, where 5-LO was mainly found in the nucleus, while FLAP was localized at the nuclear envelope. The overlay of the proteins at the nuclear membrane could be detected both in Ca<sup>2+</sup>-ionophore A23187-stimulated control cells as well as in archazolid-treated macrophages. Archazolid did therefore not result in defects of 5-LO translocation followed by impaired AA conversion. These results led us to investigate catalytically active 5- and 15-LO in cell homogenates, whereby cellular regulatory mechanisms can be excluded since in this assay large amounts of substrate and activity determining factors are supplied exogenously and spatial barriers are removed. Due to the inhibition of 5-LO products by archazolid in homogenates as well, it can be assumed that archazolid exhibits a direct effect on the enzyme, which is further supported by the impact on both macrophage subtypes. Apart from AA, 5-LO converts other fatty acids, such as eicosatrienoic acid (ETA, 20:3  $\omega$ -9) and eicosapentaenoic acid (EPA, 20:5  $\omega$ -3). Archazolid also inhibited ETA-derived 5-HETrE and EPA-derived 5-HEPE in a similar strength as AA-derived 5-HETE, concluding that archazolid directly interferes with 5-LO. Moreover, these findings are in agreement with previous studies that revealed direct inhibition of 5-LO by archazolid in a cell-free assay [256]. Pharmacophore studies emphasized a large compliance of pharmacophoric features between AA and archazolid (Figure 5.2) that could further be confirmed for bafilomycin and apicularen [256]. Contrarily, it was shown that the active-site pocket of COX-

2 is too buried and narrow for archazolid to access it, which might be an explanation for the opposing effects found for archazolid on 5-LO and COX-2 of macrophages. To exclude the possibility of an effect of archazolid on protein levels of 5-LO, immunoblotting of 5-LO in M1 and M2 was done which confirmed unaffected 5-LO expression levels.

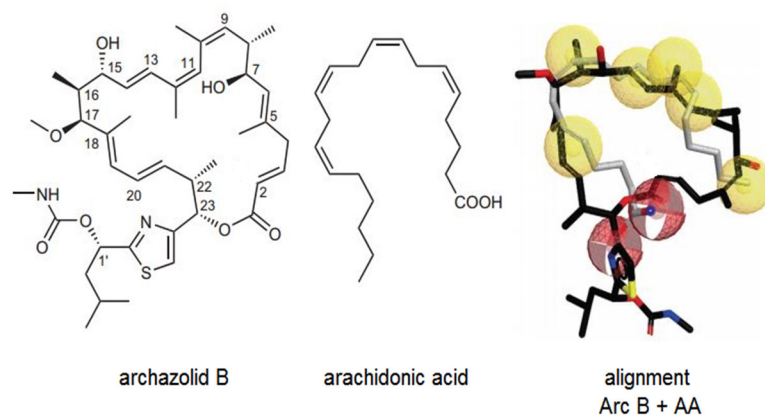


**Figure 5.2: Pharmacophore alignment of archazolid and AA.** Yellow: hydrophobic interaction points; red: hydrogen-bond acceptor positions. Adapted from Reker et al [256]. Reprinted by permission from Macmillan Publishers Ltd: *Nature Chemistry* 6, 1072–1078, copyright 2014.

Nevertheless, homogenates of M1 and M2 revealed unexpected results regarding the product formation of 5-LO, namely an inhibition of 15-HETE in M2 but an increase of 15-HETE in M1, even though this was not as strong as in intact cells. There are reports about some differences with respect to the 5-LO in M1 and M2 which could give a clue for the opposing effects by archazolid. Examples are the higher expression of 15-LOX-2 towards 15-LOX-1 in M1 [105], the higher substrate specificity for AA of 15-LOX-2 [105, 297], low suicide inactivation of 15-LOX-2 [297], and its higher specificity for the position of oxygen insertion at C-15 [298]. Although these features might explain higher 15-HETE production in M1 in general (considering those, the stimulation with AA for 15 min taking only 15- not 12-HETE into account are adverse conditions for 15-LOX-1), they do not reveal clear explanations for the effects achieved by archazolid. Since 5-LO converts 15-HETE into lipoxins and 5-LO is inhibited by archazolid, increased 15-HETE levels in M1 might result from an accumulation of non-transformed 15-HETE. However, 5-LO is inhibited in M2 as well but 15-HETE elevation could only be observed in M1. Other possibilities might base on 15-HETE found in some cells to be a by-product of COX and even suppressing the 5-LO pathway [299], or on a cross-talk between the pathways of COX and 5-LO leading to a mutual activation [300]. Incubation of M and M1 with the COX-inhibitor dexamethasone showed indeed an inhibition of 15-HETE formation, supporting the idea of COX-2 being responsible for 15-HETE elevation. However, inhibition of 15-HETE formation by archazolid in homogenates of M2 cannot

be explained by 15-HETE being a by-product of COX-2 since PGE<sub>2</sub> and other COX-2 products were not affected by archazolid in M2. Finally, lacking the elevating effect of archazolid on 15-HETE in M2 might result from an increased incorporation of 15-HETE in membranes induced especially by IL-4 stimulation [301], resulting in less amounts of 15-HETE in supernatants of M2. Concluding, although there are some conceivable approaches for increased 15-HETE by archazolid in M1, the accompanying inhibitory effect of the compound on 15-HETE in M2 remains incompletely understood.

In conclusion, the results of this thesis show that archazolid selectively elevates TNF $\alpha$  release from LPS- and LPS/IFN- $\gamma$ -stimulated macrophages whereas IL-4-stimulated macrophages remain unaffected. We could attribute increased TNF $\alpha$  levels to an elevation of transcription of TNF $\alpha$  by archazolid due to enhanced NF-kB activity. However, no effects on other investigated cytokines could be revealed by archazolid in neither M, M1 nor M2, which supports the selectivity of the compound's effect on TNF $\alpha$ . As expected of a v-ATPase inhibitor, archazolid was shown to elevate vesicular pH but nevertheless, cell viability as well as cellular integrity of polarized macrophages were not impaired. This fact combined with selective TNF $\alpha$  elevation by archazolid highlights the beneficial effects in terms of cancer treatment besides purely cytotoxic effects of archazolid on cancer cells. Furthermore, we revealed the AA cascade as target of archazolid due to its various effects on involved LOs. Inhibited 5-LO product formation in polarized macrophages besides elevated 15-HETE production in M1 by archazolid emphasizes the relevance of the v-ATPase in eicosanoid formation and additionally demonstrates the potential of v-ATPase inhibitors to promote an anti-inflammatory pro-resolving eicosanoid status.

## 6 REFERENCES

1. Forgac, M., *Vacuolar ATPases: rotary proton pumps in physiology and pathophysiology*. Nat Rev Mol Cell Biol, 2007. **8**(11): p. 917-29.
2. Wagner, C.A., et al., *Renal vacuolar H<sup>+</sup>-ATPase*. Physiol Rev, 2004. **84**(4): p. 1263-314.
3. Forgac, M., *Structure, function and regulation of the vacuolar (H<sup>+</sup>)-ATPases*. FEBS Lett, 1998. **440**(3): p. 258-63.
4. Hoefle, G., et al., *Archazolides, method of preparing them and agents containing them*. 1993, Google Patents.
5. von Schwarzenberg, K., et al., *Mode of cell death induction by pharmacological vacuolar H<sup>+</sup>-ATPase (V-ATPase) inhibition*. J Biol Chem, 2013. **288**(2): p. 1385-96.
6. Wang, N., H. Liang, and K. Zen, *Molecular mechanisms that influence the macrophage m1-m2 polarization balance*. Front Immunol, 2014. **5**: p. 614.
7. Mantovani, A., et al., *The chemokine system in diverse forms of macrophage activation and polarization*. Trends Immunol, 2004. **25**(12): p. 677-86.
8. Lacy, P. and J.L. Stow, *Cytokine release from innate immune cells: association with diverse membrane trafficking pathways*. Blood, 2011. **118**(1): p. 9-18.
9. Carswell, E.A., et al., *An endotoxin-induced serum factor that causes necrosis of tumors*. Proceedings of the National Academy of Sciences, 1975. **72**(9): p. 3666-3670.
10. Mocellin, S., et al., *Tumor necrosis factor, cancer and anticancer therapy*. Cytokine & Growth Factor Reviews, 2005. **16**(1): p. 35-53.
11. Peters-Golden, M. and W.R. Henderson, *Leukotrienes*. New England Journal of Medicine, 2007. **357**(18): p. 1841-1854.
12. Levy, B.D., et al., *Human alveolar macrophages have 15-lipoxygenase and generate 15(S)-hydroxy-5,8,11-cis-13-trans-eicosatetraenoic acid and lipoxins*. J Clin Invest, 1993. **92**(3): p. 1572-9.
13. Smith, W.L., Y. Urade, and P.J. Jakobsson, *Enzymes of the cyclooxygenase pathways of prostanoid biosynthesis*. Chem Rev, 2011. **111**(10): p. 5821-65.
14. Scher, J.U. and M.H. Pillinger, *The anti-inflammatory effects of prostaglandins*. J Investig Med, 2009. **57**(6): p. 703-8.
15. Medzhitov, R., *Inflammation 2010: New Adventures of an Old Flame*. Cell, 2010. **140**(6): p. 771-776.
16. Kumar, R., et al., *The dynamics of acute inflammation*. Journal of Theoretical Biology, 2004. **230**(2): p. 145-155.
17. Medzhitov, R., *Origin and physiological roles of inflammation*. Nature, 2008. **454**(7203): p. 428-435.
18. Sherwood, E.R. and T. Toliver-Kinsky, *Mechanisms of the inflammatory response*. Best Practice & Research Clinical Anaesthesiology, 2004. **18**(3): p. 385-405.
19. Serhan, C.N., et al., *Fundamentals of Inflammation*. 2010: Cambridge University Press.
20. Serhan, C.N. and J. Savill, *Resolution of inflammation: the beginning programs the end*. Nat Immunol, 2005. **6**(12): p. 1191-7.
21. Serhan, C.N., et al., *Resolution of inflammation: state of the art, definitions and terms*. FASEB J, 2007. **21**(2): p. 325-32.
22. Nathan, C. and A. Ding, *Nonresolving Inflammation*. Cell, 2010. **140**(6): p. 871-882.

23. Arnold, L., et al., *Inflammatory monocytes recruited after skeletal muscle injury switch into antiinflammatory macrophages to support myogenesis*. The Journal of Experimental Medicine, 2007. **204**(5): p. 1057-1069.
24. Serhan, C.N., *Resolution phase of inflammation: novel endogenous anti-inflammatory and proresolving lipid mediators and pathways*. Annu Rev Immunol, 2007. **25**: p. 101-37.
25. Gilroy, D.W., et al., *Inducible cyclooxygenase may have anti-inflammatory properties*. Nature medicine, 1999. **5**(6): p. 698-701.
26. Aggarwal, B.B., et al., *Inflammation and cancer: How hot is the link?* Biochemical Pharmacology, 2006. **72**(11): p. 1605-1621.
27. Nathan, C., *Points of control in inflammation*. Nature, 2002. **420**(6917): p. 846-52.
28. Manabe, I., *Chronic Inflammation Links Cardiovascular, Metabolic and Renal Diseases*. Circulation Journal, 2011. **75**(12): p. 2739-2748.
29. Coussens, L.M. and Z. Werb, *Inflammation and cancer*. Nature, 2002. **420**(6917): p. 860-867.
30. Mantovani, A., *Cancer: inflammation by remote control*. Nature, 2005. **435**(7043): p. 752-3.
31. Balkwill, F. and A. Mantovani, *Inflammation and cancer: back to Virchow?* The Lancet, 2001. **357**(9255): p. 539-545.
32. Allavena, P., et al., *The chemokine receptor switch paradigm and dendritic cell migration: its significance in tumor tissues*. Immunological Reviews, 2000. **177**(1): p. 141-149.
33. Iwasaki, A. and R. Medzhitov, *Toll-like receptor control of the adaptive immune responses*. Nat Immunol, 2004. **5**(10): p. 987-95.
34. Viriyakosol, S., et al., *MD-2 binds to bacterial lipopolysaccharide*. J Biol Chem, 2001. **276**(41): p. 38044-51.
35. Nagai, Y., et al., *Essential role of MD-2 in LPS responsiveness and TLR4 distribution*. Nat Immunol, 2002. **3**(7): p. 667-672.
36. Tapia-Abellan, A., et al., *Role of MAP kinases and PI3K-Akt on the cytokine inflammatory profile of peritoneal macrophages from the ascites of cirrhotic patients*. Liver Int, 2013. **33**(4): p. 552-60.
37. Karin, M., *Inflammation-activated protein kinases as targets for drug development*. Proc Am Thorac Soc, 2005. **2**(4): p. 386-90; discussion 394-5.
38. Swantek, J.L., M.H. Cobb, and T.D. Geppert, *Jun N-terminal kinase/stress-activated protein kinase (JNK/SAPK) is required for lipopolysaccharide stimulation of tumor necrosis factor alpha (TNF-alpha) translation: glucocorticoids inhibit TNF-alpha translation by blocking JNK/SAPK*. Mol Cell Biol, 1997. **17**(11): p. 6274-82.
39. Bhat, N.R., et al., *Extracellular signal-regulated kinase and p38 subgroups of mitogen-activated protein kinases regulate inducible nitric oxide synthase and tumor necrosis factor-alpha gene expression in endotoxin-stimulated primary glial cultures*. J Neurosci, 1998. **18**(5): p. 1633-41.
40. Lee, J.C., et al., *A protein kinase involved in the regulation of inflammatory cytokine biosynthesis*. Nature, 1994. **372**(6508): p. 739-46.
41. Mahtani, K.R., et al., *Mitogen-activated protein kinase p38 controls the expression and posttranslational modification of tristetraprolin, a regulator of tumor necrosis factor alpha mRNA stability*. Mol Cell Biol, 2001. **21**(19): p. 6461-9.
42. Dumitru, C.D., et al., *TNF- $\alpha$  Induction by LPS Is Regulated Posttranscriptionally via a Tpl2/ERK-Dependent Pathway*. Cell, 2000. **103**(7): p. 1071-1083.

43. Kaisho, T. and S. Akira, *Toll-like receptor function and signaling*. J Allergy Clin Immunol, 2006. **117**(5): p. 979-87; quiz 988.
44. Kawai, T. and S. Akira, *The role of pattern-recognition receptors in innate immunity: update on Toll-like receptors*. Nat Immunol, 2010. **11**(5): p. 373-84.
45. Song, G., G. Ouyang, and S. Bao, *The activation of Akt/PKB signaling pathway and cell survival*. Journal of cellular and molecular medicine, 2005. **9**(1): p. 59-71.
46. Nidai Ozes, O., et al., *NF-[kappa]B activation by tumour necrosis factor requires the Akt serine-threonine kinase*. Nature, 1999. **401**(6748): p. 82-85.
47. Pengal, R.A., et al., *Lipopolysaccharide-induced production of interleukin-10 is promoted by the serine/threonine kinase Akt*. Molecular Immunology, 2006. **43**(10): p. 1557-1564.
48. Antoniv, T.T. and L.B. Ivashkiv, *Interleukin-10-induced gene expression and suppressive function are selectively modulated by the PI3K-Akt-GSK3 pathway*. Immunology, 2011. **132**(4): p. 567-577.
49. Nicholson, K.M. and N.G. Anderson, *The protein kinase B/Akt signalling pathway in human malignancy*. Cellular Signalling, 2002. **14**(5): p. 381-395.
50. Perkins, N.D. and T.D. Gilmore, *Good cop, bad cop: the different faces of NF-kappaB*. Cell Death Differ, 2006. **13**(5): p. 759-72.
51. Karin, M. and Y. Ben-Neriah, *Phosphorylation meets ubiquitination: the control of NF-kB activity*. Annual review of immunology, 2000. **18**(1): p. 621-663.
52. Campbell, K. and N. Perkins, *Post-translational modification of RelA (p65) NF-kB*. Biochemical Society Transactions, 2004. **32**(6): p. 1087-1089.
53. Chen, L.-F. and W.C. Greene, *Shaping the nuclear action of NF-[kappa]B*. Nat Rev Mol Cell Biol, 2004. **5**(5): p. 392-401.
54. Shishodia, S. and B.B. Aggarwal, *Nuclear factor-kB: a friend or a foe in cancer?* Biochemical Pharmacology, 2004. **68**(6): p. 1071-1080.
55. Viatour, P., et al., *Phosphorylation of NF-kappaB and IkappaB proteins: implications in cancer and inflammation*. Trends Biochem Sci, 2005. **30**(1): p. 43-52.
56. Huang, S., et al., *Nuclear Factor-kB Activity Correlates with Growth, Angiogenesis, and Metastasis of Human Melanoma Cells in Nude Mice*. Clinical Cancer Research, 2000. **6**(6): p. 2573-2581.
57. Darnell, J., I. Kerr, and G. Stark, *Jak-STAT pathways and transcriptional activation in response to IFNs and other extracellular signaling proteins*. Science, 1994. **264**(5164): p. 1415-1421.
58. O'Shea, John J. and R. Plenge, *JAK and STAT Signaling Molecules in Immunoregulation and Immune-Mediated Disease*. Immunity, 2012. **36**(4): p. 542-550.
59. Turkson, J., *STAT proteins as novel targets for cancer drug discovery*. Expert Opinion on Therapeutic Targets, 2004. **8**(5): p. 409-422.
60. Yu, H. and R. Jove, *The STATs of cancer—new molecular targets come of age*. Nature Reviews Cancer, 2004. **4**(2): p. 97-105.
61. Buettner, R., L.B. Mora, and R. Jove, *Activated STAT signaling in human tumors provides novel molecular targets for therapeutic intervention*. Clinical cancer research, 2002. **8**(4): p. 945-954.
62. Sica, A. and V. Bronte, *Altered macrophage differentiation and immune dysfunction in tumor development*. The Journal of clinical investigation, 2007. **117**(5): p. 1155-1166.
63. Dinarello, C.A., *PRo-inflammatory cytokines\**. Chest, 2000. **118**(2): p. 503-508.
64. Lippitz, B.E., *Cytokine patterns in patients with cancer: a systematic review*. The Lancet Oncology, 2013. **14**(6): p. e218-e228.

65. Lin, W.W. and M. Karin, *A cytokine-mediated link between innate immunity, inflammation, and cancer*. J Clin Invest, 2007. **117**(5): p. 1175-83.
66. O'Malley, W.E., B. Achinstein, and M.J. Shear, *Action of Bacterial Polysaccharide on Tumors. II. Damage of Sarcoma 37 by Serum of Mice Treated With Serratia Marcescens Polysaccharide, and Induced Tolerance*. Journal of the National Cancer Institute, 1962. **29**(6): p. 1169-1175.
67. Aggarwal, B.B., et al., *Human tumor necrosis factor. Production, purification, and characterization*. Journal of Biological Chemistry, 1985. **260**(4): p. 2345-2354.
68. Bradley, J.R., *TNF-mediated inflammatory disease*. J Pathol, 2008. **214**(2): p. 149-60.
69. Tracey, K.J. and A. Cerami, *Tumor necrosis factor, other cytokines and disease*. Annual review of cell biology, 1993. **9**(1): p. 317-343.
70. Baud, V. and M. Karin, *Signal transduction by tumor necrosis factor and its relatives*. Trends in Cell Biology, 2001. **11**(9): p. 372-377.
71. Eggermont, A.M.M., J.H.W. de Wilt, and T.L.M. ten Hagen, *Current uses of isolated limb perfusion in the clinic and a model system for new strategies*. The Lancet Oncology, 2003. **4**(7): p. 429-437.
72. Lejeune, F.J., C. Rüegg, and D. Liénard, *Clinical applications of TNF- $\alpha$  in cancer*. Current opinion in immunology, 1998. **10**(5): p. 573-580.
73. Malik, S.T.A., et al., *Paradoxical effects of tumour necrosis factor in experimental ovarian cancer*. International Journal of Cancer, 1989. **44**(5): p. 918-925.
74. Balkwill, F.R., et al., *Human tumor xenografts treated with recombinant human tumor necrosis factor alone or in combination with interferons*. Cancer Res, 1986. **46**(8): p. 3990-3.
75. Talmadge, J.E., et al., *Immunomodulatory properties of recombinant murine and human tumor necrosis factor*. Cancer Res, 1988. **48**(3): p. 544-50.
76. Balkwill, F.R., *Tumour necrosis factor*. British Medical Bulletin, 1989. **45**(2): p. 389-400.
77. Balkwill, F., *Tumour necrosis factor and cancer*. Nature Reviews Cancer, 2009. **9**(5): p. 361-371.
78. Creasey, A.A., M.T. Reynolds, and W. Laird, *Cures and partial regression of murine and human tumors by recombinant human tumor necrosis factor*. Cancer research, 1986. **46**(11): p. 5687-5690.
79. Balkwill, F., *Tumor necrosis factor or tumor promoting factor?* Cytokine and Growth Factor Reviews, 2002. **13**(2): p. 135-141.
80. Havell, E.A., W. Fiers, and R.J. North, *The antitumor function of tumor necrosis factor (TNF), I. Therapeutic action of TNF against an established murine sarcoma is indirect, immunologically dependent, and limited by severe toxicity*. J Exp Med, 1988. **167**(3): p. 1067-85.
81. de Paula Rogerio, A., et al., *The role of lipids mediators in inflammation and resolution*. Biomed Res Int, 2015. **2015**: p. 605959.
82. Needleman, P., et al., *Arachidonic acid metabolism*. Annual review of biochemistry, 1986. **55**(1): p. 69-102.
83. Smith, W.L., D.L. DeWitt, and R.M. Garavito, *Cyclooxygenases: structural, cellular, and molecular biology*. Annual review of biochemistry, 2000. **69**(1): p. 145-182.
84. Mestre, J.R., et al., *Redundancy in the signaling pathways and promoter elements regulating cyclooxygenase-2 gene expression in endotoxin-treated macrophage/monocytic cells*. J Biol Chem, 2001. **276**(6): p. 3977-82.

85. Murakami, M. and I. Kudo, *Recent advances in molecular biology and physiology of the prostaglandin E2-biosynthetic pathway*. Progress in Lipid Research, 2004. **43**(1): p. 3-35.
86. Scheinman, R.I., et al., *Role of transcriptional activation of I kappa B alpha in mediation of immunosuppression by glucocorticoids*. Science, 1995. **270**(5234): p. 283-6.
87. Auphan, N., et al., *Immunosuppression by glucocorticoids: Inhibition of NF- $\kappa$ B activity through induction of I $\kappa$ B synthesis*. Science, 1995. **270**(5234): p. 286-290.
88. Gilbert, N.C., et al., *The structure of human 5-lipoxygenase*. Science, 2011. **331**(6014): p. 217-9.
89. Radmark, O., et al., *5-Lipoxygenase: regulation of expression and enzyme activity*. Trends Biochem Sci, 2007. **32**(7): p. 332-41.
90. Borgeat, P. and B. Samuelsson, *Arachidonic acid metabolism in polymorphonuclear leukocytes: Effects of ionophore A23187*. Proceedings of the National Academy of Sciences, 1979. **76**(5): p. 2148-2152.
91. Puustinen, T., M.M. Scheffer, and B. Samuelsson, *Regulation of the human leukocyte 5-lipoxygenase: stimulation by micromolar Ca<sup>2+</sup> levels and phosphatidylcholine vesicles*. Biochimica et Biophysica Acta (BBA) - Lipids and Lipid Metabolism, 1988. **960**(3): p. 261-267.
92. Kulkarni, S., et al., *Molecular Basis of the Specific Subcellular Localization of the C2-like Domain of 5-Lipoxygenase*. Journal of Biological Chemistry, 2002. **277**(15): p. 13167-13174.
93. Noguchi, M., et al., *Human 5-lipoxygenase associates with phosphatidylcholine liposomes and modulates LTA4 synthetase activity*. Biochimica et Biophysica Acta (BBA) - Lipids and Lipid Metabolism, 1994. **1215**(3): p. 300-306.
94. Rakonjac, M., et al., *Coactosin-like protein supports 5-lipoxygenase enzyme activity and up-regulates leukotriene A4 production*. Proceedings of the National Academy of Sciences, 2006. **103**(35): p. 13150-13155.
95. Rådmark, O. and B. Samuelsson, *Regulation of 5-lipoxygenase enzyme activity*. Biochemical and biophysical research communications, 2005. **338**(1): p. 102-110.
96. Ochi, K., et al., *Arachidonate 5-lipoxygenase of guinea pig peritoneal polymorphonuclear leukocytes. Activation by adenosine 5'-triphosphate*. Journal of Biological Chemistry, 1983. **258**(9): p. 5754-5758.
97. Luo, M., et al., *Protein Kinase A Inhibits Leukotriene Synthesis by Phosphorylation of 5-Lipoxygenase on Serine 523*. Journal of Biological Chemistry, 2004. **279**(40): p. 41512-41520.
98. Leslie, C.C., *Regulation of the specific release of arachidonic acid by cytosolic phospholipase A2*. Prostaglandins, Leukotrienes and Essential Fatty Acids, 2004. **70**(4): p. 373-376.
99. Dixon, R.A.F., et al., *Requirement of a 5-lipoxygenase-activating protein for leukotriene synthesis*. Nature, 1990. **343**(6255): p. 282-284.
100. Chen, X.S. and C.D. Funk, *Structure-function properties of human platelet 12-lipoxygenase: chimeric enzyme and in vitro mutagenesis studies*. The FASEB Journal, 1993. **7**(8): p. 694-701.
101. Kuhn, H., M. Walther, and R.J. Kuban, *Mammalian arachidonate 15-lipoxygenases: Structure, function, and biological implications*. Prostaglandins & Other Lipid Mediators, 2002. **68-69**: p. 263-290.

102. Conrad, D.J., et al., *Specific inflammatory cytokines regulate the expression of human monocyte 15-lipoxygenase*. Proceedings of the National Academy of Sciences, 1992. **89**(1): p. 217-221.
103. Brash, A.R., W.E. Boeglin, and M.S. Chang, *Discovery of a second 15S-lipoxygenase in humans*. Proc Natl Acad Sci U S A, 1997. **94**(12): p. 6148-52.
104. Setsu, N., et al., *Interferon- $\gamma$ -induced 15-lipoxygenase-2 expression in normal human epidermal keratinocytes and a pathogenic link to psoriasis vulgaris*. European Journal of Dermatology, 2006. **16**(2): p. 141-145.
105. Wuest, S.J., et al., *Expression and regulation of 12/15-lipoxygenases in human primary macrophages*. Atherosclerosis, 2012. **225**(1): p. 121-7.
106. Hennig, R., et al., *15-Lipoxygenase-1 Production is Lost in Pancreatic Cancer and Overexpression of the Gene Inhibits Tumor Cell Growth*. Neoplasia, 2007. **9**(11): p. 917-926.
107. Feng, Y., et al., *Downregulation of 15-lipoxygenase 2 by glucocorticoid receptor in prostate cancer cells*. International journal of oncology, 2010. **36**(6): p. 1541-1549.
108. Funk, C.D., *Prostaglandins and leukotrienes: advances in eicosanoid biology*. Science, 2001. **294**(5548): p. 1871-5.
109. Serhan, C.N., N. Chiang, and T.E. Van Dyke, *Resolving inflammation: dual anti-inflammatory and pro-resolution lipid mediators*. Nat Rev Immunol, 2008. **8**(5): p. 349-361.
110. Frolov, A., et al., *Anti-inflammatory properties of prostaglandin E2: deletion of microsomal prostaglandin E synthase-1 exacerbates non-immune inflammatory arthritis in mice*. Prostaglandins Leukot Essent Fatty Acids, 2013. **89**(5): p. 351-8.
111. Fadok, V.A., et al., *Macrophages that have ingested apoptotic cells in vitro inhibit proinflammatory cytokine production through autocrine/paracrine mechanisms involving TGF- $\beta$ , PGE2, and PAF*. Journal of Clinical Investigation, 1998. **101**(4): p. 890-898.
112. Freire-de-Lima, C.G., et al., *Apoptotic Cells, through Transforming Growth Factor- $\beta$ , Coordinately Induce Anti-inflammatory and Suppress Pro-inflammatory Eicosanoid and NO Synthesis in Murine Macrophages*. Journal of Biological Chemistry, 2006. **281**(50): p. 38376-38384.
113. Levy, B.D., et al., *Lipid mediator class switching during acute inflammation: signals in resolution*. Nat Immunol, 2001. **2**(7): p. 612-9.
114. Bandeira-Melo, C., et al., *Cyclooxygenase-2-Derived Prostaglandin E2 and Lipoxin A4 Accelerate Resolution of Allergic Edema in Angiostrongylus costaricensis-Infected Rats: Relationship with Concurrent Eosinophilia*. The Journal of Immunology, 2000. **164**(2): p. 1029-1036.
115. Pons, F., et al., *Pro-inflammatory and anti-inflammatory effects of the stable prostaglandin D2 analogue, ZK 118.182*. European Journal of Pharmacology, 1994. **261**(3): p. 237-247.
116. Rajakariar, R., et al., *Hematopoietic prostaglandin D2 synthase controls the onset and resolution of acute inflammation through PGD2 and 15-deoxyDelta12 14 PGJ2*. Proc Natl Acad Sci U S A, 2007. **104**(52): p. 20979-84.
117. Smyth, E.M., *Thromboxane and the thromboxane receptor in cardiovascular disease*. Clinical lipidology, 2010. **5**(2): p. 209-219.
118. Ricciotti, E. and G.A. FitzGerald, *Prostaglandins and inflammation*. Arterioscler Thromb Vasc Biol, 2011. **31**(5): p. 986-1000.

119. Ding, X. and P.A. Murray, *Cellular mechanisms of thromboxane A<sub>2</sub>-mediated contraction in pulmonary veins*. American Journal of Physiology-Lung Cellular and Molecular Physiology, 2005. **289**(5): p. L825-L833.
120. Cheng, Y., et al., *Role of Prostacyclin in the Cardiovascular Response to Thromboxane A<sub>2</sub>*. Science, 2002. **296**(5567): p. 539-541.
121. Kobayashi, T., et al., *Roles of thromboxane A<sub>2</sub> and prostacyclin in the development of atherosclerosis in apoE-deficient mice*. The Journal of clinical investigation, 2004. **114**(6): p. 784-794.
122. Ishizuka, et al., *Stimulation with thromboxane A<sub>2</sub> (TXA<sub>2</sub>) receptor agonist enhances ICAM-1, VCAM-1 or ELAM-1 expression by human vascular endothelial cells*. Clinical & Experimental Immunology, 1998. **112**(3): p. 464-470.
123. Nie, D., et al., *Thromboxane A<sub>2</sub> Regulation of Endothelial Cell Migration, Angiogenesis, and Tumor Metastasis*. Biochemical and Biophysical Research Communications, 2000. **267**(1): p. 245-251.
124. Ashton, A.W. and J.A. Ware, *Thromboxane A<sub>2</sub> receptor signaling inhibits vascular endothelial growth factor-induced endothelial cell differentiation and migration*. Circ Res, 2004. **95**(4): p. 372-9.
125. Peters-Golden, M. and R.W. McNish, *Redistribution of 5-lipoxygenase and cytosolic phospholipase A<sub>2</sub> to the nuclear fraction upon macrophage activation*. Biochem Biophys Res Commun, 1993. **196**(1): p. 147-53.
126. Peters-Golden, M. and T.G. Brock, *5-lipoxygenase and FLAP*. Prostaglandins Leukot Essent Fatty Acids, 2003. **69**(2-3): p. 99-109.
127. Spector, A.A., J.A. Gordon, and S.A. Moore, *Hydroxyeicosatetraenoic acids (HETEs)*. Progress in Lipid Research, 1988. **27**(4): p. 271-323.
128. Borgeat, P. and B. Samuelsson, *Arachidonic acid metabolism in polymorphonuclear leukocytes: unstable intermediate in formation of dihydroxy acids*. Proc Natl Acad Sci U S A, 1979. **76**(7): p. 3213-7.
129. Hammarstrom, S., *Leukotrienes*. Annual review of biochemistry, 1983. **52**(1): p. 355-377.
130. Yokomizo, T., T. Izumi, and T. Shimizu, *Leukotriene B<sub>4</sub>: Metabolism and Signal Transduction*. Archives of Biochemistry and Biophysics, 2001. **385**(2): p. 231-241.
131. Devchand, P.R., et al., *The PPAR $\alpha$ -leukotriene B<sub>4</sub> pathway to inflammation control*. Nature, 1996. **384**(6604): p. 39-43.
132. Nicosia, S., V. Capra, and G.E. Rovati, *Leukotrienes as Mediators of Asthma*. Pulmonary Pharmacology & Therapeutics, 2001. **14**(1): p. 3-19.
133. Samuelsson, B., *Leukotrienes: mediators of immediate hypersensitivity reactions and inflammation*. Science, 1983. **220**(4597): p. 568-575.
134. Serhan, C.N., M. Hamberg, and B. Samuelsson, *Lipoxins: novel series of biologically active compounds formed from arachidonic acid in human leukocytes*. Proceedings of the National Academy of Sciences, 1984. **81**(17): p. 5335-5339.
135. Stables, M.J. and D.W. Gilroy, *Old and new generation lipid mediators in acute inflammation and resolution*. Progress in Lipid Research, 2011. **50**(1): p. 35-51.
136. Serhan, C.N., *Lipoxin biosynthesis and its impact in inflammatory and vascular events*. Biochim Biophys Acta, 1994. **1212**(1): p. 1-25.
137. Takata, S., et al., *Remodeling of neutrophil phospholipids with 15(S)-hydroxyeicosatetraenoic acid inhibits leukotriene B<sub>4</sub>-induced neutrophil migration across endothelium*. J Clin Invest, 1994. **93**(2): p. 499-508.

138. Girton, R.A., A.A. Spector, and J.A. Gordon, *15-HETE: selective incorporation into inositol phospholipids of MDCK cells*. *Kidney international*, 1994. **45**(4): p. 972-980.
139. Takano, T., et al., *Neutrophil-mediated changes in vascular permeability are inhibited by topical application of aspirin-triggered 15-epi-lipoxin A4 and novel lipoxin B4 stable analogues*. *Journal of Clinical Investigation*, 1998. **101**(4): p. 819.
140. Maddox, J.F. and C.N. Serhan, *Lipoxin A4 and B4 are potent stimuli for human monocyte migration and adhesion: selective inactivation by dehydrogenation and reduction*. *J Exp Med*, 1996. **183**(1): p. 137-46.
141. Godson, C., et al., *Cutting edge: lipoxins rapidly stimulate nonphlogistic phagocytosis of apoptotic neutrophils by monocyte-derived macrophages*. *The Journal of Immunology*, 2000. **164**(4): p. 1663-1667.
142. Mitchell, S., et al., *Lipoxins, Aspirin-Triggered Epi-Lipoxins, Lipoxin Stable Analogues, and the Resolution of Inflammation: Stimulation of Macrophage Phagocytosis of Apoptotic Neutrophils In Vivo*. *Journal of the American Society of Nephrology*, 2002. **13**(10): p. 2497-2507.
143. Hume, D.A., *The mononuclear phagocyte system*. *Current Opinion in Immunology*, 2006. **18**(1): p. 49-53.
144. Mosser, D.M. and J.P. Edwards, *Exploring the full spectrum of macrophage activation*. *Nat Rev Immunol*, 2008. **8**(12): p. 958-69.
145. Pollard, J.W., *Trophic macrophages in development and disease*. *Nat Rev Immunol*, 2009. **9**(4): p. 259-70.
146. Gordon, S. and P.R. Taylor, *Monocyte and macrophage heterogeneity*. *Nat Rev Immunol*, 2005. **5**(12): p. 953-64.
147. Kono, H. and K.L. Rock, *How dying cells alert the immune system to danger*. *Nat Rev Immunol*, 2008. **8**(4): p. 279-289.
148. Gordon, S., *Pattern Recognition Receptors: Doubling Up for the Innate Immune Response*. *Cell*, 2002. **111**(7): p. 927-930.
149. Mills, C.D., et al., *M-1/M-2 Macrophages and the Th1/Th2 Paradigm*. *The Journal of Immunology*, 2000. **164**(12): p. 6166-6173.
150. Martinez, F.O., et al., *Macrophage activation and polarization*. *Front Biosci*, 2008. **13**: p. 453-61.
151. Mosser, D.M., *The many faces of macrophage activation*. *Journal of Leukocyte Biology*, 2003. **73**(2): p. 209-212.
152. Schwartz, Y. and A.V. Svisltnik, *Functional phenotypes of macrophages and the M1-M2 polarization concept. Part I. Proinflammatory phenotype*. *Biochemistry (Mosc)*, 2012. **77**(3): p. 246-60.
153. Boehm, U., et al., *Cellular responses to interferon- $\gamma$* . *Annual review of immunology*, 1997. **15**(1): p. 749-795.
154. Alan, R., B. Ezekowitz, and S. Gordon, *Alterations of Surface Properties by Macrophage Activation: Expression of Receptors for Fc and Mannose-Terminal Glycoproteins and Differentiation Antigens*, in *Macrophage Activation*, D.O. Adams and M.G. Hanna, Editors. 1984, Springer US: Boston, MA. p. 33-56.
155. Murray, H.W. and Z.A. Cohn, *Macrophage oxygen-dependent antimicrobial activity. III. Enhanced oxidative metabolism as an expression of macrophage activation*. *The Journal of Experimental Medicine*, 1980. **152**(6): p. 1596-1609.

156. Gruenheid, S. and P. Gros, *Genetic susceptibility to intracellular infections: Nramp1, macrophage function and divalent cations transport*. *Current Opinion in Microbiology*, 2000. **3**(1): p. 43-48.
157. Sica, A., et al., *Macrophage polarization in tumour progression*. *Semin Cancer Biol*, 2008. **18**(5): p. 349-55.
158. Stein, M., et al., *Interleukin 4 potently enhances murine macrophage mannose receptor activity: a marker of alternative immunologic macrophage activation*. *The Journal of experimental medicine*, 1992. **176**(1): p. 287-292.
159. Gordon, S., *Alternative activation of macrophages*. *Nat Rev Immunol*, 2003. **3**(1): p. 23-35.
160. Kristiansen, M., et al., *Identification of the haemoglobin scavenger receptor*. *Nature*, 2001. **409**(6817): p. 198-201.
161. Hesse, M., et al., *Differential Regulation of Nitric Oxide Synthase-2 and Arginase-1 by Type 1/Type 2 Cytokines In Vivo: Granulomatous Pathology Is Shaped by the Pattern of l-Arginine Metabolism*. *The Journal of Immunology*, 2001. **167**(11): p. 6533-6544.
162. Wang, H.-W. and J.A. Joyce, *Alternative activation of tumor-associated macrophages by IL-4: priming for protumoral functions*. *Cell Cycle*, 2010. **9**(24): p. 4824-35.
163. Condeelis, J. and J.W. Pollard, *Macrophages: Obligate Partners for Tumor Cell Migration, Invasion, and Metastasis*. *Cell*, 2006. **124**(2): p. 263-266.
164. Fidler, I.J. and A.J. Schroit, *Recognition and destruction of neoplastic cells by activated macrophages: discrimination of altered self*. *Biochimica et Biophysica Acta (BBA) - Reviews on Cancer*, 1988. **948**(2): p. 151-173.
165. Qian, B.-Z. and J.W. Pollard, *Macrophage Diversity Enhances Tumor Progression and Metastasis*. *Cell*, 2010. **141**(1): p. 39-51.
166. Maeda, H. and T. Akaike, *Nitric oxide and oxygen radicals in infection, inflammation, and cancer*. *Biochemistry (Mosc)*, 1998. **63**(7): p. 854-65.
167. Hudson, J.D., et al., *A proinflammatory cytokine inhibits p53 tumor suppressor activity*. *J Exp Med*, 1999. **190**(10): p. 1375-82.
168. Dranoff, G., *Cytokines in cancer pathogenesis and cancer therapy*. *Nat Rev Cancer*, 2004. **4**(1): p. 11-22.
169. Bingle, L., N.J. Brown, and C.E. Lewis, *The role of tumour-associated macrophages in tumour progression: implications for new anticancer therapies*. *The Journal of Pathology*, 2002. **196**(3): p. 254-265.
170. Lin, E.Y., et al., *Colony-Stimulating Factor 1 Promotes Progression of Mammary Tumors to Malignancy*. *The Journal of Experimental Medicine*, 2001. **193**(6): p. 727-740.
171. Lewis, J.S., et al., *Expression of vascular endothelial growth factor by macrophages is up-regulated in poorly vascularized areas of breast carcinomas*. *J Pathol*, 2000. **192**(2): p. 150-8.
172. Voronov, E., et al., *IL-1 is required for tumor invasiveness and angiogenesis*. *Proc Natl Acad Sci U S A*, 2003. **100**(5): p. 2645-50.
173. Pollard, J.W., *Tumour-educated macrophages promote tumour progression and metastasis*. *Nat Rev Cancer*, 2004. **4**(1): p. 71-78.
174. Menetrier-Caux, C., et al., *Inhibition of the differentiation of dendritic cells from CD34(+) progenitors by tumor cells: role of interleukin-6 and macrophage colony-stimulating factor*. *Blood*, 1998. **92**(12): p. 4778-91.
175. Beissert, S., et al., *IL-10 inhibits tumor antigen presentation by epidermal antigen-presenting cells*. *The Journal of Immunology*, 1995. **154**(3): p. 1280-6.

176. Saccani, A., et al., *p50 Nuclear Factor- $\kappa$ B Overexpression in Tumor-Associated Macrophages Inhibits M1 Inflammatory Responses and Antitumor Resistance*. *Cancer Research*, 2006. **66**(23): p. 11432-11440.
177. Klimp, A.H., et al., *A potential role of macrophage activation in the treatment of cancer*. *Critical Reviews in Oncology/Hematology*, 2002. **44**(2): p. 143-161.
178. Dunn, G.P., et al., *Cancer immunoediting: from immunosurveillance to tumor escape*. *Nature immunology*, 2002. **3**(11): p. 991-998.
179. Clark, W.H., et al., *Model predicting survival in stage I melanoma based on tumor progression*. *Journal of the National Cancer Institute*, 1989. **81**(24): p. 1893-1904.
180. Shankaran, V., et al., *IFN $\gamma$  and lymphocytes prevent primary tumour development and shape tumour immunogenicity*. *Nature*, 2001. **410**(6832): p. 1107-1111.
181. Kaplan, D.H., et al., *Demonstration of an interferon  $\gamma$ -dependent tumor surveillance system in immunocompetent mice*. *Proceedings of the National Academy of Sciences*, 1998. **95**(13): p. 7556-7561.
182. Street, S.E., E. Cretney, and M.J. Smyth, *Perforin and interferon- $\gamma$  activities independently control tumor initiation, growth, and metastasis*. *Blood*, 2001. **97**(1): p. 192-197.
183. Duluc, D., et al., *Interferon-gamma reverses the immunosuppressive and protumoral properties and prevents the generation of human tumor-associated macrophages*. *Int J Cancer*, 2009. **125**(2): p. 367-73.
184. Guiducci, C., et al., *Redirecting in vivo elicited tumor infiltrating macrophages and dendritic cells towards tumor rejection*. *Cancer Res*, 2005. **65**(8): p. 3437-46.
185. Ostrand-Rosenberg, S., M.J. Grusby, and V.K. Clements, *Cutting Edge: STAT6-Deficient Mice Have Enhanced Tumor Immunity to Primary and Metastatic Mammary Carcinoma*. *The Journal of Immunology*, 2000. **165**(11): p. 6015-6019.
186. Kortylewski, M., et al., *Inhibiting Stat3 signaling in the hematopoietic system elicits multicomponent antitumor immunity*. *Nature medicine*, 2005. **11**(12): p. 1314-1321.
187. Luo, Y., et al., *Targeting tumor-associated macrophages as a novel strategy against breast cancer*. *The Journal of Clinical Investigation*. **116**(8): p. 2132-2141.
188. Rauh, M.J., et al., *The role of SHIP1 in macrophage programming and activation*. *Biochemical Society Transactions*, 2004. **32**(5): p. 785-788.
189. Krieg, A.M., *Therapeutic potential of Toll-like receptor 9 activation*. *Nat Rev Drug Discov*, 2006. **5**(6): p. 471-484.
190. Ruiz-Cabello, F., et al., *Impaired surface antigen presentation in tumors: implications for T cell-based immunotherapy*. *Seminars in Cancer Biology*, 2002. **12**(1): p. 15-24.
191. Finbow, M.E.a.H., Michael A. , <*The vacuolar H-ATPase, a universal proton pump of eukaryotes.pdf*>. 1997.
192. Yoshida, M., E. Muneyuki, and T. Hisabori, *ATP synthase--a marvellous rotary engine of the cell*. *Nat Rev Mol Cell Biol*, 2001. **2**(9): p. 669-77.
193. Cidon, S. and N. Nelson, *A novel ATPase in the chromaffin granule membrane*. *J Biol Chem*, 1983. **258**(5): p. 2892-98.
194. Forgac, M., et al., *Clathrin-coated vesicles contain an ATP-dependent proton pump*. *Proc Natl Acad Sci U S A*, 1983. **80**(5): p. 1300-3.
195. Wilkens, S. and M. Forgac, *Three-dimensional Structure of the Vacuolar ATPase Proton Channel by Electron Microscopy*. *Journal of Biological Chemistry*, 2001. **276**(47): p. 44064-44068.
196. Grinstein, S., et al., *V-ATPases in phagocytic cells*. *The Journal of experimental biology*, 1992. **172**(1): p. 179-192.

197. Harvey, W.R., *Physiology of v-ATPases*. Journal of Experimental Biology, 1992: p. 1-1.
198. Nishi, T. and M. Forgac, *The vacuolar (H<sup>+</sup>)-ATPases--nature's most versatile proton pumps*. Nat Rev Mol Cell Biol, 2002. **3**(2): p. 94-103.
199. Toyomura, T., et al., *From lysosomes to the plasma membrane: localization of vacuolar-type H<sup>+</sup>-ATPase with the a3 isoform during osteoclast differentiation*. J Biol Chem, 2003. **278**(24): p. 22023-30.
200. Pietrement, C., et al., *Distinct expression patterns of different subunit isoforms of the V-ATPase in the rat epididymis*. Biol Reprod, 2006. **74**(1): p. 185-94.
201. WERNER, G., et al., *Metabolic products of microorganisms. 224. Bafilomycins, a new group of macrolide antibiotics. Production, isolation, chemical structure and biological activity*. The Journal of antibiotics, 1984. **37**(2): p. 110-117.
202. Anderson, A.S. and E.M. Wellington, *The taxonomy of Streptomyces and related genera*. Int J Syst Evol Microbiol, 2001. **51**(Pt 3): p. 797-814.
203. Bowman, E.J., A. Siebers, and K. Altendorf, *Bafilomycins: a class of inhibitors of membrane ATPases from microorganisms, animal cells, and plant cells*. Proc Natl Acad Sci U S A, 1988. **85**(21): p. 7972-6.
204. Bowman, B.J. and E.J. Bowman, *Mutations in Subunit c of the Vacuolar ATPase Confer Resistance to Bafilomycin and Identify a Conserved Antibiotic Binding Site*. Journal of Biological Chemistry, 2002. **277**(6): p. 3965-3972.
205. Weissman, K.J. and R. Müller, *Myxobacterial secondary metabolites: bioactivities and modes-of-action*. Natural product reports, 2010. **27**(9): p. 1276-1295.
206. Reichenbach, H., *The ecology of the myxobacteria*. Environmental Microbiology, 1999. **1**(1): p. 15-21.
207. Kunze, B., et al., *Apicularens A and B, new cytostatic macrolides from Chondromyces species (myxobacteria): production, physico-chemical and biological properties*. The Journal of antibiotics, 1998. **51**(12): p. 1075-1080.
208. Su, Q. and J.S. Panek, *Total Synthesis of (-)-Apicularen A*. Journal of the American Chemical Society, 2004. **126**(8): p. 2425-2430.
209. Jansen, R., et al., *Apicularen A and B, Cytotoxic 10-Membered Lactones with a Novel Mechanism of Action from Chondromyces Species (Myxobacteria): Isolation, Structure Elucidation, and Biosynthesis*. European Journal Of Organic Chemistry, 2000. **2000**(6): p. 913-919.
210. Huss, M., et al., *Archazolid and apicularen: novel specific V-ATPase inhibitors*. BMC Biochem, 2005. **6**: p. 13.
211. Osteresch, C., et al., *The binding site of the V-ATPase inhibitor apicularen is in the vicinity of those for bafilomycin and archazolid*. J Biol Chem, 2012. **287**(38): p. 31866-76.
212. Sasse, F., et al., *Archazolids, new cytotoxic macrolactones from Archangium gephyra (Myxobacteria). Production, isolation, physico-chemical and biological properties*. J Antibiot (Tokyo), 2003. **56**(6): p. 520-5.
213. Sasse, F., et al., *Archazolids, new cytotoxic macrolactones from Archangium gephyra (Myxobacteria). Production, isolation, physico-chemical and biological properties*. J Antibiot (Tokyo), 2003. **56**(6): p. 520-5.
214. Hassfeld, J., et al., *Stereochemical determination of Archazolid A and B, highly potent vacuolar-type ATPase inhibitors from the Myxobacterium Archangium gephyra*. Org Lett, 2006. **8**(21): p. 4751-4.
215. Roethle, P.A., I.T. Chen, and D. Trauner, *Total synthesis of (-)-archazolid B*. J Am Chem Soc, 2007. **129**(29): p. 8960-1.

216. Menche, D., et al., *Modular total synthesis of archazolid A and B*. J Org Chem, 2009. **74**(19): p. 7220-9.
217. Toshima, K., et al., *Total Synthesis of Bafilomycin A1*. The Journal of organic chemistry, 1997. **62**(10): p. 3271-3284.
218. Gruenberg, J. and F.G. Van der Goot, *Mechanisms of pathogen entry through the endosomal compartments*. Nature reviews Molecular cell biology, 2006. **7**(7): p. 495-504.
219. Frattini, A., et al., *Defects in TCIRG1 subunit of the vacuolar proton pump are responsible for a subset of human autosomal recessive osteopetrosis*. Nature genetics, 2000. **25**(3): p. 343-346.
220. Murakami, T., et al., *Elevated expression of vacuolar proton pump genes and cellular PH in cisplatin resistance*. International journal of cancer, 2001. **93**(6): p. 869-874.
221. Sennoune, S.R., et al., *Vacuolar H<sup>+</sup>-ATPase in human breast cancer cells with distinct metastatic potential: distribution and functional activity*. American Journal of Physiology - Cell Physiology, 2004. **286**(6): p. C1443-C1452.
222. Wiedmann, R.M., et al., *The V-ATPase-inhibitor archazolid abrogates tumor metastasis via inhibition of endocytic activation of the Rho-GTPase Rac1*. Cancer Res, 2012. **72**(22): p. 5976-87.
223. Kubisch, R., et al., *V-ATPase inhibition by archazolid leads to lysosomal dysfunction resulting in impaired cathepsin B activation in vivo*. Int J Cancer, 2014. **134**(10): p. 2478-88.
224. Rojas, J.D., et al., *Vacuolar-type H<sup>+</sup>-ATPases at the plasma membrane regulate pH and cell migration in microvascular endothelial cells*. American Journal of Physiology-Heart and Circulatory Physiology, 2006. **291**(3): p. H1147-H1157.
225. De Milito, A., et al., *Proton Pump Inhibitors Induce Apoptosis of Human B-Cell Tumors through a Caspase-Independent Mechanism Involving Reactive Oxygen Species*. Cancer Research, 2007. **67**(11): p. 5408-5417.
226. Wu, Y.C., et al., *Inhibition of macroautophagy by bafilomycin A1 lowers proliferation and induces apoptosis in colon cancer cells*. Biochem Biophys Res Commun, 2009. **382**(2): p. 451-6.
227. von Schwarzenberg, K., et al., *V-ATPase inhibition overcomes trastuzumab resistance in breast cancer*. Molecular Oncology, 2014. **8**(1): p. 9-19.
228. Hinton, A., S. Bond, and M. Forgac, *V-ATPase functions in normal and disease processes*. Pflugers Arch, 2009. **457**(3): p. 589-98.
229. Schempp, C.M., et al., *V-ATPase inhibition regulates anoikis resistance and metastasis of cancer cells*. Mol Cancer Ther, 2014. **13**(4): p. 926-37.
230. Dunn, G.P., L.J. Old, and R.D. Schreiber, *The Immunobiology of Cancer Immunosurveillance and Immunoediting*. Immunity, 2004. **21**(2): p. 137-148.
231. Dranoff, G., *Immune recognition and tumor protection*. Current Opinion in Immunology, 2002. **14**(2): p. 161-164.
232. Pergola, C., et al., *Testosterone suppresses phospholipase D, causing sex differences in leukotriene biosynthesis in human monocytes*. FASEB J, 2011. **25**(10): p. 3377-87.
233. Solinas, G., et al., *Tumor-conditioned macrophages secrete migration-stimulating factor: a new marker for M2-polarization, influencing tumor cell motility*. J Immunol, 2010. **185**(1): p. 642-52.
234. Mosmann, T., *Rapid colorimetric assay for cellular growth and survival: Application to proliferation and cytotoxicity assays*. Journal of Immunological Methods, 1983. **65**(1): p. 55-63.

235. Zheng, N., X. Zhang, and G.R. Rosania, *Effect of phospholipidosis on the cellular pharmacokinetics of chloroquine*. *J Pharmacol Exp Ther*, 2011. **336**(3): p. 661-71.
236. Bidani, A., et al., *Cytoplasmic pH in pulmonary macrophages: recovery from acid load is Na<sup>+</sup> independent and NEM sensitive*. *American Journal of Physiology-Cell Physiology*, 1989. **257**(1): p. C65-C76.
237. Nuutila, J. and E.-M. Lilius, *Flow cytometric quantitative determination of ingestion by phagocytes needs the distinguishing of overlapping populations of binding and ingesting cells*. *Cytometry Part A*, 2005. **65A**(2): p. 93-102.
238. Livak, K.J. and T.D. Schmittgen, *Analysis of Relative Gene Expression Data Using Real-Time Quantitative PCR and the 2- $\Delta\Delta$ CT Method*. *Methods*, 2001. **25**(4): p. 402-408.
239. Yokomakura, A., et al., *Increased production of reactive oxygen species by the vacuolar-type (H<sup>+</sup>)-ATPase inhibitors bafilomycin A1 and concanamycin A in RAW 264 cells*. *J Toxicol Sci*, 2012. **37**(5): p. 1045-8.
240. Spina, D., *Statistics in pharmacology*. *British journal of pharmacology*, 2007. **152**(3): p. 291-293.
241. Tapper, H. and R. Sundler, *Cytosolic pH regulation in mouse macrophages. Proton extrusion by plasma-membrane-localized H<sup>+</sup>-ATPase*. *Biochem J*, 1992. **281 ( Pt 1)**: p. 245-50.
242. Lafourcade, C., et al., *Regulation of the V-ATPase along the endocytic pathway occurs through reversible subunit association and membrane localization*. *PLoS One*, 2008. **3**(7): p. e2758.
243. Kamachi, F., et al., *Involvement of Na<sup>+</sup>/H<sup>+</sup> exchangers in induction of cyclooxygenase-2 by vacuolar-type (H<sup>+</sup>)-ATPase inhibitors in RAW 264 cells*. *FEBS Lett*, 2007. **581**(24): p. 4633-8.
244. Kazami, S., et al., *Iejimalide C is a potent V-ATPase inhibitor, and induces actin disorganization*. *Biol Pharm Bull*, 2014. **37**(12): p. 1944-7.
245. Ohkuma, S. and B. Poole, *Fluorescence probe measurement of the intralysosomal pH in living cells and the perturbation of pH by various agents*. *Proc Natl Acad Sci U S A*, 1978. **75**(7): p. 3327-31.
246. Bergman, J., et al., *Use of the pH-sensitive dye BCECF to study pH regulation in cultured human kidney proximal tubule cells*. *Journal of tissue culture methods*, 1991. **13**(3): p. 205-209.
247. Sobota, J.A., et al., *Inhibitors of the V0 subunit of the vacuolar H<sup>+</sup>-ATPase prevent segregation of lysosomal-and secretory-pathway proteins*. *Journal of cell science*, 2009. **122**(19): p. 3542-3553.
248. Zurier, R.B., S. Hoffstein, and G. Weissmann, *Cytochalasin B: Effect on Lysosomal Enzyme Release from Human Leukocytes*. *Proceedings of the National Academy of Sciences*, 1973. **70**(3): p. 844-848.
249. Sobell, H.M., *Actinomycin and DNA transcription*. *Proceedings of the National Academy of Sciences*, 1985. **82**(16): p. 5328-5331.
250. Li, Y. and M.A. Trush, *Diphenyleneiodonium, an NAD(P)H oxidase inhibitor, also potently inhibits mitochondrial reactive oxygen species production*. *Biochem Biophys Res Commun*, 1998. **253**(2): p. 295-9.
251. Bray, M.A. and D. Gordon, *Prostaglandin production by macrophages and the effect of anti-inflammatory drugs*. *Br J Pharmacol*, 1978. **63**(4): p. 635-42.
252. Masferrer, J.L. and K. Seibert, *Regulation of prostaglandin synthesis by glucocorticoids*. *Receptor*, 1994. **4**(1): p. 25-30.

253. Norris, P.C., et al., *Specificity of eicosanoid production depends on the TLR-4-stimulated macrophage phenotype*. J Leukoc Biol, 2011. **90**(3): p. 563-74.
254. Beyenbach, K.W. and H. Wieczorek, *The V-type H<sup>+</sup> ATPase: molecular structure and function, physiological roles and regulation*. J Exp Biol, 2006. **209**(Pt 4): p. 577-89.
255. Breton, S. and D. Brown, *Regulation of luminal acidification by the V-ATPase*. Physiology (Bethesda), 2013. **28**(5): p. 318-29.
256. Reker, D., et al., *Revealing the macromolecular targets of complex natural products*. Nat Chem, 2014. **6**(12): p. 1072-8.
257. Arias-Negrete, S., K. Keller, and K. Chadee, *Proinflammatory cytokines regulate cyclooxygenase-2 mRNA expression in human macrophages*. Biochem Biophys Res Commun, 1995. **208**(2): p. 582-9.
258. Auphan, N., et al., *Immunosuppression by glucocorticoids: inhibition of NF-kappa B activity through induction of I kappa B synthesis*. Science, 1995. **270**(5234): p. 286-90.
259. Tateson, J., et al., *Selective inhibition of arachidonate 5-lipoxygenase by novel acetohydroxamic acids: biochemical assessment in vitro and ex vivo*. British journal of pharmacology, 1988. **94**(2): p. 528-539.
260. Larsen, G.L. and P.M. Henson, *Mediators of inflammation*. Annual review of immunology, 1983. **1**(1): p. 335-359.
261. Libby, P., *Inflammatory Mechanisms: the Molecular Basis of Inflammation and Disease*. Nutrition Reviews, 2007. **65**(suppl 3): p. S140-S146.
262. Ong, S.-M., et al., *Macrophages in human colorectal cancer are pro-inflammatory and prime T cells towards an anti-tumour type-1 inflammatory response*. European Journal of Immunology, 2012. **42**(1): p. 89-100.
263. Goubau, D., et al., *Transcriptional re-programming of primary macrophages reveals distinct apoptotic and anti-tumoral functions of IRF-3 and IRF-7*. Eur J Immunol, 2009. **39**(2): p. 527-40.
264. Baay, M., et al., *Tumor cells and tumor-associated macrophages: secreted proteins as potential targets for therapy*. Clin Dev Immunol, 2011. **2011**: p. 565187.
265. Scherer, O., et al., *Targeting V-ATPase in primary human monocytes by archazolid potently represses the classical secretion of cytokines due to accumulation at the endoplasmic reticulum*. Biochem Pharmacol, 2014. **91**(4): p. 490-500.
266. Bidani, A., et al., *Bactericidal activity of alveolar macrophages is suppressed by V-ATPase inhibition*. Lung, 2000. **178**(2): p. 91-104.
267. Wiedmann, R.M., et al., *The V-ATPase-inhibitor archazolid abrogates tumor metastasis via inhibition of endocytic activation of the Rho-GTPase Rac1*. Cancer Res, 2012. **72**(22): p. 5976-87.
268. Zajac, E., et al., *Angiogenic capacity of M1- and M2-polarized macrophages is determined by the levels of TIMP-1 complexed with their secreted proMMP-9*. Blood, 2013. **122**(25): p. 4054-4067.
269. Cassol, E., et al., *M1 and M2a Polarization of Human Monocyte-Derived Macrophages Inhibits HIV-1 Replication by Distinct Mechanisms*. The Journal of Immunology, 2009. **182**(10): p. 6237-6246.
270. Gwinn, M.R. and V. Vallyathan, *Respiratory burst: role in signal transduction in alveolar macrophages*. J Toxicol Environ Health B Crit Rev, 2006. **9**(1): p. 27-39.
271. Marshansky, V. and M. Futai, *The V-type H<sup>+</sup>-ATPase in vesicular trafficking: targeting, regulation and function*. Current Opinion in Cell Biology, 2008. **20**(4): p. 415-426.

272. Latchman, D.S., *Transcription factors: an overview*. The international journal of biochemistry & cell biology, 1997. **29**(12): p. 1305-1312.
273. Collart, M.A., P. Baeuerle, and P. Vassalli, *Regulation of tumor necrosis factor alpha transcription in macrophages: involvement of four kappa B-like motifs and of constitutive and inducible forms of NF-kappa B*. Mol Cell Biol, 1990. **10**(4): p. 1498-506.
274. Shakhov, A.N., et al., *Kappa B-type enhancers are involved in lipopolysaccharide-mediated transcriptional activation of the tumor necrosis factor alpha gene in primary macrophages*. J Exp Med, 1990. **171**(1): p. 35-47.
275. Sasaki, C.Y., et al., *Phosphorylation of RelA/p65 on serine 536 defines an I{kappa}B{alpha}-independent NF-{kappa}B pathway*. J Biol Chem, 2005. **280**(41): p. 34538-47.
276. Bohuslav, J., et al., *p53 induces NF-kB activation by an Ikb kinase-independent mechanism involving phosphorylation of p65 by ribosomal S6 kinase 1*. Journal of Biological Chemistry, 2004. **279**(25): p. 26115-26125.
277. Hohmann, H.P., et al., *Tumor necrosis factors-alpha and -beta bind to the same two types of tumor necrosis factor receptors and maximally activate the transcription factor NF-kappa B at low receptor occupancy and within minutes after receptor binding*. Journal of Biological Chemistry, 1990. **265**(25): p. 15183-8.
278. Geppert, T.D., et al., *Lipopolysaccharide signals activation of tumor necrosis factor biosynthesis through the ras/raf-1/MEK/MAPK pathway*. Mol Med, 1994. **1**(1): p. 93-103.
279. Ip, Y.T. and R.J. Davis, *Signal transduction by the c-Jun N-terminal kinase (JNK) — from inflammation to development*. Current Opinion in Cell Biology, 1998. **10**(2): p. 205-219.
280. Madrid, L.V., et al., *Akt stimulates the transactivation potential of the RelA/p65 subunit of NF-kB through utilization of the Ikb kinase and activation of the mitogen-activated protein kinase p38*. Journal of Biological Chemistry, 2001. **276**(22): p. 18934-18940.
281. Yu, H., D. Pardoll, and R. Jove, *STATs in cancer inflammation and immunity: a leading role for STAT3*. Nat Rev Cancer, 2009. **9**(11): p. 798-809.
282. Shen, Y., et al., *Constitutively activated Stat3 protects fibroblasts from serum withdrawal and UV-induced apoptosis and antagonizes the proapoptotic effects of activated Stat1*. Proc Natl Acad Sci U S A, 2001. **98**(4): p. 1543-8.
283. Wang, J. and J. Yi, *Cancer cell killing via ROS: to increase or decrease, that is the question*. Cancer Biol Ther, 2008. **7**(12): p. 1875-84.
284. Schumacker, P.T., *Reactive oxygen species in cancer cells: Live by the sword, die by the sword*. Cancer Cell, 2006. **10**(3): p. 175-176.
285. Morgan, M.J., Y.S. Kim, and Z. Liu, *Lipid rafts and oxidative stress-induced cell death*. Antioxid Redox Signal, 2007. **9**(9): p. 1471-83.
286. Yuan, F., et al., *Induction of Murine Macrophage M2 Polarization by Cigarette Smoke Extract via the JAK2/STAT3 Pathway*. PLoS ONE, 2014. **9**(9): p. e107063.
287. Ott, M., et al., *Mitochondria, oxidative stress and cell death*. Apoptosis, 2007. **12**(5): p. 913-922.
288. Ushio-Fukai, M., *Compartmentalization of redox signaling through NADPH oxidase-derived ROS*. Antioxid Redox Signal, 2009. **11**(6): p. 1289-99.
289. Morgan, M. and Z.-g. Liu, *Reactive oxygen species in TNFa-induced signaling and cell death*. Molecules and Cells, 2010. **30**(1): p. 1-12.
290. Gilroy, D.W., *Eicosanoids and the endogenous control of acute inflammatory resolution*. The International Journal of Biochemistry & Cell Biology, 2010. **42**(4): p. 524-528.

291. Kuehl, F. and R. Egan, *Prostaglandins, arachidonic acid, and inflammation*. Science, 1980. **210**(4473): p. 978-984.
292. Park, J.Y., M.H. Pillinger, and S.B. Abramson, *Prostaglandin E2 synthesis and secretion: The role of PGE2 synthases*. Clinical Immunology, 2006. **119**(3): p. 229-240.
293. Bonventre, J.V., *Phospholipase A2 and signal transduction*. J Am Soc Nephrol, 1992. **3**(2): p. 128-50.
294. Hwang, D., et al., *Expression of mitogen-inducible cyclooxygenase induced by lipopolysaccharide: Mediation through both mitogen-activated protein kinase and nf-kb signaling pathways in macrophages*. Biochemical Pharmacology, 1997. **54**(1): p. 87-96.
295. Gilroy, D.W., A. Tomlinson, and D.A. Willoughby, *Differential effects of inhibitors of cyclooxygenase (cyclooxygenase 1 and cyclooxygenase 2) in acute inflammation*. Eur J Pharmacol, 1998. **355**(2-3): p. 211-7.
296. Rouzer, C.A., et al., *MK886, a potent and specific leukotriene biosynthesis inhibitor blocks and reverses the membrane association of 5-lipoxygenase in ionophore-challenged leukocytes*. Journal of Biological Chemistry, 1990. **265**(3): p. 1436-1442.
297. Kilty, I., A. Logan, and P.J. Vickers, *Differential characteristics of human 15-lipoxygenase isozymes and a novel splice variant of 15S-lipoxygenase*. European Journal of Biochemistry, 1999. **266**(1): p. 83-93.
298. Brash, A.R., W.E. Boeglin, and M.S. Chang, *Discovery of a second 15S-lipoxygenase in humans*. Proceedings of the National Academy of Sciences, 1997. **94**(12): p. 6148-6152.
299. Bailey, J.M., et al., *Characterization of 11-HETE and 15-HETE, together with prostacyclin, as major products of the cyclooxygenase pathway in cultured rat aorta smooth muscle cells*. J Lipid Res, 1983. **24**(11): p. 1419-28.
300. Xu, Z.G., et al., *Relationship between 12/15-lipoxygenase and COX-2 in mesangial cells: potential role in diabetic nephropathy*. Kidney Int, 2006. **69**(3): p. 512-9.
301. Profita, M., et al., *Interleukin-4 enhances 15-lipoxygenase activity and incorporation of 15 (S)-HETE into cellular phospholipids in cultured pulmonary epithelial cells*. American journal of respiratory cell and molecular biology, 1999. **20**(1): p. 61-68.

## **APPENDIX 1: Acknowledgements**

Mein besonderer Dank gilt Prof. Dr. Oliver Werz für die Möglichkeit, an diesem hochinteressanten, vielschichtigen und herausfordernden Thema zu arbeiten sowie für die wertvolle wissenschaftliche Betreuung, die mir jederzeit Raum ließ, eigene Ideen einzubringen und umzusetzen.

Bei Herrn Prof. Dr. Gerhard Scriba möchte ich mich herzlich für die Übernahme des Zweitgutachtens bedanken.

Herrn Prof. Dr. Eugen Proschak danke ich für die Erstellung des dritten Gutachtens meiner Arbeit.

Beim Institut für Transfusionsmedizin des Universitätsklinikums Jena und im Besonderen bei Frau Dr. C. Weinigel und Frau Dr. S. Rummler bedanke ich mich für die Bereitstellung der Buffy Coats.

Prof. Dr. D. Menche und seiner Arbeitsgruppe danke ich für die Synthese und Bereitstellung der V-ATPase-Inhibitoren Archazolid und Apicularen. Desweiteren gilt mein Dank allen Beteiligten der DFG Forschergruppe 1406 für die fachlichen Diskussionen rund um die V-ATPase.

Für den Zugang zu Nanodrop und qPCR System bedanke ich mich beim Lehrstuhl für Genetik.

Den Arbeitskreisen von Prof. Werz und Prof. Scriba bin ich für die gute Zusammenarbeit, die jederzeitige Hilfsbereitschaft aller und die hervorragende Arbeitsatmosphäre dankbar und nicht zu vergessen, die vielen leckeren Kuchen zu so mancher Kaffeepause.

Hierunter möchte ich ganz herzlich den Personen danken, die mich während meiner Promotionszeit auf besondere Weise unterstützt haben:

Dr. Ulrike Garscha möchte ich für die Einarbeitung in die Betreuung des Praktikums „Qualitative anorganische Analytik von Arznei-, Hilfs- und Schadstoffen“ sowie die vielen gemeinsamen Stunden während der Praktikumszeiten bedanken. Vielen Dank außerdem für die guten und anregenden Diskussionen sowohl auf wissenschaftlicher Basis als auch darüber hinaus, für das jederzeit offene Ohr und die kritische Betrachtung aller Fragestellungen.

PD Dr. Andreas Koeberle danke ich für die Einführung in die LC-MS/MS-Analytik sowie seine Hilfsbereitschaft und guten Ratschläge rund um dieses Thema.

Bei Katrin Schubert möchte ich mich für die ausgezeichnete praktische Einarbeitung in die Welt der Makrophagen bedanken.

Katrin Fischer danke ich für ihr außergewöhnliches Engagement hinsichtlich jeglicher Materialbeschaffungen und die Kunst, den Überblick über unsere unzähligen LC-MS/MS Proben zu behalten.

Bei allen Mitbetreuern des 1. Semesters bedanke ich mich für die gute und effektive Zusammenarbeit und die unterhaltsamen Stunden während des Praktikums.

Dr. Olga Scherer, Bettina Mönch und Saskia Lindner danke ich für die gemeinsame Zeit während unserer Forschergruppe-Treffen sowie die damit verbundenen kritischen und produktiven Gespräche.

Felix Nikels und Verena Krauth danke ich als meinen zwei wunderbaren Labornachbarn für die tolle Arbeitsatmosphäre, den fachlichen Austausch, die jederzeitige Hilfsbereitschaft und die ausgezeichnete Zusammenarbeit, die guten Gespräche und alles andere, das dazu beigetragen hat, den Arbeitsalltag immer wieder aufs Neue zu etwas Besonderem zu machen.

Mein herzlichster Dank gilt meinen Eltern, die mich jederzeit und in allen Dingen unterstützen, mir ihr absolutes Vertrauen schenken, immer für mich da sind und mir diesen akademischen Lebensweg ermöglichten. Meiner Schwester und besten Freundin Saskia bin ich unglaublich dankbar, dass sie allzeit ein offenes Ohr für mich hat, mir mit konstruktiven Ratschlägen fortwährend beiseite steht und ich mir ihrer vollen Unterstützung immer gewiss sein kann. Mitunter durch die vielen wertvollen Gespräche und anregenden Diskussionen mit der gesamten Familie stehe ich heute dort wo ich bin.

Meinem Lieblingsmenschen Tobias danke ich dafür, dass er immer für mich da ist und für die wundervolle Fähigkeit, mich in jeder Lebenssituation aufheitern zu können, was auch in der Promotionszeit eine unschätzbare Unterstützung war. Für die vielen hilfreichen Tipps und Ratschläge, das geduldige Zuhören, die Denkanstöße und nicht zuletzt das Krisenbeheben neben unzähligen weiteren Dingen bin ich unendlich dankbar.

## **APPENDIX 2: List of publications**

### **Posterpresentation**

05/2015                      DFG Symposium “Vacuolar ATPase: A novel anti-tumor target”  
in Mailand, Italien (Poster)

### **Manuscripts**

Dawczynski C, Dittrich M, Neumann T, Goetze K, Welzel A, Oelzner P, Völker S, Schaible AM, Troisi F, Thomas L, Pace S, Koeberle A, Werz O, Schlattmann P, Lorkowski S, Jahreis G

Docosahexaenoic acid in the treatment of rheumatoid arthritis: A double-blind, placebo-controlled, randomized cross-over study with microalgae vs. sunflower oil.

### **Manuscript in print**

Thomas L, Zhigang R, Gerstmeier J, Raasch M, Weinigel C, Rummler S, Menche D, Müller R, Pergola C, Mosig A, Werz O

Selective upregulation of TNF $\alpha$  expression in classically-activated human monocyte-derived macrophages (M1) through pharmacological interference with V-ATPase

### **Manuscript in preparation**

Thomas L, Weinigel C, Rummler S, Menche D, Müller R, Werz O

Suppression of V-ATPase differentially affects the biosynthesis of eicosanoids in polarized macrophages

## **APPENDIX 3: Eigenständigkeitserklärung**

Hiermit erkläre ich, dass mir die Promotionsordnung der Biologisch-Pharmazeutischen Fakultät der Friedrich-Schiller-Universität Jena bekannt ist. Die vorliegende Dissertation habe ich selbst angefertigt, keine Textabschnitte eines Dritten oder eigener Prüfungsarbeiten ohne Kennzeichnung übernommen und alle von mir benutzten Hilfsmittel, persönlichen Mitteilungen und Quellen angegeben.

Ich versichere, dass ich die Hilfe eines Promotionsberaters nicht in Anspruch genommen habe und dass Dritte weder unmittelbar noch mittelbar geldwerte Leistungen von mir für Arbeiten erhalten haben, die im Zusammenhang mit dem Inhalt der vorgelegten Dissertation stehen.

Diese Dissertation wurde für keine staatliche oder andere wissenschaftliche Prüfung als Prüfungsarbeit von mir eingereicht. Weiterhin versichere ich, dass ich die gleiche, eine in wesentlichen Teilen ähnliche oder eine andere Abhandlung nicht bei einer anderen Universität als Dissertation eingereicht habe.

---

Ort, Datum

---

Lea Thomas